

Aus dem
Walther-Straub-Institut für Pharmakologie und Toxikologie
Ludwig-Maximilians-Universität München

Institut für Pharmakologie und Toxikologie der Bundeswehr



**Interaction of Sulfur Mustard and other Alkylating
Compounds with human Transient Receptor Potential
(TRPA1) Channels**

Dissertation
zum Erwerb des Doctor of Philosophy (Ph.D.)
an der Medizinischen Fakultät der
Ludwig-Maximilians-Universität München

vorgelegt von
Katharina Müller-Dott

aus
Frankfurt am Main

Jahr
2024

Mit Genehmigung der Medizinischen Fakultät der
Ludwig-Maximilians-Universität München

Erstes Gutachten:	Prof. Dr. Dirk Steinritz
Zweites Gutachten:	Priv. Doz. Dr. Claudia Staab-Weijnitz
Drittes Gutachten:	Prof. Dr. Alexander Faußner
Viertes Gutachten:	Prof. Dr. Franz Worek
Dekan:	Prof. Dr. med. Thomas Gudermann
Tag der mündlichen Prüfung:	22.01.2024

*To my daughter Lilly,
with endless love*

Affidavit



Affidavit

Müller-Dott, Katharina
(Surname, first name)

Neuherbergstr. 11
(Street)

80937 München, Germany
(Zip code, town, country)

I hereby declare, that the submitted thesis entitled:

Interaction of Sulfur Mustard and other Alkylating Compounds with human Transient Receptor Potential (TRPA1) Channels

is my own work. I have only used the sources indicated and have not made unauthorised use of services of a third party. Where the work of others has been quoted or reproduced, the source is always given.

I further declare that the dissertation presented here has not been submitted in the same or similar form to any other institution for the purpose of obtaining an academic degree.

München, 02.02.2024

Katharina Müller-Dott

(Katharina Müller-Dott)

Confirmation of congruency



**Confirmation of congruency between printed and electronic version
of the doctoral thesis**

Müller-Dott, Katharina
(Surname, first name)

Neuherbergstr. 11
(Street)

80937 München, Germany
(Zip code, town, country)

I hereby declare, that the submitted thesis entitled:

Interaction of Sulfur Mustard and other Alkylating Compounds with human Transient Receptor Potential (TRPA1) Channels

is congruent with the printed version both in content and format.

München, 02.02.2024

Katharina Müller-Dott

(Katharina Müller-Dott)

Contents

Affidavit	I
Confirmation of congruency	II
Table of content	III
List of abbreviations	IV
List of publications	V
1 Authors contribution to the publications	1
1.1 Contribution to Paper I	1
1.2 Contribution to Paper II	3
2 Introductory Summary	5
2.1 Sulfur mustard	5
2.1.1 Clinical picture of SM poisoning	6
2.1.2 Molecular toxicology	6
2.2 Transient receptor potential channels	8
2.2.1 Transient receptor potential ankyrin 1 channels	9
2.3 SM-related alkylating agents	10
2.3.1 Nitrogen mustard	11
2.3.2 Chemotherapeutic agents	11
2.4 Identification of SM-induced hTRPA1 channel modifications (Paper I)	12
2.5 hTRPA1 activation potential of SM-related alkylating agents (Paper II)	13
2.6 Concluding remarks	15
3 Paper I	16
3.1 Supplementary material Paper I	27
4 Paper II	38
4.1 Supplementary material Paper I	47
5 Summary	49
6 Bibliography	50
Acknowledgements	58

List of abbreviations

AITC	allyl isothiocyanate
AP18	4-(4-chlorophenyl)-3-methyl-3-buten-2-one oxime
Ca ²⁺ _i	intracellular calcium concentration
CEES	2-chloroethyl ethyl sulfide
CWC	Chemical Weapon Convention
CYP	cytochrome P450
HD	Hun Stuff distilled
HEK-A1	HEK293 cells overexpression hTRPA1 channel
HEK-wt	HEK293-wildtype
HETE	Hydroxyethylthioethyl
HN1	bis(2-chloroethyl)ethylamine
HN2	bis(2-chloroethyl)methylamine
HN3	tris(2-chloroethyl)amine
hTRPA1	human TRP ankyrin 1 channel
IAA	iodoacetamide
IARC	International Agency for Research on Cancer
IMS	immunomagnetic separation
LC ₅₀	lethal concentration resulting in 50% cell viability
N7-HETE-G	7-(2-hydroxyethylthioethyl) guanine
NATO	North Atlantic Treaty Organization
OPCW	Organisation for the Prohibition of Chemical Weapons
Q	sesquimustard
SM	sulfur mustard
T	O-mustard
THC	tetrahydrocannabinol
TRP	transient receptor potential
TRPC	canonical TRP channel
TRPM	melastatin TRP channel
TRPML	mucolipin TRP channel
TRPN	no-mechanoreceptor potential channels
TRPP	polycystin TRP channel
TRPV	vanilloid TRP channel
WWI	World War I
WWII	World War II
μLC-ESI MS/HR MS	micro liquid chromatography-electrospray ionization high-resolution tandem-mass spectrometry

List of publications

Publications of the cumulative dissertation

Publication I

Katharina Müller-Dott, Horst Thiermann, Harald John, Dirk Steinritz (2022). Isolation of human TRPA1 channel from transfected HEK293 cells and identification of alkylation sites after sulfur mustard exposure. *Archives of Toxicology*, 97, pp. 429–439. doi: 10.1007/s00204-022-03411-1.

The publication is an open access article under the CC BY 4.0 DEED license.

Publication II

Katharina Müller-Dott, Sarah-Christine Raßmuß, Marc-Michael Blum, Horst Thiermann, Harald John, Dirk Steinritz (2023). Activation of the human TRPA1 channel by different alkylating sulfur and nitrogen mustards and structurally related chemotherapeutic drugs. *Toxicology Letters*, 376, pp. 51–59. doi: 10.1016/j.toxlet.2023.01.007.

The publication is an open access article under the CC BY-NC-ND license.

Additional publications

Katharina Müller-Dott, Horst Thiermann, Dirk Steinritz, Tanja Popp (2020). Effect of sulfur mustard on melanogenesis in vitro. *Toxicology Letters*, 319, pp. 197-203. doi: 10.1016/j.toxlet.2019.11.014.

Katharina Müller-Dott, Cornelia Muschik, Tanja Popp, Horst Thiermann, Dirk Steinritz (2020). In vitro Untersuchungen zum Einfluss von Schwefel-Lost auf die Melanogenese' *Wehrmedizinische Monatszeitschrift*, 64(1), pp. 38–39.

Conference contributions

Poster presentation: Katharina Müller-Dott, Tanja Popp, Thomas Gudermann, Ingrid Boekhoff, Horst Thiermann, Dirk Steinritz (2019). The effect of sulfur mustard on human melanocytes. 4th Pharm-Tox Summit - 85th Annual Meeting of the German Society for Experimental and Clinical Pharmacology and Toxicology (DGPT), Stuttgart.

Poster presentation: Katharina Müller-Dott, Dirk Steinritz, Horst Thiermann, Tanja Popp (2019). Affection of melanogenesis after exposure to sulfur mustard in vitro. 17. Medical Chemical Defense Conference, München.

Poster presentation: Katharina Müller-Dott, Cornelia Muschik, Tanja Popp, Horst Thiermann, Dirk Steinritz (2019). In vitro Untersuchungen zum Einfluss von S-Lost auf die Melanogenese. 50. Jahreskongress der Deutschen Gesellschaft für Wehrmedizin und Wehrpharmazie e. V., Leipzig.

Poster presentation: Katharina Müller-Dott, Thomas Gudermann, Horst Thiermann, Harald John, Dirk Steinritz (2022). Isolation of TRPA1 channel from HEK293 cells as a target for alkylating agents. 7th Pharm-Tox Summit - 88th Annual Meeting of the German Society for Experimental and Clinical Pharmacology and Toxicology (DGPT), digital.

1 Authors contribution to the publications

1.1 Contribution to Paper I

Katharina Müller-Dott, Horst Thiermann, Harald John, Dirk Steinritz (2022). Isolation of human TRPA1 channel from transfected HEK293 cells and identification of alkylation sites after sulfur mustard exposure. *Archives of Toxicology*, 97, pp. 429–439. doi: 10.1007/s00204-022-03411-1.

The publication is an open access article under the CC BY 4.0 DEED license.

I investigated amino acid modifications within the human transient receptor potential ankyrin 1 (hTRPA1) channel after exposure to the chemical warfare agent sulfur mustard (SM). This was performed to elucidate hTRPA1 activation mechanism, thus, to identify specific amino acid modifications which might be involved in hTRPA1 activation. During this research, a broad spectrum of proteomic assays was applied such as recombinant expression of the hTRPA1 channel in HEK293 cells, cell lysis, protein purification, and identification of hTRPA1 modifications using micro liquid chromatography-electrospray ionization high-resolution tandem mass spectrometry (μ LC-ESI MS/HR MS). The results from this study were published in *Archives of Toxicology*. In the following, I list my contributions to the publication „Isolation of human TRPA1 from transfected HEK293 cells and identification of alkylation sites after sulfur mustard exposure“ published in *Archives of Toxicology*.

- Literature research
- Planning of the experimental design
- Cell cultivation of HEK293 cells
- Transfection of HEK293 cells with His-tagged hTRPA1 plasmid
- Optimization of cell lysis buffer
- Identification of hTRPA1 protein expression using Western blot experiments
- Purification of hTRPA1 using immunomagnetic separation with hTRPA1 and His-tag specific antibodies
- Functionality testing of hTRPA1 using Fura-2 calcium measurements
- Development of a μ LC-ESI MS/HR MS method for the sensitive and selective detection of alkylation sites

- Analytical characterization of the different peptides containing alkylated amino acid residues
- Preparation of the manuscript draft
- Preparation of the revised manuscript

The following contributions to the publication *Müller-Dott et al.* (2022) in *Archives of Toxicology* were made by the co-authors:

Author Horst Thiermann:

- Scientific advice

Authors Harald John and Dirk Steinritz:

- Project supervision and scientific advice
- Data discussion
- Preparation of the manuscript and manuscript revision

1.2 Contribution to Paper II

Katharina Müller-Dott, Sarah-Christine Raßmuß, Marc-Michael Blum, Horst Thiermann, Harald John, Dirk Steinritz (2023). Activation of the human TRPA1 channel by different alkylating sulfur and nitrogen mustards and structurally related chemotherapeutic drugs. *Toxicology Letters*, 376, pp. 51–59. doi: 10.1016/j.toxlet.2023.01.007.

The publication is an open access article under the CC BY-NC-ND license.

In this study, I investigated the activation of hTRPA1 by additional alkylating agents, including SM-related agents such as sesquimustard (Q) and O-mustard (T), but also nitrogen mustards and related chemotherapeutic drugs. This was performed using the aequorin assay for calcium measurements. Furthermore, I determined cytotoxicity of the different compounds and calculated an activation-cytotoxicity ratio to evaluate a correlation between activation potential and cytotoxicity. In a final step, I performed pre-treatment of the cells using the hTRPA1 specific antagonist 4-(4-chlorophenyl)-3-methyl-3-buten-2-one oxime (AP18) to elucidate the role of hTRPA1 in cytotoxicity. The results from this study were published in *Toxicology Letters*. In the following, I list my contributions to the publication „Activation of the human TRPA1 channel by different alkylating sulfur and nitrogen mustards and structurally related chemotherapeutic drugs“ in *Toxicology Letters*.

- Literature research
- Planning of the experimental design
- Cell cultivation of HEK293 and hTRPA1 overexpressing HEK-A1 cells
- Identification of hTRPA1 gene and protein using PCR and Western blot experiments
- Supervision and project planning for calcium measurements and XTT assay
- Performing calcium measurements using the aequorin assay
- Cell viability assay using XTT for nitrogen mustards and chemotherapeutic agents
- XTT with pre-treatment of HEK293 cells using the hTRPA1 specific antagonist AP18
- Data discussion
- Preparation of the manuscript draft
- Preparation of the revised manuscript

The following contributions to the publication *Müller-Dott et al. (2023)* in *Archives of Toxicology* were made by the co-authors:

Author Sarah-Christine Raßmuß:

- Cell cultivation of HEK293 and HEK-A1 cells
- Performing calcium measurements using aequorin assay for SM-related agents (SM, Q, and T)
- Cell viability assay using XTT for SM-related agents (SM, Q, and T)

Author Marc-Michael Blum:

- Synthesis of Q and T

Author Horst Thiermann:

- Scientific advice

Author Harald John:

- Scientific advice
- Preparation of the manuscript

Author Dirk Steinritz:

- Project supervision and scientific advice
- Data analysis using R and data discussion
- Preparation of the manuscript and manuscript revision

2 Introductory Summary

2.1 Sulfur mustard

The chemical warfare agent sulfur mustard (CAS-No. 505-60-2, bis(2-chloroethyl) sulfide, SM, chemical structure shown in Figure 2.1 (A)) was initially employed during World War I (WWI) and led to 1.3 million wounded soldiers (Wattana & Bey, 2009) as SM exposure for few minutes caused cutaneous, respiratory, and ocular damage (Ghabili et al., 2011; Razavi et al., 2012). After WWI, it has been documented that SM has been repeatedly utilized (Balali-Mood & Hefazi, 2005; Paromov et al., 2007; Ghabili et al., 2011; Rose et al., 2018). Although the Organization for the Prohibition of Chemical Weapons (OPCW), which is responsible for enforcing the Chemical Weapons Convention (CWC), forbids the use of SM, the Islamic State's deployment of SM in Syria in 2013 has brought back concerns about chemical attacks (John et al., 2019; Sezigen et al., 2019). Furthermore, the lack of an effective antidote, as well as the simplicity with which SM may be synthesized, has accelerated SM research (Smith et al., 1995).

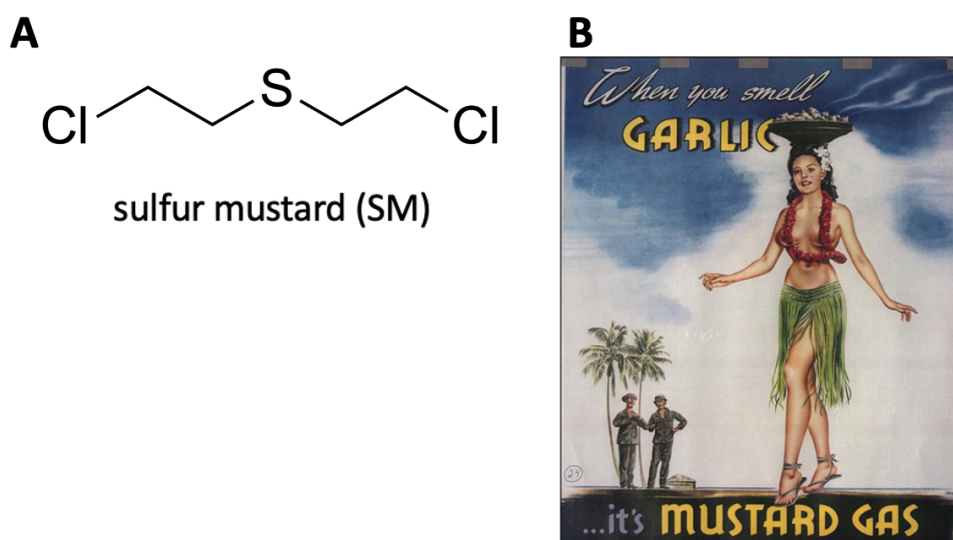


Figure 2.1: (A) Chemical structure of sulfur mustard (bis(2-chloroethyl) sulfide, SM) containing two reactive side chains with chlorine atoms at each end. (B) SM warning during World War II (WWII). Posters were intended to alert soldiers and locals about the distinct odor of technical SM (Phillips, 2005).

While the Belgian scientist César-Mansuete Despretz was the first to synthesize an oily liquid in 1822, Niemann and Guthrie described the strong mustard and garlic

odor of SM as well as the blistering action on the skin shortly after (Kehe & Szinicz, 2005; Paromov et al., 2007; Wattana & Bey, 2009; Ghabili et al., 2011; Razavi et al., 2013). Despite being a liquid at ambient temperature, SM is also known as mustard gas due to its unique odor, which was used to alert people and troops (Fig. 2.1 (B)) (Young & Bast, 2009). Lommel and Steinkopf, two chemists from the laboratory of Fritz Haber in Berlin, explored the compound's military use and developed a method for the large-scale synthesis of SM. The first initials of the two chemists were used to create the acronym „S-Lost“. Haber then recommended utilizing SM on the battlefield, which Germany did against French soldiers during WWI in Ypres, Belgium. As a result, SM is also known as Yperite (Rice, 2003; Paromov et al., 2007; Ghabili et al., 2011; Graham & Schoneboom, 2013). Other names include the NATO code HD, which stands for „Hun Stuff Distilled“ (Kehe & Szinicz, 2005; Kehe et al., 2008; Ghabili et al., 2011).

2.1.1 Clinical picture of SM poisoning

SM quickly penetrates the skin and has vesicant and blistering properties. It also targets the eyes and the respiratory system. Thus, these three major organ systems are typically affected by SM (Kehe et al., 2008; Firooz et al., 2011; Ghabili et al., 2011; Rose et al., 2018). After skin contact, at first no pain or any symptoms occur, however, several hours after exposure typical symptoms include reddening of the skin, blister formation and wound healing disorder (Kehe & Szinicz, 2005; Ghabili et al., 2011; Schmidt et al., 2018). Additionally, hyper- and hypopigmentation have been described (Firooz et al., 2011; Müller-Dott et al., 2020). After respiratory tract exposure, symptoms such as irritation of nasal mucosa were reported. SM mostly affects the upper respiratory tract; but, due to its poor water solubility and at larger dosages, it can reach lower lung compartments (Kehe & Szinicz, 2005; Razavi et al., 2012). The lung epithelium, like the epidermis, can detach. Cell debris interacts with exudative fluids, resulting in the formation of pseudo membranes and tracheal or other airway blockage, which can be deadly, whereas cutaneous exposure to SM is seldom fatal (Anderson et al., 1996; Kehe & Szinicz, 2005; Veress et al., 2010; Graham & Schoneboom, 2013; Rose et al., 2018). Unfortunately, even more than 100 years after its first use in WWI, there is no specific therapy for SM exposure (Evison, 2002; Bobb et al., 2005; Kehe et al., 2008; Rodgers & Condurache, 2010; Jenner & Graham, 2013; Rose et al., 2018).

2.1.2 Molecular toxicology

SM is a chemical that is extremely reactive. It has the ability to alkylate biomolecules such as DNA, RNA, proteins, and lipid membranes. It is cytotoxic, genotoxic, mutagenic and a dose-related carcinogen according to the International Agency for Research on Cancer (IARC) (Papirmeister et al., 1991; Firooz et al., 2011). DNA damage caused by alkylation is thought to be the major mechanism of SM toxicity (Kehe et al., 2009). As seen in Figure 2.2, SM toxicity is depending on the spontaneous formation of sulfonium ions in aqueous environments. These are formed as a result of first order intramolecular cyclization of the 2-chloroethyl

side chains. The highly reactive carbonium ion can then immediately react with electron-rich structures such as amines, purine and pyrimidine bases (Ludlum et al., 1994; Shakarjian et al., 2009). Alkylation of the purine bases guanine and adenine can be detected directly after exposure (Rose et al., 2018). Mono- as well as bifunctional SM adducts can be formed. The N7 of guanine is alkylated in 61 % of all alkylation resulting in 7-(2-hydroxyethylthioethyl) guanine (N7-HETE-G). Additionally, the formation of DNA crosslinks slows down DNA replication and can cause DNA double strand breaks, which together can trigger apoptosis (Batal et al., 2013). Alkylation of other biomolecules such as cysteine residues in proteins like albumin, creatine kinase, α 1-antitrypsin and transthyretin by adding a HETE moiety has been described (Lüling et al., 2018, 2021; John et al., 2019; Schmeißer et al., 2022). Recently, Stenger *et al.* (2015) demonstrated activation of the human transient receptor potential ankyrin 1 channel (hTRPA1) by SM or its monofunctional analogue 2-chloroethyl ethyl sulfide (CEES). However, it is yet unclear how SM activates hTRPA1.

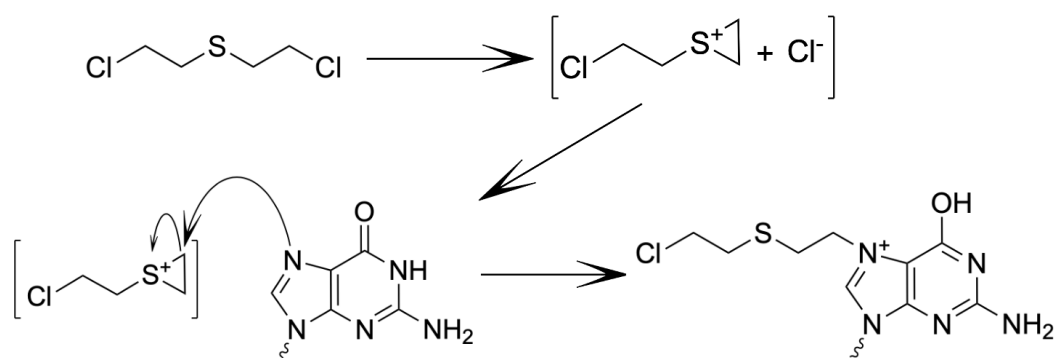


Figure 2.2: Mechanism of SM induced alkylation at the N7 position of guanine. Chloroethyl side chain undergoes intramolecular cyclization forming a sulfonium ring. The intermediate reacts with the N7 of guanine forming the DNA adduct.

Although the primary mechanism of SM toxicity is thought to be the formation of DNA adducts (Masta et al., 1996; Batal et al., 2013; Mangerich et al., 2016), the characteristic garlic-like smell of SM points a direct interaction with the sensory system (Steinritz et al., 2018). Olfactory receptors and chemosensory ion channels like the TRP channel family are primarily involved in chemical sensing at the molecular level (Bessac & Jordt, 2010). A direct interaction of SM with the organism was also confirmed in cockroaches, which also respond promptly to alkylating agents, indicating that beyond DNA alkylation other cellular effects occur (Worek et al., 2016; Popp et al., 2018). These results suggest that a prompt interaction might also occur in humans after being exposed to SM (Popp et al., 2018).

2.2 Transient receptor potential channels

TRP channels have been studied for more than 30 years and have emerged to be one of the most important families of sensory transducers due to the fact that they may be triggered by a range of chemicals found in plants, food, cosmetics, and pollution (Cosens & Manning, 1969; Montell & Rubin, 1989; Bandell et al., 2004; H. Wang & Woolf, 2005; Andersson et al., 2008). They have therefore received increasing interest as a potential therapeutic target for pharmaceuticals as well as harmful substances (Hinman et al., 2006; Macpherson et al., 2007; Nilius & Flockerzi, 2014; Paulsen et al., 2015). The TRP family is a heterogenous group of ion channels which are composed of seven subgroups as shown in Figure 2.3: no-mechanoreceptor potential channels (NOMPC = TRPN), polycystin TRP channels (TRPP), canonical TRP channels (TRPC), melastatin TRP channels (TRPM), mucolipin TRP channels (TRPML), vanilloid TRP channels (TRPV), and TRPA channels named after its ankyrin repeats at the N-terminus (Clapham, 2003; Pedersen et al., 2005).

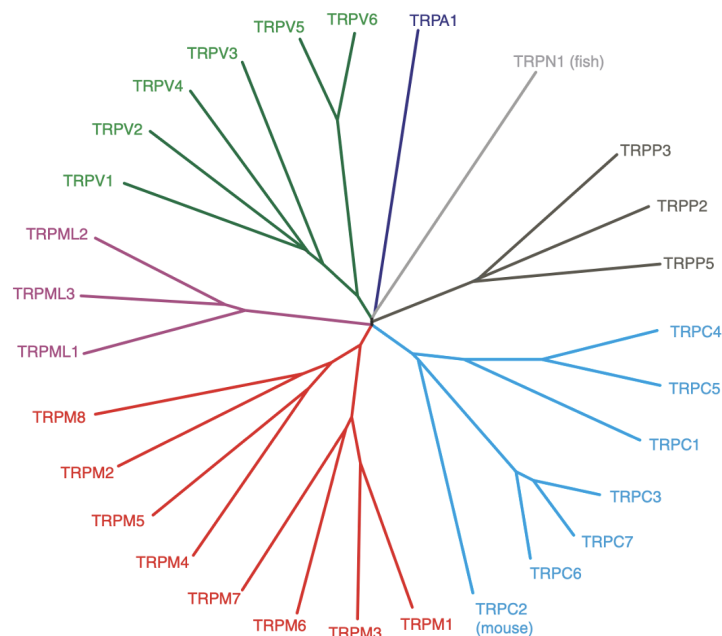


Figure 2.3: Phylogenetic tree of TRP family. The phylogenetic tree shows the seven subgroups of the TRP family: no-mechanoreceptor potential channels (NOMPC = TRPN), polycystin TRP channels (TRPP), canonical TRP channels (TRPC), melastatin TRP channels (TRPM), mucolipin TRP channels (TRPML), vanilloid TRP channels (TRPV), and TRP ankyrin 1 channels (TRPA1) (Nilius & Owsianik, 2013).

As seen in Figure 2.4, TRP channels are typically non-selective cation channels made up of six transmembrane domains with an intracellular N- and C-terminus and a pore loop between domains five and six (Story et al., 2003; Nilius et al., 2012; Paulsen et al., 2015). Depending on the kind of TRP channel, heteromeric and homomeric tetramers have been identified (Cheng et al., 2010; Nilius & Flockerzi, 2014; Paulsen

et al., 2015). Phosphorylation, ubiquitination, and protein-protein interactions, such as G protein receptor coupling or ligand gating, have all been reported (Nilius et al., 2012; Nilius & Flockerzi, 2014; Hall et al., 2018).

Several of these channels transmit a wide range of sensations, including mechanosensation, pain, sensitivity to warmth or cold, various flavors, pressure, and vision (Hardie & Minke, 1992; Bautista et al., 2007; Bessac & Jordt, 2008, 2010; Ishimaru & Matsunami, 2009). Certain TRP channels are for example triggered by the garlic component allicin (TRPA1, TRPV1) (Bautista et al., 2005; Macpherson et al., 2005), capsaicin (TRPV1) (Caterina et al., 1997), or the wasabi ingredient allyl isothiocyanate (AITC) (TRPA1) (Bandell et al., 2004; Jordt et al., 2004; Hinman et al., 2006).

2.2.1 Transient receptor potential ankyrin 1 channels

The TRPA1 channel is the only mammalian member in the TRPA group. It is named after the ankyrin repeats found near the N-terminus as shown in Figure 2.4. These channels are expressed by primary afferent nociceptors but are also found in non-neuronal tissues including skin, skeletal muscle, lung and digestive organs (Mukhopadhyay et al., 2011; Meents et al., 2019). Their main function is to act as a mechanical and chemical stress sensor for environmental irritants which mediates pain and inflammation (Jordt et al., 2004; Bautista et al., 2006). TRPA1 channels are triggered by several stimuli such as temperature (Bandell et al., 2004; Andersson et al., 2008), mechanical disturbances (Kwan et al., 2006), hypoxic water, reactive oxygen species (Koivisto & Pertovaara, 2015), endogenous compounds linked with tissue injury (Bautista et al., 2013) and several chemicals. Different substances have been identified to activate the TRPA1 channel such as icilin (Story et al., 2003), isothiocyanates (e.g. AITC) (Bandell et al., 2004; Jordt et al., 2004; Hinman et al., 2006), garlic (Bautista et al., 2005; Macpherson et al., 2005), tetrahydrocannabinol (THC) (Jordt et al., 2004), cinnamon (cinnamaldehyde) (Bandell et al., 2004; Macpherson et al., 2006) and bradykinin (Bandell et al., 2004; Bautista et al., 2006). In addition, TRPA1 mediates the effect of environmental irritants such as acrolein which is present in e.g. vehicle exhaust and tobacco products (Bautista et al., 2006). As mentioned above, Stenger *et al.* (2015) demonstrated hTRPA1 activation by SM and CEES.

Most activators are electrophiles that bind preferably to cysteines in the ankyrin region which includes Cys⁶²¹, Cys⁶⁴¹ and Cys⁶⁶⁵ and in addition two lysines at position 620 and 710 (Lys⁶²⁰, Lys⁷¹⁰) (Hinman et al., 2006; Bahia et al., 2016). Furthermore, the structure of TRPA1 is dynamically mediated by electrophilic activation and contains a network of disulfide bonds which potentially plays a role in activation and desensitization of the channel (Hinman et al., 2006; Macpherson et al., 2007; Takahashi et al., 2008; Fischer et al., 2010; L. Wang et al., 2012; Paulsen et al., 2015; Bahia et al., 2016; Meents et al., 2019; Suo et al., 2019; Talavera et al., 2020). Covalent alteration of cysteine residues by reactive intermediates, as previously ex-

plored by Macpherson *et al.* (2007), might be responsible for the observed activation of TRPA1 (Hinman *et al.*, 2006; Macpherson *et al.*, 2007; Sadofsky *et al.*, 2011; Bahia *et al.*, 2016). It is unknown if SM targets the same amino acids for channel activation.

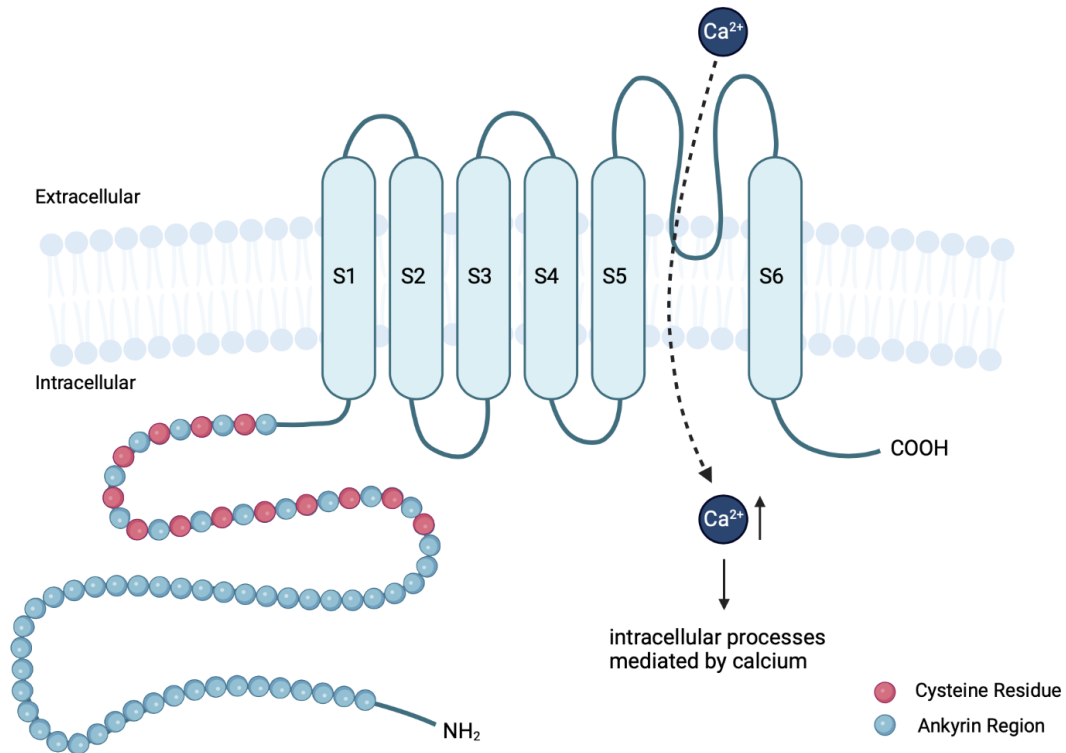


Figure 2.4: Structure of the hTRPA1 channel. The ion channel subunits' transmembrane structure is depicted. TRPA1 is made up of six transmembrane domains and a pore region between S5 and S6. The ankyrin region's cysteine residues are highlighted in red (Structure of hTRPA1 created with BioRender.com).

2.3 SM-related alkylating agents

Besides SM, there are structurally related alkylating chemicals such as O-mustard (T) and sesquimustard (Q) (Fig. 2.5) which might also be able to activate the hTRPA1 channel. However, neither substance has received considerable scientific attention. T and Q are far more toxic than the original SM. T was first synthesized in the 1930s to improve the persistence of SM. It is 3.5 times more vesicant than SM. In WWII, it was combined with SM to keep it liquid at lower temperatures during the winter. This mixture was called „winter lost“ (Watson & Griffin, 1992). Bennett and Whincop synthesized Q for the first time in 1921 (Bennett & Whincop, 1921). Blister development is five times greater than in SM, which might be attributed to increased alkylation (Gasson *et al.*, 1948; Blum *et al.*, 2020).

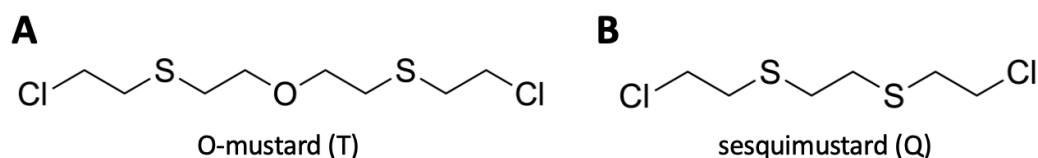


Figure 2.5: Chemical structure of (A) O-mustard (bis(2-(2-chloroethylsulfanyl)ethyl) ether, T) and (B) sesquimustard (1,2-bis(2-chloroethylsulfanyl) ethane, Q). Similar to SM, T and Q are characterized by the presence of two reactive side chains with chlorine atoms at both ends.

2.3.1 Nitrogen mustard

Nitrogen mustards were first designed as chemical warfare weapons in the 1920s and 1930s. They were never utilized as chemical agents, but were the first compounds used in chemotherapy (Gilman, 1963). Similar to SM, they have a severe irritating impact that is harmful to the skin, eyes, and respiratory system. Nitrogen mustards can quickly infiltrate the body's cells and harm the immune system and bone marrow. HN1 (bis(2-chloro-ethyl)ethylamine), HN2 (bis(2-chloroethyl)methylamine) and HN3 (tris(2-chloroethyl)amine) are categorized as alkylating agents (Fig. 2.6) (Mattes et al., 1986). HN1 was created to eradicate warts. HN2 was originally intended as a military agent, but it was eventually utilized to cure cancer. HN3 was also used in chemotherapy, especially to treat Hodgkin's disease (DeVita & Chu, 2008; Mangerich & Esser, 2014; Singh et al., 2018). Due to the high toxicity of the mentioned nitrogen mustards, they are no longer utilized in chemotherapy. Derivatives of the nitrogen mustards, e.g. bendamustine, were introduced as chemotherapeutic agent and have resurfaced as a possible therapy option due to their lower toxicity (Cheson & Rummel, 2009).

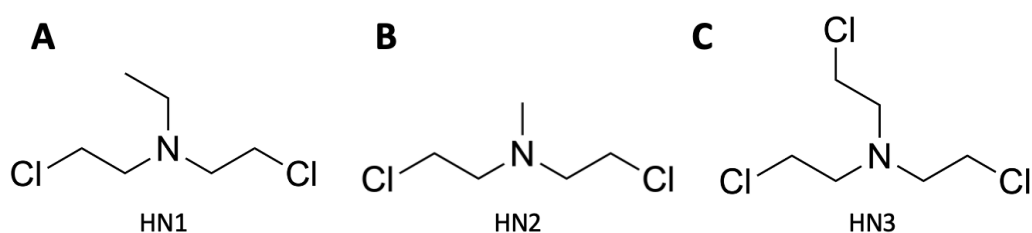


Figure 2.6: Chemical structure of nitrogen mustards: (A) HN1 (bis(2-chloroethyl) ethylamine), (B) HN2 (bis(2-chloroethyl)methylamine) and (C) HN3 (tris(2-chloroethyl)amine) which are tertiary amines with vesicant activity (National Defense Research Committee, 1946).

2.3.2 Chemotherapeutic agents

Nitrogen mustard-based chemotherapeutic compounds exhibiting a lower toxicity than H1, HN2 and HN3 include for example bendamustine, cyclophosphamide and

ifosfamide (Fig. 2.7). Bendamustine is used to treat chronic lymphocytic leukemia and multiple myeloma. It also functions as an alkylating agent, resulting in intra- and inter-strand DNA cross-links (Cheson & Rummel, 2009; Chang & Kahl, 2012; Gentile et al., 2015; Lehmann & Wennerberg, 2021). Cyclophosphamide and ifosfamide are used to treat various forms of cancer and are non-toxic prodrugs. Thus, they need to be enzymatically transformed into its pharmacologically active form by cytochrome P450 (mainly CYP2B6 and CYP3A4) (Zhang et al., 2008). All three chemotherapeutic drugs show side effects such as exhaustion, nausea, and vomiting, as well as skin irritations and coughing or hoarseness. Burning, numbness, and unpleasant feelings have also been reported (Zhang et al., 2008; Cheson & Rummel, 2009).

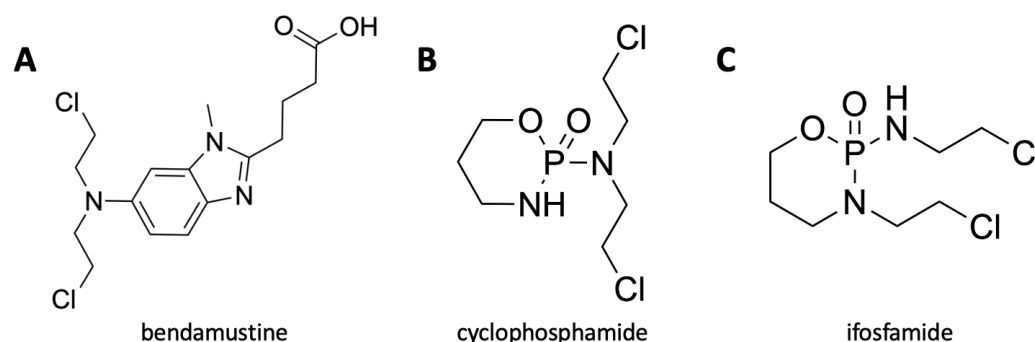


Figure 2.7: Chemical structure of chemotherapeutic compounds: (A) bendamustine, (B) cyclophosphamide and (C) ifosfamide. These are nitrogen mustard-based chemotherapeutics with structural similarities to alkylating agents and purine analogs (Cheson & Rummel, 2009).

2.4 Identification of SM-induced hTRPA1 channel modifications (Paper I)

The hTRPA1 channel is a target for various reactive, electrophilic chemicals and is activated through covalent modification of cysteine residues mainly in the ankyrin region (Hinman et al., 2006; Macpherson et al., 2007; L. Wang et al., 2012; Bahia et al., 2016). The chemical warfare agent SM was shown to also activate hTRPA1 by a so far unknown mechanism (Stenger et al., 2015). Since SM is a highly reactive compound, it is able to react with a variety of biomolecules such as amino acid residues e.g., cysteines (Lüling et al., 2018, 2021; John et al., 2019; Schmeißer et al., 2022). It was therefore postulated that SM would also react with hTRPA1 by modification of cysteine residues in the ankyrin region.

In Paper I, SM-induced hTRPA1 channel modifications were therefore investigated. A hTRPA1 overexpressing cell line was generated using HEK293 cells. A His-tagged hTRPA1 plasmid was used for a facilitated isolation and purification of the hTRPA1 channel. Verification of the successful expression and proper functionality of the

channel was performed by Western blot experiments and calcium measurements using Fura-2, respectively. To analyze the postulated modifications, native and SM-treated hTRPA1 channel was isolated from overexpressing HEK293 cells and purified using immunomagnetic separation (IMS). For IMS, an anti-hTRPA1 and an anti-His-tag antibody were used. Possibly alkylated peptides were subjected to analytical examination utilizing the purified hTRPA1 channel, which was proteolyzed with trypsin. Alkylation of eligible amino acid residues after SM exposure was analyzed using micro liquid chromatography-electrospray ionization high-resolution tandem-mass spectrometry (μ LC-ESI MS/HR MS) analysis.

μ LC-ESI MS/HR MS was performed and revealed a sequence coverage of 40 % for both extraction procedures (anti-hTRPA1 antibody and anti-His-tag antibody) and enabled protein identification with a Mascot score of about 800. These results were obtained from lysates of different cell passages showing the same peptide pattern after proteolysis and were comparable to results found by Macpherson *et al.* (2007). Initial SM incubations were performed using purified hTRPA1 from cell lysates. Up to 10 mM of SM was added to whole cell lysates to induce optimal adduct formation. After SM incubation, alkylation of hTRPA1 was detected at Cys⁴⁶² and Cys⁶⁶⁵. In addition, SM-induced modifications were observed at the Asp³³⁹ and the Glu³⁴¹ residue. To confirm the detected modifications, hTRPA1 overexpressing HEK293 cells were exposed to SM concentrations ranging from 50 μ M to 1000 μ M. Concentrations as low as 250 μ M SM were able to alkylate Cys⁶⁶⁵ and Cys⁴⁶². It was therefore shown that hTRPA1 is alkylated by SM at cysteine as well as aspartic and glutamic acid residues in the ankyrin repeat sequence.

In the presented Paper I, the effective separation of the hTRPA1 channel from overexpressing HEK293 cells was demonstrated using IMS. Furthermore, SM exposure *in vitro* revealed hTRPA1 modifications of Cys⁴⁶² and Cys⁶⁶⁵, Asp³³⁹ and Glu³⁴¹ residues. As already shown by other agonists such as AITC and also iodoacetamide (IAA) (Hinman *et al.*, 2006; Macpherson *et al.*, 2007), especially Cys⁶⁶⁵ that is involved in hTRPA1 channel activation is also alkylated by SM. Further research will focus on determination of additional sites of alkylation. Since hTRPA1 might also be a target for other chemical warfare agents, formation of corresponding adducts is expected and can be identified by the presented μ LC-ESI MS/HR MS procedure.

2.5 hTRPA1 activation potential of SM-related alkylating agents (Paper II)

The hTRPA1 is considered as the most promiscuous TRP channel because it is activated by a variety of chemicals found in many plants, food and pollutants. Although SM is an agonist of the hTRPA1 channel (Stenger *et al.*, 2015), this finding has been controversially discussed since exposure to SM does not lead to acute pain as described for other hTRPA1 agonists (Story *et al.*, 2003; Nilius &

Flockerzi, 2014; Paulsen et al., 2015). Thus, the focus of Paper II was to verify hTRPA1 activation by SM as well as to investigate the activation potential of structurally related alkylating agents. Examples of structural analogs of SM include T and Q, nitrogen mustards HN1, HN2, and HN3, as well as the chemotherapeutic drugs bendamustine, cyclophosphamide, and ifosfamide. T and Q have not been extensively studied, however, both chemicals are more toxic than SM. Nitrogen mustards were initially developed as chemical warfare agents but never were utilized in that manner. They were instead used as the first chemotherapeutic drugs. Because of their high toxicity, a number of chemically similar chemotherapeutics with lower toxicity, including bendamustine, cyclophosphamide, and ifosfamide, were developed. We assessed the hTRPA1 activation capacity of these alkylating compounds.

Additionally, the effect of hTRPA1 activation on cytotoxicity was studied because an immediate interaction with the organism in addition to DNA alkylation has already been shown (Worek et al., 2016; Popp et al., 2018; Steinritz et al., 2018). This is supported by the characteristic mustard-like odor of SM and hTRPA1 activation by mustard-like substances such as SM (Stenger et al., 2015). A direct interaction of SM with the organism was further confirmed *in vivo* using cockroaches (Popp et al., 2018). Therefore, Paper II also focuses on the correlation of hTRPA1 activation and cytotoxicity of the different alkylating compounds.

To validate hTRPA1 activation by SM and further explore the activation potential of the structurally similar compounds HEK293-wildtype (HEK-wt) cells and HEK293 cells stably expressing hTRPA1 channel (HEK-A1) were utilized. According to research by Stenger *et al.* (2015), Fura-2 measurements are considered as unsuitable for detecting changes in intracellular calcium concentration ($[Ca^{2+}]_i$) in the presence of alkylating compounds due to an interaction between the fluorescent dye Fura-2 and the alkylating agents. Thus, the calcium-sensitive photoprotein aequorin was used. XTT viability assays were used to determine lethal concentration, resulting in a 50 % decreased *in vitro* cell viability (LC_{50}) after exposure to the alkylating agents. The hTRPA1 specific antagonist AP18 was used to determine if cytotoxicity could be reduced or even inhibited after exposure to SM-related agents, which would suggest that hTRPA1 plays a significant role in SM-mediated cytotoxicity. In addition, a correlation between hTRPA1 activation and cytotoxicity was determined.

In Paper II, it was verified that the hTRPA1 channel was activated by SM. Aequorin measurements furthermore demonstrated that almost all tested structurally SM-related compounds activated the hTRPA1 with the exception for the two prodrugs cyclophosphamide and ifosfamide. The XTT assay demonstrated that SM, T and Q are generally more toxic than nitrogen mustards. HN2 showed comparable toxicity to SM, which was also shown by Mangerich *et al.* (2016). The chemotherapeutic drugs showed the lowest toxicity. The activation potential as well as the cytotoxicity of the alkylating compounds was normalized and a correlation was found: Compounds with a high activation potential also demonstrated a high toxicity, while low activation potential was correlated to a lower toxicity. This was furthermore confirmed by the

activation-cytotoxicity ratio where a relationship was observed for all compounds except for HN2. Since the hTRPA1 specific antagonist AP18 had no discernible impact on cytotoxicity, it can be concluded that hTRPA1 does not control cytotoxicity in the first line.

2.6 Concluding remarks

Activation of hTRPA1 by SM has been controversially discussed since acute pain is not a typical symptom after SM exposure. hTRPA1 activation by SM was therefore successfully verified. In addition, it was shown that also the SM-related agents Q and T, the nitrogen mustards HN1, HN2, and HN3, and the nitrogen mustard-derived chemotherapeutic compound bendamustine consistently activated hTRPA1. Alkylating chemicals with lower activation potential were found to be less cytotoxic than SM, and vice versa, indicating a connection between hTRPA1 activation and cytotoxicity. However, hTRPA1 inhibition using the specific antagonist AP18 had no effect on LC₅₀, demonstrating that hTRPA1 activation might not mainly be involved in cytotoxicity by the different alkylating agents. Therefore, it was concluded that the activation of hTRPA1 by various alkylating agents merely reflects the overall chemical reactivity. Future studies should focus on examining cellular effects beyond cytotoxicity that result from hTRPA1 activation by alkylating substances.

In addition, it was proven for the first time that SM alkylates Asp³³⁹ and Glu³⁴¹ as well as at least two cysteine residues (Cys⁴⁶² and Cys⁶⁶⁵) in hTRPA1. Similar adducts are anticipated and might be found using the analytical strategy outlined in Paper I, as hTRPA1 may be a target for additional chemical warfare agents structurally related to SM, such as Q (Blum et al., 2020; Hemme et al., 2021) or T. Other TRP channels may also use this method to identify potential binding sites. Future research will focus on mutation studies to evaluate the significance of the detected modified amino acids during hTRPA1 activation. In this scenario, the altered glutamic or aspartic acid will be changed to e.g., alanine, and calcium measurements will be used to ascertain the function of the mutated amino acid. This will give more knowledge about how hTRPA1 is activated as well as about certain amino acid residues that might be directly involved in hTRPA1 activation.

3 Paper I

Archives of Toxicology (2023) 97:429–439
<https://doi.org/10.1007/s00204-022-03411-1>

MOLECULAR TOXICOLOGY



Isolation of human TRPA1 channel from transfected HEK293 cells and identification of alkylation sites after sulfur mustard exposure

Katharina Müller-Dott^{1,2} · Horst Thiermann¹ · Harald John¹ · Dirk Steinritz¹

Received: 5 August 2022 / Accepted: 3 November 2022 / Published online: 12 November 2022
 © The Author(s) 2022

Abstract

Transient receptor potential (TRP) channels are important in the sensing of pain and other stimuli. They may be triggered by electrophilic agonists after covalent modification of certain cysteine residues. Sulfur mustard (SM) is a banned chemical warfare agent and its reactivity is also based on an electrophilic intermediate. The activation of human TRP ankyrin 1 (hTRPA1) channels by SM has already been documented, however, the mechanism of action is not known in detail. The aim of this work was to purify hTRPA1 channel from overexpressing HEK293 cells for identification of SM-induced alkylation sites. To confirm hTRPA1 isolation, Western blot analysis was performed showing a characteristic double band at 125 kDa. Immunomagnetic separation was carried out using either an anti-His-tag or an anti-hTRPA1 antibody to isolate hTRPA1 from lysates of transfected HEK293 cells. The identity of the channel was confirmed by micro liquid chromatography-electrospray ionization high-resolution tandem-mass spectrometry. Following SM exposure, hTRPA1 channel modifications were found at Cys⁴⁶² and Cys⁶⁶⁵, as well as at Asp³³⁹ and Glu³⁴¹ described herein for the first time. Since Cys⁶⁶⁵ is a well-known target of hTRPA1 agonists and is involved in hTRPA1 activation, SM-induced modifications of cysteine, as well as aspartic acid and glutamic acid residues may play a role in hTRPA1 activation. Considering hTRPA1 as a target of other SM-related chemical warfare agents, analogous adducts may be predicted and identified applying the analytical approach described herein.

Keywords Agonists of hTRPA1 · Amino acid modifications · HETE · Hydroxyethylthioethyl-moiety · Immunomagnetic separation · μ LC-ESI MS/HR MS

Abbreviations

AITC	Allyl isothiocyanate
[Ca ²⁺] _i	Intracellular calcium concentration
CBB	Coomassie brilliant blue
CEES	2-Chloroethyl ethyl sulfide
CWC	Chemical Weapons Convention
d ₃ -atr	Triple deuterated atropine
DMEM	Dulbecco's modified eagle medium

DMP	Dimethyl-pimelimidate-dihydrochloride
DTT	1,4-Dithiothreitol
ESI	Electrospray ionization
FCS	Fetal calf serum
fwhm	Full-width at half-maximum
HEK-A1	HEK293 cells transfected and overexpressing His-tagged hTRPA1
HEK-wt	Human embryonic kidney 293 wildtype
HETE	Hydroxyethylthioethyl
hTRPA1	Human transient receptor potential ankyrin 1
IAA	Iodoacetamide
IMAC	Immobilized metal affinity chromatography
IMS	Immunomagnetic separation
MS/HR MS	High-resolution tandem-mass spectrometry
OPCW	Organisation for the Prohibition of Chemical Weapons
P/S	Penicillin/streptomycin solution
PBS	Phosphate-buffered saline
PRM	Parallel reaction monitoring
PVDF	Polyvinylidene difluoride

✉ Dirk Steinritz
dirksteinritz@bundeswehr.org

Katharina Müller-Dott
k.muellerdott@campus.lmu.de

Horst Thiermann
horstthiermann@bundeswehr.org

Harald John
haraldjohn@bundeswehr.org

¹ Bundeswehr Institute of Pharmacology and Toxicology, Neuherbergstr. 11, 80937 Munich, Germany

² Walther-Straub-Institute of Pharmacology and Toxicology, Ludwig-Maximilians-University, 80336 Munich, Germany

RT	Room temperature
SDS-PAGE	Sodium dodecyl sulfate–polyacrylamide gel electrophoresis
SM	Sulfur mustard
TBS	Tris-buffered saline
TCEP-HCl	Tris(2-carboxyethyl) phosphine-hydrochloride
TEA	Triethanolamine
THC	Tetrahydrocannabinol
t_R	Retention time
TRP	Transient receptor potential
UF	Ultrafiltration
μ LC	Micro liquid chromatography

Introduction

Transient receptor potential (TRP) channels are cation permeable channels that are responsible for both mechanical- and chemo-sensation. They are composed of six transmembrane domains with a pore loop between domain five and six and intracellular N- and C-termini (Story et al. 2003; Nilius et al. 2012; Paulsen et al. 2015). The TRP ankyrin 1 (TRPA1) channel is the only mammalian member of the TRPA group. One characteristic of human TRPA1 (hTRPA1) channels is its ankyrin repeat sequence located at the N-terminus. hTRPA1 is expressed by primary afferent nociceptors but is also found in non-neuronal tissues and cells including skin, skeletal muscle, lung and digestive organs (Büch et al. 2013; Steinritz et al. 2018; Meents et al. 2019).

hTRPA1 channels are triggered by multiple stimuli such as temperature (Bandell et al. 2004; Andersson et al. 2008), mechanical stress (Kwan et al. 2006), hypoxia, reactive oxygen species (Koivisto and Pertovaara 2015), endogenous compounds linked with tissue injury (Bautista et al. 2013) and reactive chemicals. The latter group includes different substances such as ilicin (Story et al. 2003), isothiocyanates (e.g., allyl isothiocyanate, AITC) (Bandell et al. 2004; Jordt et al. 2004; Hinman et al. 2006), garlic (Bautista et al. 2005; Macpherson et al. 2005), tetrahydrocannabinol (THC) (Jordt et al. 2004), cinnamon (cinnamaldehyde) (Bandell et al. 2004; Macpherson et al. 2006) and acrolein (Bautista et al. 2006).

Most activators are electrophiles which were found to covalently modify certain amino acid residues in the ankyrin region including especially the cysteine residues Cys⁶²¹, Cys⁶⁴¹ and Cys⁶⁶⁵ and the lysine residues Lys⁶²⁰ and Lys⁷¹⁰ (Hinman et al. 2006; Bahia et al. 2016). In addition to cysteine modifications, disulfide bridges between cysteines also appear to play a role in hTRPA1 activation and therefore have an impact on the functional conformation of the channel (Hinman et al. 2006; Macpherson et al. 2007; Takahashi

et al. 2008; Fischer et al. 2010; Wang et al. 2012; Paulsen et al. 2015; Bahia et al. 2016; Meents et al. 2019; Suo et al. 2019; Talavera et al. 2020). Covalent modifications of the referred cysteine residues were shown to be involved in hTRPA1 activation (Hinman et al. 2006; Macpherson et al. 2007; Sadofsky et al. 2011; Bahia et al. 2016). Accordingly, Stenger et al. (2015) demonstrated hTRPA1 activation by the alkylating chemical warfare agent sulfur mustard (SM) and its analog 2-chloroethyl ethyl sulfide (CEES) but the relevant mechanism still remained unknown.

SM is a chemical warfare agent and was first used during World War I (Paromov et al. 2007; Ghabili et al. 2011; Rose et al. 2018). Even though the use of SM is prohibited under the Chemical Weapons Convention (CWC), which is supervised by the Organisation for the Prohibition of Chemical Weapons (OPCW), SM has been used for chemical attacks in Syria since 2013 by the terrorist group known as "Islamic State" (John et al. 2019; Sezigen et al. 2019). SM alkylates a wide range of biomolecules such as DNA, RNA and proteins (Ludlum et al. 1994; Shakarjian et al. 2009) thereby causing its toxic effects on skin, eyes and the respiratory system (Kehe et al. 2008; Ghabili et al. 2011; Rose et al. 2018; Müller-Dott et al. 2020). Since SM was already shown to alkylate cysteine residues by adding a hydroxyethylthioethyl (HETE) moiety to a multitude of proteins including albumin, creatine kinase, α 1-antitrypsin and transthyretin (Lüling et al. 2018, 2021; John et al. 2019; Schmeißer et al. 2022), it is conceivable that the alkylation of intracellular cysteine residues in the ankyrin region of hTRPA1 is also linked to ThRPA1 activation. This mechanism has already been demonstrated for other reactive compounds such as cinnamaldehyde, iodoacetamide (IAA) and AITC (Hinman et al. 2006; Macpherson et al. 2007; Paulsen et al. 2015). Whether SM as a highly electrophilic molecule alkylates amino acid residues in hTRPA1 was investigated in the present in vitro study providing insights into hTRPA1 activation by SM. Therefore, hTRPA1 overexpressing HEK293 cells were used and hTRPA1 expression was monitored by Western blot analysis. Immunomagnetic separation (IMS) was used to extract the channel, followed by micro liquid chromatography-electrospray ionization high-resolution tandem-mass spectrometry (μ LC-ESI MS/HR MS) to detect and identify SM-induced hTRPA1 channel alkylation sites.

Materials and methods

Chemicals

Dulbecco's modified eagle medium (DMEM), fetal calf serum (FCS), penicillin/streptomycin solution (P/S), 0.05% trypsin–EDTA and phosphate-buffered saline (PBS) were purchased from Gibco by Life Technologies (Karlsruhe,

Germany). PromoFectin transfection reagent was obtained from PromoCell GmbH (Heidelberg, Germany). The DNA construct pcDNA3.1V5-HisB_A123 and the HisPur™ Ni-NTA Spin Purification kit were purchased from ThermoFisher Scientific (Darmstadt, Germany). NuPAGE MES SDS running buffer (20x), NuPAGE transfer buffer (20x), 4–12% Bis-Tris gels, polyvinylidene difluoride (PVDF) membranes (0.2 µm pore size) and Dynabeads protein G were purchased from Invitrogen by Life Technologies (Karlsruhe, Germany). Digitonin, tris(2-carboxyethyl)phosphine-hydrochloride (TCEP-HCl), NaCl, dimethyl-pimelimidate-dihydrochloride (DMP), Tween-20, IAA, NH₄HCO₃, acetonitrile, triethanolamine (TEA), NaN₃, trypsin and the corresponding trypsin reaction buffer from the Trypsin Profile IGD kit were obtained from Sigma-Aldrich (Steinheim, Germany). Tris, acetic acid, formic acid (FA ≥ 98%) and NaOCl solution for decontamination (12% Cl₂) were obtained from Carl Roth (Karlsruhe, Germany). Threefold deuterated atropine (d₃-atr) was from CDN Isotopes (Pointe Claire, Quebec, Canada). Chameleon Duo marker, 4× protein loading dye, intercept blocking buffer PBS and IR dye 800CW goat anti-mouse antibody were obtained from Licor (Bad Homburg, Germany). PhastGel Blue tablets were from GE Healthcare (Munich, Germany). Methanol was purchased from Merck (Darmstadt, Germany). 1,4-dithiothreitol (DTT) was purchased from Roche (Penzberg, Germany). The primary anit-hTRPA1 antibody ANKTM-1 (C-5) was obtained from Santa-Cruz Biotechnology (Heidelberg, Germany) and anti-6xHis antibody from abcam (Cambridge, UK). SM (purity and integrity were assessed in-house by nuclear magnetic resonance, NMR, spectroscopy) was made available by the German Ministry of Defense.

Cell culture

Human embryonic kidney wildtype (HEK-wt) cells, kindly donated by the Walther-Straub-Institute (Ludwig-Maximilians-University, Munich), were cultured in DMEM containing 10% (v/v) FCS and 1% (v/v) P/S in a humidified atmosphere at 37 °C, 5% (v/v) CO₂. For transfection, 4–5 × 10⁶ HEK-wt cells were seeded in a T175 flask. The next day, cells reached approx. 50% confluency and were transfected with pcDNA3.1V5-HisB_A123 using PromoFectin as follows: 10 µg of the DNA construct and 20 µL PromoFectin solution were each mixed with 1 mL DMEM without supplements. Afterwards, 1 mL PromoFectin solution was added to 1 mL DNA solution. The DNA-PromoFectin mix was incubated for 20 min at room temperature (RT). After removal of the cell culture medium, 2 mL of PromoFectin-DNA solution was added to the flask and filled up with 15 mL DMEM and incubated for 72 h. Transfected and thus hTRPA1 overexpressing HEK293 cells are further referred to as HEK-A1 cells.

Cell lysis

A digitonin lysis buffer was used according to Suo et al. (2019). It was freshly prepared and contained 20 mM Tris, adjusted to pH 8.0, 150 mM NaCl, 5 mM TCEP-HCl and 1% (w/v) digitonin. Protease inhibitors and DNase were not part of the lysis buffer. For cell lysis, 2 mL lysis buffer was added to each T175 flask. Cells were incubated at 4 °C for 1 h before being gently detached by scraping. The whole content was transferred to another Eppendorf tube. The mixture was further incubated on ice for 1 h and intermittently vortexed. The mixture was centrifuged at 14,000 RCF for 15 min and supernatants were stored at –80 °C.

Immobilized metal affinity chromatography

Cell lysates were purified using immobilized metal affinity chromatography (IMAC). The HisPur™ Ni-NTA spin purification kit, containing 1 mL columns, was used according to the manufacturer's protocol. In brief, the equilibration buffer contained 10 mM imidazole, the wash buffer 25 mM imidazole and the elution buffer 300 mM imidazole. All centrifugation steps were carried out at 700 RCF for 2 min at 4 °C. The column was equilibrated with 2 mL equilibration buffer at 4 °C for 1 h. The column was then centrifuged and the equilibration fraction was collected (F1). The column was washed four-times with 2 mL wash buffer each, centrifuged, and the wash fractions were collected in separate tubes (W1–W4). The His-tagged protein was eluted with two-times 1 mL elution buffer followed by centrifugation and collection of the eluates in separate vials (E1–E2). All samples were stored at –80 °C.

Sodium dodecyl sulfate–polyacrylamide gel electrophoresis

The loading buffer contained 60 µL of 4× loading dye mixed with 40 µL DTT (500 mM). HEK-A1 whole cell lysate (15 µL) was mixed with 8 µL of the loading buffer and loaded onto a 4–12% Bis-Tris gel. As a marker, 3 µL Chameleon Duo marker was used. Sodium dodecyl sulfate–polyacrylamide gel electrophoresis (SDS-PAGE) was run in ice-cold 1× NuPAGE MES SDS running buffer at constant voltage (200 V) for 40 min. The gel was either stained with Coomassie brilliant blue (CBB) or Western blotting was performed.

Staining of proteins

Proteins were visualized in gel using CBB. A CBB stock solution was composed of one PhastGel Blue tablet dissolved in 200 mL H₂O/methanol (40:60 v/v). For protein staining, CBB working solution was freshly prepared and

contained 6 mL methanol, 12 mL water, 2 mL acetic acid (100%) and 2.2 mL of CBB stock solution (0.2% w/v). After SDS-PAGE, the gel was carefully removed from the chamber and placed in the CBB solution. The gel was incubated for 45 min on a swirl plate until bands were noticeably stained. CBB solution was then removed and the gel was washed twice with water for 15 min followed by additional de-staining overnight in water. The next day, the protein double band considered as hTRPA1 channel was cut out and subjected to nano-LC MS/MS analysis for protein identification.

Western blot analysis

After SDS-PAGE, proteins were transferred from the gel onto a 0.2 µm PVDF membrane using the wet blotting technique. The membrane was activated in methanol for 30 s and blotting was performed using 1 × transfer buffer containing 20% (v/v) methanol at 25 V for 1 h. The membrane was then blocked in PBS blocking buffer for 1 h on an orbital shaker. As primary antibody solution, either 4 µg anti-hTRPA1 (ANKTM1 C-5) or 4 µg anti-His-tag (anti-6xHis) antibody was diluted in 4 mL 0.2% (v/v) Tween-20 in PBS blocking buffer and incubated overnight. The membrane was washed twice for 10 min with a washing buffer containing 0.1% (v/v) Tween-20 in PBS. The commercial solution of the secondary antibody (800CW goat anti-mouse antibody) was diluted 1:7500 in 11 mL 0.2% (v/v) Tween-20 in PBS blocking buffer and the membrane was incubated for 1 h. Afterwards, the membrane was washed twice as described above. Images were recorded with an Odyssey[®] DLx imaging system using the software Image studio 5.2 (Licor, Bad Homburg, Germany).

Measurement of the intracellular calcium concentration with Fura-2 AM

Fura-2 AM was used according to the manufacturer's instructions. A stock solution (1 mM) was prepared. Cells were harvested in the same manner as described before (see section: cell culture) and counted using a CASY Cell Counter and Analyzer TT. Approximately 2×10^6 cells/mL was used and the cell suspension was centrifuged for 5 min at 500 RCF. Afterwards, cells were loaded with Fura-2 AM (c_{final} 2 µM) and incubated for 1 h at 37 °C. The cells were then centrifuged (500 RCF, 3 min), rinsed with DMEM, and centrifuged again (500 RCF, 3 min). Cells were resuspended in DMEM before plating 190 µL of cell suspension into each well of a black 96-well plate. In the case of AP18 pre-treatment, cells were resuspended in DMEM with AP18 (final concentrations: 5 µM, 10 µM and 25 µM). The photometer was adjusted to 37.0 °C. The injector was then primed with the before prepared AITC solution (1 mL). DMEM was used as negative control. The excitation

wavelengths for Ca²⁺-bound and Ca²⁺-free fura-2 AM were set to 340 nm and 380 nm, respectively. The wavelength of maximum emission in both forms was 510 nm. The ratios 510 nm/340 nm and 510 nm/380 nm are proportional to the quantity of Ca²⁺ present intracellularly. After recording the baseline for 20 cycles (approx. 40 s), 10 µL of the agonist was injected and changes in fluorescence were measured for 150 s. A 340 nm to 380 nm ratio was determined to assess changes in intracellular calcium levels ($[Ca^{2+}]_i$).

Immunomagnetic separation

Preparing IMS of hTRPA1, commercially available Dynabead protein G slurry (1 mL) was transferred into a 5 mL reaction vial. Beads were fixed using a magnet and the supernatant was discarded. Beads were washed three-times with 2 mL PBST (0.05% v/v Tween-20 in PBS, pH 7.4). Afterwards, 4 mL PBST was added to the beads and either 200 µL of anti-His-tag antibody (1 mg/mL) or 1 mL of anti-hTRPA1 antibody solution (200 µg/mL) was added for immobilization. The mixture was incubated on a rolling shaker for 15 min at RT. The supernatant was removed, and beads were washed twice with 200 mM TEA (0.025% w/v NaN₃, pH 7.8). Afterwards, beads were incubated with a freshly prepared DMP solution (2 mL, 5.4 mg/mL in TEA solution) on a rolling shaker for 30 min at RT. The supernatant was again removed and 2 mL Tris-buffered saline (TBS) (0.9% w/v NaCl in 20 mM Tris, pH 7.6) was added. The mixture was incubated for 15 min at RT on a rolling shaker. The beads were washed twice with 1 mL PBST. Finally, 950 µL PBST was added to the labeled beads which were stored at 4 °C.

The labeled beads slurry (50 µL) was transferred into a 1.5 mL reaction vial. Beads were fixed with a magnet and the supernatant was discarded. Afterwards, 200 µL cell lysate was added and the mixture was incubated for 2 h at 20 °C. The supernatant was removed, and beads with the bound protein were washed twice with 500 µL PBST, each. Next, 200 µL PBS and 8 µL DTT (20 mg/mL in water) were added to the vial. Samples were incubated for 30 min at 47 °C. Afterwards, 16 µL IAA (40 mg/mL in water) was added following a 30 min incubation at RT in the dark. The protein labeled beads were washed three-times with 250 µL NH₄HCO₃ (4 mg/mL) and the supernatant was removed. For proteolysis, 25 µL trypsin solution (20 µg/mL in trypsin solubilization reagent) and 50 µL trypsin reaction buffer (40 mM NH₄HCO₃ in 9% v/v acetonitrile) was added and incubated overnight at 37 °C under gentle shaking. Afterwards, the supernatant was transferred into a 10 kDa ultrafiltration (UF) device for UF (10,000 RCF, 10 min, 15 °C). The retentate was washed twice by UF with 50 µL d₃-atp solution (3 ng/mL in 0.5% v/v FA). The filtrates were centrifuged

and subjected to μ LC-ESI MS/HR MS analysis or stored at $-20\text{ }^{\circ}\text{C}$.

Exposure of extracted hTRPA1 protein to SM

HEK-A1 cell lysate (200 μL) was incubated with antibody-labeled beads for 2 h for extraction of hTRPA1 by IMS. Beads with bound hTRPA1 were mixed with 195 μL PBS and incubated (1 h, RT) with 5 μL ethanolic SM solution (diluted in ethanol yielding final concentrations of 1 to 10 mM SM). Blanks had a final concentration of 2.5% (v/v) ethanol only. The liquid layer was discarded and IMS was performed as described above (see section: Immunomagnetic separation).

Exposure of cell culture to SM

HEK-A1 cells were exposed to SM as follows: cell culture medium was removed from the T175 flask 72 h after transfection and 6 mL of an ethanolic SM solution diluted in DMEM (final concentrations: 50 μM , 100 μM , 200 μM , 250 μM , 500 μM and 1000 μM) was added to each flask. As a negative control (blank), 2.5% (v/v) ethanol was used. The cells were incubated for 1 h at $37\text{ }^{\circ}\text{C}$. Due to the detachment of the cells after exposure to SM concentrations above 500 μM , cell-containing supernatants were collected and centrifuged for 5 min at 500 RCF. The cell pellet was washed with PBS. Cells were again centrifuged and 2 mL lysis buffer (see section: Cell lysis) was added. The pellet was resuspended in lysis buffer and incubated for 1 h on ice. The lysate was further incubated for 1 h and vortexed several times. Cell lysates were centrifuged for 15 min at 14,000 RCF and the supernatants were subjected to clean tubes. Lysates were stored at $-80\text{ }^{\circ}\text{C}$.

μ LC-ESI MS/HR MS analysis

A MicroPro pump (Eldex Laboratories, Napa, CA, USA) with an Integrity autosampler and a Mistral column oven (both Spark Holland, Emmen, The Netherlands) were used for chromatography that was online coupled to a QExactive plus Orbitrap mass spectrometer by an HESI II ion source (Thermo Scientific, Bremen, Germany). Eldex MicroPro 1.0.54 software (Eldex Laboratories) was used to control the system (Blum et al. 2020; John et al. 2022a). The Excalibur 4.1 software (Thermo Scientific) was used to manage the MS system. Calibration was done daily using the Pierce LTQ Velos ESI positive ion calibration solution (Thermo Fisher Scientific). The lock masses of protonated ubiquitous molecules ($\text{C}_{24}\text{H}_{39}\text{O}_4$, m/z 391.28429, and $\text{C}_{10}\text{H}_{16}\text{O}_2\text{NS}$, m/z 214.08963) were used for internal mass calibration (John et al. 2022a). To identify peptides obtained from proteolysis of the adducted

hTRPA1 channel initial MS/HR MS detection was carried out in the ddMS2 approach. Proteome Discoverer Software 2.5.0.400 (Thermo Scientific) was used to analyze the obtained data.

Using the ddMS2 approach, peptides were separated at $45\text{ }^{\circ}\text{C}$ using a binary mobile phase (30 $\mu\text{L}/\text{min}$) of solvent A (0.05% v/v FA) and solvent B (ACN/ H_2O 80:20 v/v, 0.05% v/v FA) on an Acquity UPLC HSS T3 column (150 \times 1.0 mm I.D., 1.8 μm , Waters, Eschborn, Germany) protected by a precolumn (Security Guard Ultra cartridge C18 peptide; Phenomenex, Aschaffenburg, Germany). Solvent A and solvent B were applied in gradient mode: $t[\text{min}]/B[\%]$ 0/4; 3/4; 60/40; 60.5/95; 68.5/95; 69/4; 70/4 with an initial 15 min equilibration period under starting conditions. Eluates between retention time (t_R) 4.5 min and 60 min were directed toward the mass spectrometer using a six-port valve. For full scan MS analysis, resolution was 70,000 full-width at half-maximum (fwhm) (John et al. 2022a) and the scan range was from m/z 290 to m/z 2,000. The ddMS2 was recorded with a resolution of 17,500 fwhm and loop count was set to 10. A stepped normalized collision energy of 25 was chosen and m/z 100 was selected as fixed first mass. Analysis of the detected peptides was performed using the Proteome Discoverer software. All possible HETE modifications at e.g., cysteine, glutamic acid and aspartic acid residues were added to the inclusion list. Detailed settings are listed in supplementary information (Protocol SI 1).

For more sensitive and selective detection of identified modified peptides, the parallel reaction monitoring (PRM) mode was chosen as a second targeted approach and chromatography was carried out on an Acquity HSS T3 column (50 \times 1 mm I.D. 1.8 μm , Waters) with solvent A and solvent B in gradient mode (30 $\mu\text{L}/\text{min}$, $40\text{ }^{\circ}\text{C}$, $t[\text{min}]/B[\%]$: 0/2; 2.5/10; 3/20; 15/45; 16/98; 18/98; 19/2; 20/2, 10 min equilibration under starting conditions). Spray voltage was optimized to 3.0 kV. Eluates from t_R 0 min to 20 min were directed toward the mass spectrometer. First, full scan MS (resolution 70,000 fwhm, scan range m/z 100 to m/z 1,500) was carried out followed by PRM scans. Resolution was set to 17,500 fwhm and fixed first mass was m/z 100. PRM analyses were carried out for: GAKPC¹⁹²(-HETE) K $[\text{M} + 2\text{H}]^{2+}$ (m/z 354.18258); KGAKPC¹⁹²(-HETE) KSNK $[\text{M} + 2\text{H}]^{2+}$ (m/z 582.81502); WGC¹⁹⁹(-HETE)FPI-HQAAFSGSK M + 3H³⁺ (m/z 580.60593); EC²¹³(-HETE) MEILR $[\text{M} + 2\text{H}]^{2+}$ (m/z 555.77143); EC²¹³(-HETE) MEILR $[\text{M} + 3\text{H}]^{3+}$ (m/z 370.85005); ID³³⁹(-HETE) SEGR $[\text{M} + 2\text{H}]^{2+}$ and IDSE³⁴¹(-HETE)GR $[\text{M} + 2\text{H}]^{2+}$ (m/z 390.68145); INTC⁴⁶²(-HETE)QR $[\text{M} + 2\text{H}]^{2+}$ (m/z 419.69912); WDEC⁶⁰⁸(-HETE)LK $[\text{M} + 2\text{H}]^{2+}$ (m/z 449.19588) and YLQC⁶⁶⁵(-HETE)PLEFTK $[\text{M} + 2\text{H}]^{2+}$ (m/z 673.33017). The FreeStyle 1.3 software was used for data processing (Thermo Scientific).

Results and discussion

While the activation mechanism of hTRPA1 has been unraveled for some compounds including AITC (Jordt et al. 2004; Hinman et al. 2006; Macpherson et al. 2007), only little is known about SM. Therefore, we isolated the hTRPA1 channel from overexpressing HEK-A1 cells and used μ LC-ESI MS/HR MS to identify SM-modifications that may cause hTRPA1 activation.

Isolation and identification of hTRPA1 from overexpressing HEK-A1 cells

Successful expression of hTRPA1 was proven by Western blot analysis and Ca^{2+} -measurements. As already discussed by Virk et al. (2019), the anti-hTRPA1 and the anti-His-tag antibody showed a distinct and characteristic double band at 125 kDa corresponding to the size of the hTRPA1 channel (Fig. 1, lane 2 and 5). The double band was presumably caused by different posttranslational modifications not specified in the literature so far (UniProt No O75762, <https://www.uniprot.org/uniprotkb/O75762/entry>). HEK-wt

cells were used as negative control (blank) and thus, did not show any band (Fig. 1, lane 3 and 4).

To ascertain that these protein bands corresponded to the His-tagged hTRPA1 channel, it was purified from protein lysates using IMAC. Sequence analysis by MS/MS-based methods allowed identification of both protein bands as hTRPA1 (UniProt No O75762) with a Mascot probability score of 1165.

To prove expression in cell culture resulted in functional hTRPA1, changes in $[\text{Ca}^{2+}]_i$ were measured using Fura-2 AM (Almers and Neher 1985). HEK-A1 cells showed a concentration-dependent rise in $[\text{Ca}^{2+}]_i$ after injection of the agonist AITC (Fig. S11A) (Bandell et al. 2004; Hinman et al. 2006). To confirm that the observed signals were mediated through hTRPA1, the specific antagonist AP18 was used to block hTRPA1. Changes in $[\text{Ca}^{2+}]_i$ were reduced and nearly disappeared when AP18 concentrations increased (Fig. S11B). In addition, AITC exhibited no impact on HEK-wt cells (Fig. S11A). Thus, expression of functional hTRPA1 in HEK-A1 cells was confirmed.

Identification of alkylation sites

IMS, using either the anti-His-tag or the anti-hTRPA1 antibody, allowed the purification of hTRPA1 from total cell lysate and its identification by μ LC-ESI MS/HR MS (ddMS2 approach, sequence coverage 40%, Mascot probability score of approx. 800). These results were obtained from lysates of different non-exposed cell passages showing the same peptide pattern after proteolysis. A number of peptides was detected and identified by ddMS2 analysis as highlighted in Fig. 2. Other proteins detected in the samples were immunoglobulin κ variable 2–40 (UniProt No A0A087WW87), 3–15 (UniProt No P01624), 4–1 (UniProt No P06312), immunoglobulin λ variable 8–61 (UniProt No A0A075B6I0) and also immunoglobulin heavy constant γ 2 (UniProt No P01859). Immunoglobulins obviously originated from the antibodies used in the IMS procedure.

SM is known to alkylate thiol groups of cysteine residues by attaching a *HETE*-moiety (Lüling et al. 2018, 2021; John et al. 2019; Schmeißer et al. 2022) as well as carboxy-groups of aspartic acid and glutamic acid residues (John et al. 2019, 2022b). Based on the peptide pattern detected from non-exposed hTRPA1, we calculated the masses of the protonated and potentially alkylated peptides for subsequent targeted μ LC-ESI MS/HR MS (PRM) analysis of SM incubated samples. This procedure provided optimum selectivity and sensitivity to unravel modified peptides containing the *HETE*-moiety either as a thioether in cysteine residues (e.g., Cys¹⁹², Cys¹⁹⁹, Cys²¹³, Cys²⁵⁸, Cys²⁷³, Cys⁴⁶², Cys⁶⁰⁸, Cys⁶⁶⁵, Cys⁷⁰³, Cys⁷⁷³ and Cys⁷⁸⁶) or as an O-ester in Asp³³⁹ or Glu³⁴¹. Except for Cys⁶⁶⁵, Cys⁷⁰³, Cys⁷⁷³ and Cys⁷⁸⁶, all targeted cysteine residues are located in the ankyrin region

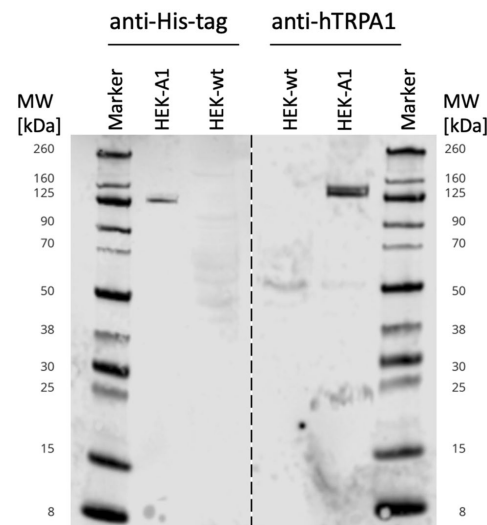


Fig. 1 Western blot analysis of HEK-A1 and HEK-wt cell lysates. Anti-His-tag antibody (left) and anti-hTRPA1 antibody (right) were used for detection of hTRPA1. Lane 1 and 6: Chameleon Due marker, lane 2 and 5: total protein lysate of transfected HEK-A1 cells; lane 3 and 4: total protein lysate of HEK-wt cells (negative control). HEK-A1 protein lysates showed a double band at 125 kDa indicating hTRPA1 expression detected with both antibodies, whereas no hTRPA1 was found in HEK-wt cells

1	MKRSRLK	KMWR	PGEK KEPQGV	VYEDVDPDTE	DFKESLK	VVF	EGSAYGLQNF
51	NK QKLRKCD	DMDTFFLHYA	AAEGQIELME	KITRDSLSLEV	LHEMDDYGN		
101	PLHCAVEK	NQ	IESVKFLLSR	GANPNLR NFN	MMAPLHIAVQ	GMNNEVMK	VL
151	LEHR TIDVNL	EGENGTAVI	IACITNNSEA	LQILKKGAK	PCKSNKWGCF		
201	PIHQAA FGSG	KECMEILRF	GEEHGYSRQL	HINFMNNGKA	TPHLAVQNG		
251	DLEM IKMCLD	NGAQIDPVEK	GRCTAIHFAA	TQGATEIVKL	MISSVSGSVD		
301	IVNTDGCHE	TMLHRASLFD	HHELADYLS	VGADINKIDS	EGRSPILAT		
351	ASASWNVNVL	LLSK GAQVDI	KDNFGRNFLH	LTVQQPYGLK	NLRPEFMQMQ		
401	QIKEL VMDI	NDGCTPLHYA	CRQGGPGSVN	NLLGFNVSIH	SKSKDKKSP		
451	HFAASYGRIN	TCQRLQDIS	DTRLLNEGDL	HGMTPLHLAA	KNGHDKVVQL		
501	LLKR GALFSL	DHNGWTALHH	ASMGGYQTQM	KVILDNLK	TDRLEDEGNT		
551	ALHFAAREGH	AKAVALLSH	NADIVLNKQ	ASFLHLALHN	KRKEVLTII		
601	RSKRWDECLK	IFSHNSPGNK	CPITEMIEYL	PECMKVLDFE	CMLHSTEDKS		
651	CRDYIYIEYFN	KYLQCPLEFT	KKTP TQDVIY	EPILTALNAMV	QNNRIELLNH		
701	PVCKEYLLMK	WLAYGFR AHM	MNLGSYCLGL	IPMTILVNI	KPGMAFNSTG		
751	IINETS	SDHSE	ILDTTNSYLI	KTCMILVFLS	SIFGYCKEAG	QIFQQR KNYF	
801	MDISNVLEWI	YTTGIIIVL	PLFVEIAPHL	QWQCGAIAVY	FYWMNLLYL		
851	QRFENQGI	FIMVLEIKTL	LRSTVVFIFL	LFAFLGSFYI	LLNLQDPFS		
901	PLLSIQFTS	MMLGDINRYR	SFLEPYLR NE	LAHPVLSFAQ	LVSFTFIVPI		
951	VLMNLLIGLA	VGDIAEVQKH	ASLKR IAMQV	ELHTSLEKLL	PLWFLKVDQ		
1001	KSTIVYPNKP	RSGGMLFHIF	CFLCTGEIR	QEIPNADKSL	EMIELKQKYR		
1051	KDLTFLLEK	QHELKLIQ	KMEISETED	DDSHCSFQDR	FKKEQMEQRN		
1101	SRWNTVLR	AV	KAKTHHLEP				

Fig. 2 Amino acid sequence of hTRPA1 (UniProt No O75762). Peptides detected by μ LC-ESI MS/HR MS obtained after tryptic cleavage of isolated not SM-exposed hTRPA1 are highlighted in yellow (sequence coverage 40%). Human TRPA1 was extracted by IMS using either an anti-His-tag or an anti-hTRPA1 antibody. Cysteine residues including Cys¹⁹², Cys¹⁹⁹, Cys²¹³, Cys²⁵⁸, Cys²⁷³, Cys⁴⁶², Cys⁶⁰⁸, Cys⁶⁶⁵, Cys⁷⁰³, Cys⁷⁷³ and Cys⁷⁸⁶ were found to be carbamidomethylated

(Paulsen et al. 2015). In addition, Cys⁶⁶⁵ has already been identified to play a pivotal role in hTRPA1 activation (Bahia et al. 2016; Meents et al. 2019; Talavera et al. 2020), thus, these cysteine residues and especially Cys⁶⁶⁵ appear as potential targets also for alkylation by SM.

Alkylation of hTRPA1 by SM

To identify alkylation sites, purified hTRPA1 from cell lysates was incubated with SM (10 mM). SM-induced hTRPA1 modifications were analyzed by μ LC-ESI MS/HR MS (PRM). Four alkylated peptides were detected containing modified amino acids: INTC⁴⁶²(-HETE)QR (Fig. S1 3 and S1 4, Table S1 2), YLQC⁶⁶⁵(-HETE)PLEFTK (Fig. 3 and S1 2, Table S1 1) as well as ID³³⁹(-HETE)SEGR (Fig. 4 and S1 5, Table S1 3) and IDSE³⁴¹(-HETE)GR (Fig. 4 and S1 5, Table S1 4).

After exposure of intact HEK-A1 cells to at least 250 μ M SM, the extracted ion chromatogram (XIC) of full scan measurement of the double-protonated and alkylated peptide YLQC⁶⁶⁵(-HETE)PLEFTK (m/z 673.3302) showed a single peak at t_R 11.46 min (Fig. 3B). In PRM analysis of this peptide, the well-known diagnostic ions at m/z 105.0369, representing the HETE-moiety [HETE]⁺, and at m/z 137.0089, indicating the HETE-moiety with a sulfur atom of the cysteine residue [HETE + S]⁺, were also detected at t_R 11.47 min (Fig. 3D, F). Additionally, product

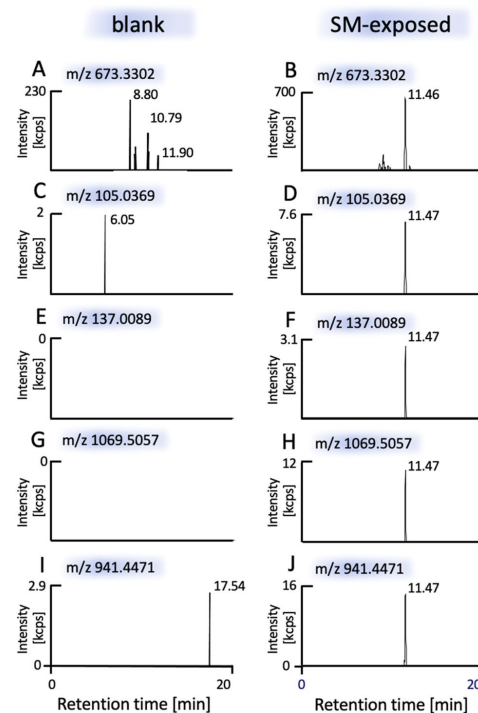


Fig. 3 Detection of the alkylated decapeptide YLQC⁶⁶⁵(-HETE)PLEFTK [M+2H]²⁺ using μ LC-ESI MS/HR MS (PRM). Results from a blank (negative control) not exposed to SM are shown in left column (A, C, E, G, I) and results of HEK-A1 cells exposed to SM are shown in right column (B, D, F, H, J). Human TRPA1 was extracted from HEK-A1 cells by IMS and subjected to trypsin-mediated proteolysis. The XIC of the alkylated peptide [M+2H]²⁺ m/z 673.3302, ± 3 ppm) is shown in Fig. 3B and showed one peak at t_R 11.46 min. The XIC of diverse product ions (± 10 ppm) assigned in Table S11 and Figure S12 are shown in part D (m/z 105.0369), F (m/z 137.0089), H (m/z 1069.5057) and J (m/z 941.4471) and revealed one peak at t_R 11.47 min. No interferences were observed in the blank (A, C, E, G, I)

ions at m/z 1069.5057 (y_8 ion) and at m/z 941.4471 (y_7 ion), both containing the HETE-moiety, were found at the same retention time. The peaks of the precursor ion as well as of the product ions were not present in the blank (HEK-A1 cells not exposed to SM, Fig. 3A, C, E, G, I) demonstrating the high selectivity and suitability of precursor and product ion detection. These results documented the unambiguous detection and identification of YLQC⁶⁶⁵(-HETE)PLEFTK containing the alkylated Cys⁶⁶⁵ residue. The MS/HR MS spectrum is shown in the supplement (Fig. S12) and product ion assignment is summarized in Table S11.

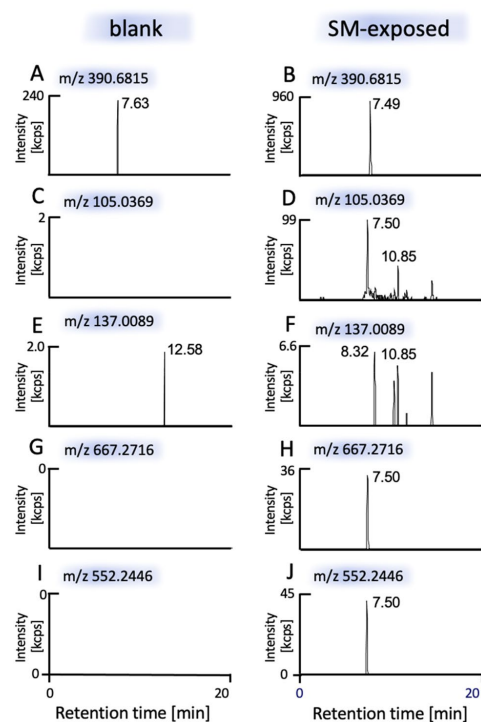


Fig. 4 Detection of the alkylated hexapeptides ID³³⁹(-HETE)SEGR [M+2H]²⁺ and IDSE³⁴¹(-HETE)GR [M+2H]²⁺ using targeted μ L-ESI MS/HR MS (PRM). Results from a blank (negative control) not exposed to SM are shown in left column (A, C, E, G, I) and results of HEK-A1 cells exposed to SM are shown in right column (B, D, F, H, J). Human TRPA1 was extracted from HEK-A1 cells by IMS and subjected to trypsin-mediated proteolysis. The XIC of the alkylated peptide [M+2H]²⁺, m/z 390.6815) is shown in Fig. 4B (± 3 ppm) and the XIC of diverse product ions (± 10 ppm) assigned in Table S1 3, S1 4 and Figure S15 are shown in part D (m/z 105.0369), H (m/z 667.2716) and J (m/z 552.2446) and revealed one peak at t_R 7.50 min. The absence of an ion peak at the relevant t_R of the XIC of m/z 137.0089 (F) indicated that no cysteine residue was alkylated. No interferences were observed in the blank (A, C, E, G, I)

Following the same strategy, INTC⁴⁶²(-HETE)QR [M+2H]²⁺ (containing alkylated Cys⁴⁶²) was also detected as a single peak in the XIC (m/z 419.6991) of a full scan analysis at t_R 7.28 min as well as single peak of diverse product ions from PRM analysis as illustrated in supplement Figs. S13, S14 and Table S12. The absence of these product ions in the blank demonstrated the selectivity of the method and suitability of this peptide (Fig. S13, left column).

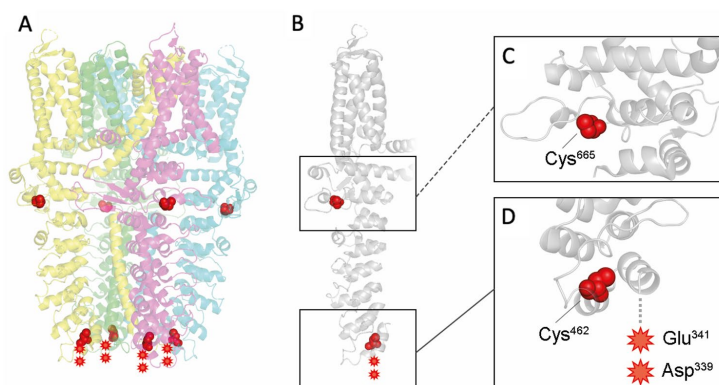
In addition, we detected alkylation sites at the Asp³³⁹ and Glu³⁴¹ residues after incubation of total protein lysate

yielding the alkylated peptides ID³³⁹(-HETE)SEGR and IDSE³⁴¹(-HETE)GR. A t_R of 7.49 min was observed for the precursor ion at m/z 390.6815 (Fig. 4B) as well as for the product ion at m/z 105.0369 (Fig. 4D) selectively indicating the presence of the HETE-moiety. No peak at the relevant t_R was detected at m/z 137.0089 (Fig. 4F) indicating that the alkylation site was not a cysteine residue. Diverse product ions containing the HETE-moiety were also detected as illustrated in Fig. 4H, J. Obviously both peptides ID³³⁹(-HETE)SEGR and IDSE³⁴¹(-HETE)GR coeluted and were simultaneously subjected to fragmentation for MS/HR MS yielding a mixed product ion spectrum documenting that the HETE-moiety was attached to the Glu³⁴¹ and also to the Asp³³⁹ residue as shown in Fig. S15. The absence of the peaks of the precursor and product ions in the blank (Fig. 4A, C, E, G, I) proved the high selectivity and suitability of the detection.

We herein identified Cys⁴⁶² and Cys⁶⁶⁵ as alkylation sites after SM exposure. In addition, we detected modifications at Asp³³⁹ and Glu³⁴¹. Different mutation studies have previously revealed that Cys⁴¹⁴, Cys⁶²¹ and also Cys⁶⁶⁵ play an essential role in hTRPA1 activation by electrophiles (Hinman et al. 2006; Macpherson et al. 2007; Takahashi et al. 2008; Fischer et al. 2010; Bahia et al. 2016). Because Cys⁶⁶⁵ is located intracellularly in a flexible loop, it is solvent accessible and might be a target for reactive chemicals (Macpherson et al. 2007; Paulsen et al. 2015). This shows that also SM reacted intracellularly and was able to alkylate Cys⁶⁶⁵ as presented in this study. For other agonists, such as AITC and IAA, it was demonstrated that Cys⁶⁶⁵ was needed for electrophile-induced hTRPA1 activation (Macpherson et al. 2005; Bahia et al. 2016). Therefore, Cys⁶⁶⁵ might also be essential in SM-induced hTRPA1 activation. Additionally, four disulfide bridges, namely Cys⁶⁶⁵-Cys⁶²¹, Cys⁶⁶⁵-Cys⁴⁶², Cys⁶⁶⁵-Cys¹⁹² and Cys⁶²¹-Cys⁶⁰⁸, were discovered in the absence of any reducing agent by Wang et al. (2012). These findings revealed that hTRPA1 channel activation involves conformational changes in the N-terminal region to provide accessibility of the cysteines (Wang et al. 2012). As Cys⁶⁶⁵ was identified as an alkylation site in our study, it is plausible that hTRPA1 conformation might be dynamically driven by electrophilic activation also by SM.

Cys⁴⁶² is also located inside the ankyrin region in the cytoplasm (Paulsen et al. 2015), supporting that SM was able to act intracellularly. Without prior protein reduction, SM alkylated Cys⁴⁶² which is in vivo disulfide-bridged with Cys⁶⁶⁵ (Wang et al. 2012) indicating that conformational changes within the hTRPA1 channel might occur after SM exposure. Furthermore, the SM concentration required for alkylation was two-times higher when compared to Cys⁶⁶⁵. Stenger et al. (2015) performed calcium measurements to evaluate hTRPA1 activation by SM, showing that 500 μ M SM caused activation. Thus, we assume that Cys⁴⁶² and

Fig. 5 Structure of human TRPA1 protein with alkylation sites at Cys⁴⁶², Cys⁶⁶⁵, Asp³³⁹ and Glu³⁴¹. **A** The homotetrameric structure (PDB ID 6PQO) of hTRPA1 is shown with herein detected and described alkylation sites indicated in red. **B** A monomeric structure (**B**) details the alkylation sites for Cys⁶⁶⁵ (**C**) and Cys⁴⁶², Asp³³⁹ and Glu³⁴¹ (**D**). The figure was created using PyMOL version 2.5.4



Cys⁶⁶⁵ might be involved in hTRPA1 activation after SM exposure.

John et al. (2019, 2022b) showed that in addition to SM-induced modifications at cysteine residues, glutamic acid modifications were found in human and avian serum albumin. It is therefore plausible that alkylation at aspartic and glutamic acid in hTRPA1 had occurred. Both amino acids possess a free carboxylic group that can react with the electrophilic SM as already shown before (Smith et al. 2008; John et al. 2019, 2022b). Additionally, TRPC channels possess similar structures to hTRPA1 channels and have three to four ankyrin repeats at the N-terminus. These also contain glutamic acid residues that promote TRPC5 channel activation (Jung et al. 2003; Jiang et al. 2011). Thus, aspartic and glutamic acid modifications might also contribute to hTRPA1 activation. In the present study, modifications were only seen at quite high SM concentrations (≤ 1 mM SM) used for cell lysate incubation. A decreased in vivo stability of SM-induced protein modifications at aspartic or glutamic acid was demonstrated by Smith et al. (2008). Thus, the HETE-moiety might have been released from the protein and may explain the lack of alkylation following exposure of the intact cell system in our study. Various competitive reactions with other proteins as well as hydrolysis of SM prior to alkylation might have occurred and reduced the amount of reactive SM.

Additional cysteine residues (Cys⁴¹⁴, Cys⁴²¹, Cys⁶²¹ and Cys⁶⁴¹) have been reported in the literature to be significant for hTRPA1 activation (Hinman et al. 2006; Macpherson et al. 2007). Especially Cys⁶²¹ has been described as a highly reactive hotspot for electrophile sensing (Bahia et al. 2016; Suo et al. 2019). Unfortunately, using the method described herein, peptide sequences covering Cys⁴¹⁴, Cys⁴²¹ as well as Cys⁶²¹ were not detected. Accordingly, it remained unclear, whether these residues were targeted by SM. The two cysteines (Cys⁴⁶² and Cys⁶⁶⁵)

detected herein are structurally resolved and are shown in Fig. 5. Both cysteine residues are located in the cytosol and appear readily accessible for SM. The Asp³³⁹ and Glu³⁴¹ are located at the N-terminal region (indicated with a red star Fig. 5D). The protein data bank entry (ID 6PQO) does not provide structural data on that region as it is characterized by a high flexibility. Access to any reactive side chain is therefore likely.

Conclusion

We demonstrated for the first time that SM alkylates at least two cysteine residues (Cys⁴⁶² and Cys⁶⁶⁵) as well as Asp³³⁹ and Glu³⁴¹ in hTRPA1. Because hTRPA1 might be a target for additional chemical warfare agents structurally related to SM such as sesquimustard (Blum et al. 2020; Hemme et al. 2021) or O-mustard, similar adducts are expected and might be discovered using the analytical approach described herein. This approach might also be used for other TRP channels to elucidate potential binding sites. Future studies will address mutation experiments to assess the impact of the discovered alterations on functional activity of the channel. In this case, the modified cysteine residues as well as glutamic or aspartic acid will be altered to e.g., alanine and calcium measurements will be performed to determine the role of the mutated amino acid. This will provide further information on hTRPA1 activation and on specific amino acid residues which may directly be essential for hTRPA1 activation.

Supplementary Information The online version contains supplementary material available at <https://doi.org/10.1007/s00204-022-03411-1>.

Funding Open Access funding enabled and organized by Projekt DEAL. This work was supported by the Deutsche

Forschungsgemeinschaft (DFG) Research Training Group (RTG) 2338 project P03.

Declarations

Conflict of interest The authors declare that they have no conflict of interest.

Open Access This article is licensed under a Creative Commons Attribution 4.0 International License, which permits use, sharing, adaptation, distribution and reproduction in any medium or format, as long as you give appropriate credit to the original author(s) and the source, provide a link to the Creative Commons licence, and indicate if changes were made. The images or other third party material in this article are included in the article's Creative Commons licence, unless indicated otherwise in a credit line to the material. If material is not included in the article's Creative Commons licence and your intended use is not permitted by statutory regulation or exceeds the permitted use, you will need to obtain permission directly from the copyright holder. To view a copy of this licence, visit <http://creativecommons.org/licenses/by/4.0/>.

References

- Almers W, Neher E (1985) The Ca signal from fura-2 loaded cells depends strongly on the method of dye-loading. *FEBS Lett* 192:13–18. [https://doi.org/10.1016/0014-5793\(85\)80033-8](https://doi.org/10.1016/0014-5793(85)80033-8)
- Andersson DA, Gentry C, Moss S, Bevan S (2008) Transient receptor potential A1 is a sensory receptor for multiple products of oxidative stress. *J Neurosci* 28:2485–2494. <https://doi.org/10.1523/JNEUROSCI.5369-07.2008>
- Bahia PK, Parks TA, Stanford KR et al (2016) The exceptionally high reactivity of Cys 621 is critical for electrophilic activation of the sensory nerve ion channel TRPA1. *J Gen Physiol* 147:451–465. <https://doi.org/10.1085/jgp.201611581>
- Bandell M, Story GM, Hwang SW et al (2004) Noxious cold ion channel TRPA1 is activated by pungent compounds and bradykinin. *Neuron* 41:849–857. [https://doi.org/10.1016/s0896-6273\(04\)00150-3](https://doi.org/10.1016/s0896-6273(04)00150-3)
- Bautista DM, Movahed P, Hinman A et al (2005) Pungent products from garlic activate the sensory ion channel TRPA1. *Proc Natl Acad Sci USA* 102:12248–12252. <https://doi.org/10.1073/pnas.0505356102>
- Bautista DM, Jordt SE, Nikai T et al (2006) TRPA1 mediates the inflammatory actions of environmental irritants and proalgesic agents. *Cell* 124:1269–1282. <https://doi.org/10.1016/j.cell.2006.02.023>
- Bautista DM, Pellegrino M, Tsunozaki M (2013) TRPA1: a gatekeeper for inflammation. *Annu Rev Physiol* 75:181–200. <https://doi.org/10.1146/annurev-physiol-030212-183811>
- Blum MM, Richter A, Siegert M et al (2020) Adduct of the blistering warfare agent sesquimustard with human serum albumin and its mass spectrometric identification for biomedical verification of exposure. *Anal Bioanal Chem* 412:7723–7737. <https://doi.org/10.1007/s00216-020-02917-w>
- Büch TRH, Schäfer EAM, Demmel MT et al (2013) Functional expression of the transient receptor potential channel TRPA1, a sensor for toxic lung inhalants, in pulmonary epithelial cells. *Chem Biol Interact* 206:462–471. <https://doi.org/10.1016/j.cbi.2013.08.012>
- Fischer MJM, Leffler A, Niedermirtl F et al (2010) The general anesthetic propofol excites nociceptors by activating TRPV1 and TRPA1 rather than GABAA receptors. *J Biol Chem* 285:34781–34792. <https://doi.org/10.1074/jbc.M110.143958>
- Ghabili K, Agutter P, Ghanei M et al (2011) Sulfur mustard toxicity: history, chemistry, pharmacokinetics, and pharmacodynamics. *Crit Rev Toxicol* 41:384–403. <https://doi.org/10.3109/1040444.2010.541224>
- Hemme M, Fidler A, van der Oeveren DR et al (2021) Mass spectrometric analysis of adducts of sulfur mustard analogues to human plasma proteins: approach towards chemical provenancing in biomedical samples. *Anal Bioanal Chem* 413:4023–4036. <https://doi.org/10.1007/s00216-021-03354-z>
- Hinman A, Chuang H-H, Bautista DM, Julius D (2006) TRP channel activation by reversible covalent modification. *Proc Natl Acad Sci* 103:19564–19568. <https://doi.org/10.1073/pnas.0609598103>
- Jiang LH, GamperBeech NDJ (2011) Properties and therapeutic potential of transient receptor potential channels with putative roles in adversity: focus on TRPC5, TRPM2 and TRPA1. *Curr Drug Targets* 12:724–736. <https://doi.org/10.2174/138945011795378568>
- John H, Koller M, Worek F et al (2019) Forensic evidence of sulfur mustard exposure in real cases of human poisoning by detection of diverse albumin-derived protein adducts. *Arch Toxicol* 93:1881–1891. <https://doi.org/10.1007/s00204-019-02461-2>
- John H, Dentzel M, Siegert M, Thiermann H (2022a) Nontargeted high-resolution mass spectrometric workflow for the detection of butyrylcholinesterase-derived adducts with organophosphorus toxicants and structural characterization of their phosphyl moiety after in-source fragmentation. *Anal Chem* 94:2048–2055. <https://doi.org/10.1021/acs.analchem.1c04116>
- John H, Hörmann P, Schrader M, Thiermann H (2022b) Alkylated glutamic acid and histidine derived from protein-adducts indicate exposure to sulfur mustard in avian serum. *Drug Test Anal.* <https://doi.org/10.1002/dta.3236>
- Jordt SE, Bautista DM, Chuang HH et al (2004) Mustard oils and cannabinoids excite sensory nerve fibres through the TRP channel ANKTM1. *Nature* 427:260–265. <https://doi.org/10.1038/nature02282>
- Jung S, Mühle A, Schaefer M et al (2003) Lanthanides potentiate TRPC5 currents by an action at extracellular sites close to the pore mouth. *J Biol Chem* 278:3562–3571. <https://doi.org/10.1074/jbc.M211484200>
- Kehe K, Balszuweit F, Emmeler J et al (2008) Sulfur mustard research—strategies for the development of improved medical therapy. *Eplasty* 8:312–332
- Koivisto A, Pertovaara A (2015) Transient receptor potential ankyrin 1 channel antagonists for pain relief. In: TRP channels as therapeutic targets: from basic science to clinical use. Elsevier Inc., pp 145–162
- Kwan KY, Allchorne AJ, Vollrath MA et al (2006) TRPA1 contributes to cold, mechanical, and chemical nociception but is not essential for hair-cell transduction. *Neuron* 50:277–289. <https://doi.org/10.1016/j.neuron.2006.03.042>
- Ludlum D, Austin-Ritchie P, Hagopian M et al (1994) Detection of sulfur mustard-induced DNA modifications. *Chem Biol Interact* 91:39–49. [https://doi.org/10.1016/0009-2797\(94\)90005-1](https://doi.org/10.1016/0009-2797(94)90005-1)
- Lüling R, John H, Gudermann T et al (2018) Transient receptor potential channel A1 (TRPA1) regulates sulfur mustard-induced expression of heat shock 70 kDa protein 6 (HSPA6) in vitro. *Cells* 7:126. <https://doi.org/10.3390/cells7090126>
- Lüling R, Schmeißer W, Siegert M et al (2021) Identification of creatine kinase and α -1 antitrypsin as protein targets of alkylation by sulfur mustard. *Drug Test Anal* 13:268–282. <https://doi.org/10.1002/dta.2916>
- Macpherson LJ, Geierstanger BH, Viswanath V et al (2005) The pungency of garlic: activation of TRPA1 and TRPV1 in response to allicin. *Curr Biol* 15:929–934. <https://doi.org/10.1016/j.cub.2005.04.018>
- Macpherson LJ, Hwang SW, Miyamoto T et al (2006) More than cool: promiscuous relationships of menthol and other sensory

- compounds. *Mol Cell Neurosci* 32:335–343. <https://doi.org/10.1016/j.mcn.2006.05.005>
- Macpherson LJ, Dubin AE, Evans MJ et al (2007) Noxious compounds activate TRPA1 ion channels through covalent modification of cysteines. *Nature* 445:541–545. <https://doi.org/10.1038/nature05544>
- Meents JE, Ciotu CI, Fischer MJM (2019) Trpa1: a molecular view. *J Neurophysiol* 121:427–443. <https://doi.org/10.1152/jn.00524.2018>
- Müller-Dott K, Thiermann H, Steinritz D, Popp T (2020) Effect of sulfur mustard on melanogenesis in vitro. *Toxicol Lett* 319:197–203. <https://doi.org/10.1016/j.toxlet.2019.11.014>
- Nilius B, Appendino G, Owsianik G (2012) The transient receptor potential channel TRPA1: from gene to pathophysiology. *Pflugers Arch Eur J Physiol* 464:425–458. <https://doi.org/10.1007/s00424-012-1158-z>
- Paromov V, Suintres Z, Smith M, Stone WL (2007) Sulfur mustard toxicity following dermal exposure: role of oxidative stress, and antioxidant therapy. *J Burns Wounds* 7:60–85
- Paulsen CE, Armache JP, Gao Y et al (2015) Structure of the TRPA1 ion channel suggests regulatory mechanisms. *Nature* 344:1173–1178. <https://doi.org/10.1126/science.1249098>. [Sleep](https://doi.org/10.1016/j.phrs.2010.11.004)
- Rose D, Schmidt A, Brandenburger M et al (2018) Sulfur mustard skin lesions: a systematic review on pathomechanisms, treatment options and future research directions. *Toxicol Lett* 293:82–90. <https://doi.org/10.1016/j.toxlet.2017.11.039>
- Sadofsky LR, Boa AN, Maher SA et al (2011) TRPA1 is activated by direct addition of cysteine residues to the *N*-hydroxysuccinyl esters of acrylic and cinnamic acids. *Pharmacol Res* 63:30–36. <https://doi.org/10.1016/j.phrs.2010.11.004>
- Schmeißer W, Lüliling R, Steinritz D et al (2022) Transthyretin as a target of alkylation and a potential biomarker for sulfur mustard poisoning: electrophoretic and mass spectrometric identification and characterization. *Drug Test Anal* 14:80–91. <https://doi.org/10.1002/dta.3146>
- Sezigen S, Ivelik K, Ortatatli M et al (2019) Victims of chemical terrorism, a family of four who were exposed to sulfur mustard. *Toxicol Lett* 303:9–15. <https://doi.org/10.1016/j.toxlet.2018.12.006>
- Shakarjian MP, Heck DE, Gray JP et al (2009) Mechanisms mediating the vesicant actions of sulfur mustard after cutaneous exposure. *Toxicol Sci* 114:5–19. <https://doi.org/10.1093/toxsci/kfp253>
- Smith JR, Capacio BR, Korte WD et al (2008) Analysis for plasma protein biomarkers following an accidental human exposure to sulfur mustard. *J Anal Toxicol* 32:17–24. <https://doi.org/10.1093/jat/32.1.17>
- Steinritz D, Stenger B, Dietrich A et al (2018) TRPs in tox: involvement of transient receptor potential-channels in chemical-induced organ toxicity—a structured review. *Cells* 7:98. <https://doi.org/10.3390/cells7080098>
- Stenger B, Zehfuß F, Mückter H et al (2015) Activation of the chemosensing transient receptor potential channel A1 (TRPA1) by alkylating agents. *Arch Toxicol* 89:1631–1643. <https://doi.org/10.1007/s00204-014-1414-4>
- Story GM, Peier AM, Reeve AJ et al (2003) ANKTM1, a TRP-like channel expressed in nociceptive neurons, is activated by cold temperatures. *Cell* 112:819–829. [https://doi.org/10.1016/S0092-8674\(03\)00158-2](https://doi.org/10.1016/S0092-8674(03)00158-2)
- Suo Y, Wang Z, Zubcevic L et al (2019) Structural insights into electrophile irritant sensing by the human TRPA1 channel. *Neuron* 105:1–13. <https://doi.org/10.1016/j.neuron.2019.11.023>
- Takahashi N, Mizuno Y, Kozai D et al (2008) Molecular characterization of TRPA1 channel activation by cysteine-reactive inflammatory mediators. *Channels* 2:287–298. <https://doi.org/10.4161/chan.2.4.6745>
- Talavera K, Startek JB, Alvarez-Collazo J et al (2020) Mammalian transient receptor potential TRPA1: from structure to disease. *Physiol Rev* 100:725–803. <https://doi.org/10.1152/physrev.00005.2019>
- Virk HS, Rekas MZ, Biddle MS et al (2019) Validation of antibodies for the specific detection of human TRPA1. *Sci Rep* 9:1–9. <https://doi.org/10.1038/s41598-019-55133-7>
- Wang L, Cvetkov TL, Chance MR, Moiseenkova-Bell VY (2012) Identification of in vivo disulfide conformation of TRPA1 ion channel. *J Biol Chem* 287:6169–6176. <https://doi.org/10.1074/jbc.M111.329748>

Publisher's Note Springer Nature remains neutral with regard to jurisdictional claims in published maps and institutional affiliations.

3.1 Supplementary material Paper I

Supplementary Information

ARCHIVES OF TOXICOLOGY

Isolation of human TRPA1 channel from transfected HEK293 cells and identification of alkylation sites after sulfur mustard exposure

Katharina Müller-Dott^{1,2}, Horst Thiermann¹, Harald John¹, Dirk Steinritz^{*1}

¹ Bundeswehr Institute of Pharmacology and Toxicology, 80937 Munich, Germany

² Walther-Straub-Institute of Pharmacology and Toxicology, Ludwig-Maximilians-University, 80336 Munich, Germany

* Address correspondence to this author

Bundeswehr Institute of Pharmacology and Toxicology,

Neuherbergstr. 11, 80937 Munich, Germany

E-Mail: dirksteinritz@bundeswehr.org

Table of Content

Protocol SI 1: Settings for Proteome Discoverer software

Table SI 1: Precursor and product ions of YLQC⁶⁶⁵(-HETE)PLEFTK

Table SI 2: Precursor and product ions of INTC⁴⁶²(-HETE)QR

Table SI 3: Precursor and product ions of ID³³⁹(-HETE)SEGR

Table SI 4: Precursor and product ions of IDSE³⁴¹(-HETE)GR

Figure SI 1: Changes in intracellular calcium concentration after stimulation with AITC using Fura-2 AM.

Figure SI 2: MS/HR MS spectrum of YLQC⁶⁶⁵(-HETE)PLEFTK containing the alkylated Cys⁶⁶⁵ residue

Figure SI 3: Detection of hexapeptide INTC⁴⁶²(-HETE)QR [M+2H]²⁺ using targeted μ LC-ESI MS/HR MS (PRM)

Figure SI 4: MS/HR MS spectrum of INTC⁴⁶²(-HETE)QR containing the alkylated Cys⁴⁶²

Figure SI 5: Mixed MS/HR MS spectrum of ID³³⁹(-HETE)SEGR containing the alkylated Asp³³⁹ and of IDSE³⁴¹(-HETE)GR containing the alkylated Glu³⁴¹

Protocol SI 1**Protocol SI 1: Settings for Proteome Discoverer software**

The following settings were applied: lowest charge was 1 and the highest charge was 6. As input data, human TRPA1 fasta file (UniProt No O75762) was selected and trypsin was selected as enzyme. Maximum number of missed cleavages was set to 3 and minimum peptide length was 4 amino acids, maximum peptide length was set to 30. Precursor mass tolerance was 5 ppm and fragment mass tolerance was set to 0.05 Da. Dynamic modifications included carbamidomethylation at cysteine and SM-modification at cysteine, glutamic acid, aspartic acid, histidine, lysine, methionine, arginine and tryptophan residues. Additionally, peptide spectral match (PSM) validator was added to the workflow. To determine Mascot probability score, the same settings as described before were used. Furthermore, as protein database SwissProt was selected and for taxonomy homo sapiens (human) was chosen.

Table SI 1

Table SI 1: Precursor and product ions of YLQC⁶⁶⁵(-HETE)PLEFTK

ion	elemental composition	<i>m/z</i> theoretical (measured)	$\Delta m/z$ [ppm]
[M+2H]²⁺	C ₆₂ H ₉₈ N ₁₂ O ₁₇ S ₂	673.3302 (673.3300)	-0.3
y₁	C ₆ H ₁₅ N ₂ O ₂	147.1128 (147.1126)	-1.4
y₂	C ₁₀ H ₂₂ N ₃ O ₄	248.1605 (248.1603)	-0.7
y₃	C ₁₉ H ₃₁ N ₄ O ₅	395.2289 (395.2285)	-1.0
y₄	C ₂₄ H ₃₈ N ₅ O ₈	524.2715 (524.2718)	0.6
y₆	C ₃₅ H ₅₆ N ₇ O ₁₀	734.4083 (734.4067)	-2.2
y₇	C ₄₂ H ₆₉ N ₈ O ₁₂ S ₂	941.4471 (941.4399)	-7.6
y₈	C ₄₇ H ₇₇ N ₁₀ O ₁₄ S ₂	1069.5057 (1069.4933)	-11.6
a₁	C ₈ H ₁₀ NO	136.0757 (136.0755)	-1.4
a₂	C ₁₄ H ₂₁ N ₂ O ₂	249.1598 (249.1593)	-1.8
b₂	C ₁₅ H ₂₁ N ₂ O ₃	277.1547 (277.1546)	-0.3
b₃	C ₂₀ H ₂₉ N ₄ O ₅	405.2132 (405.2136)	-0.9
y₈-18²⁺	C ₄₇ H ₇₅ N ₁₀ O ₁₃ S ₂	526.2512 (526.2497)	-2.8
a₈²⁺	C ₅₁ H ₇₇ N ₉ O ₁₂ S ₂	535.7561 (535.7614)	9.9
y₁₀-17²⁺	C ₆₂ H ₉₅ N ₁₁ O ₁₇ S ₂	664.8169 (664.8205)	5.4

Table SI 2

Table SI 2: Precursor and product ions of INTC⁴⁶²(-HETE)QR

ion	elemental composition	<i>m/z</i> theoretical (measured)	$\Delta m/z$ [ppm]
[M+2H]²⁺	C ₃₂ H ₆₁ N ₁₁ O ₁₁ S ₂	419.6991 (419.6981)	-2.4
y₁	C ₆ H ₁₅ N ₄ O ₂	175.1189 (175.1182)	-4.3
y₂	C ₁₁ H ₂₃ N ₆ O ₄	303.1775 (303.1779)	1.2
y₃	C ₁₈ H ₃₆ N ₇ O ₆ S ₂	510.2163 (510.2147)	-3.1
y₄	C ₂₂ H ₄₃ N ₈ O ₈ S ₂	611.2640 (611.2619)	-3.4
y₅	C ₂₆ H ₄₉ N ₁₀ O ₁₀ S ₂	725.3070 (725.3035)	-4.7
y₂-17	C ₁₁ H ₂₀ N ₅ O ₄	286.1510 (286.1495)	-5.2
y₅-17	C ₂₆ H ₄₆ N ₉ O ₁₀ S ₂	708.2803 (708.2782)	-3.05
y₅-18	C ₂₆ H ₄₇ N ₁₀ O ₉ S ₂	707.2963 (707.2949)	-2.0
a₂	C ₉ H ₁₈ N ₃ O ₂	200.1394 (200.1386)	-3.8
y₆-17²⁺	C ₃₂ H ₅₉ N ₁₀ O ₁₁ S ₂	411.1859 (411.1889)	7.4
y₆-18²⁺	C ₃₂ H ₆₀ N ₁₁ O ₁₀ S ₂	410.6938 (410.6929)	-2.3
a₆²⁺	C ₃₁ H ₅₉ N ₁₁ O ₉ S ₂	396.6964 (396.6956)	-2.0
b₆²⁺	C ₃₂ H ₅₉ N ₁₁ O ₁₀ S ₂	410.6938 (410.6929)	-2.3

Table SI 3

Table SI 3: Precursor and product ions of ID³³⁹(-HETE)SEGR

ion	elemental composition	<i>m/z</i> theoretical (measured)	$\Delta m/z$ [ppm]
[M+2H] ²⁺	C ₃₀ H ₅₅ N ₉ O ₁₃ S	390.6815 (390.6805)	-2.4
y ₁	C ₆ H ₁₅ N ₄ O ₂	175.1190 (175.1188)	-0.9
y ₄	C ₁₆ H ₃₀ N ₇ O ₈	448.2150 (448.2141)	-2.1
y ₅	C ₂₄ H ₄₃ N ₈ O ₁₂ S	667.2716 (667.2703)	-1.9

Table SI 4

Table SI 4: Precursor and product ions of IDSE³⁴¹(-HETE)GR

ion	elemental composition	<i>m/z</i> theoretical (measured)	$\Delta m/z$ [ppm]
[M+2H]²⁺	C ₃₀ H ₅₅ N ₉ O ₁₃ S	390.6815 (390.6805)	-2.4
y₁	C ₆ H ₁₅ N ₄ O ₂	175.1190 (175.1188)	-0.9
y₄	C ₂₀ H ₃₈ N ₇ O ₉ S	552.2446 (552.2425)	-3.9
y₅	C ₂₄ H ₄₃ N ₈ O ₁₂ S	667.2715 (667.2703)	-1.9
a₂	C ₉ H ₁₇ N ₂ O ₃	201.1234 (201.1229)	-2.3
a₂-18	C ₉ H ₁₅ N ₂ O	183.1128 (183.1125)	-1.7
b₂	C ₁₀ H ₁₇ N ₂ O ₄	229.1183 (229.1181)	-0.8

Figure SI 1

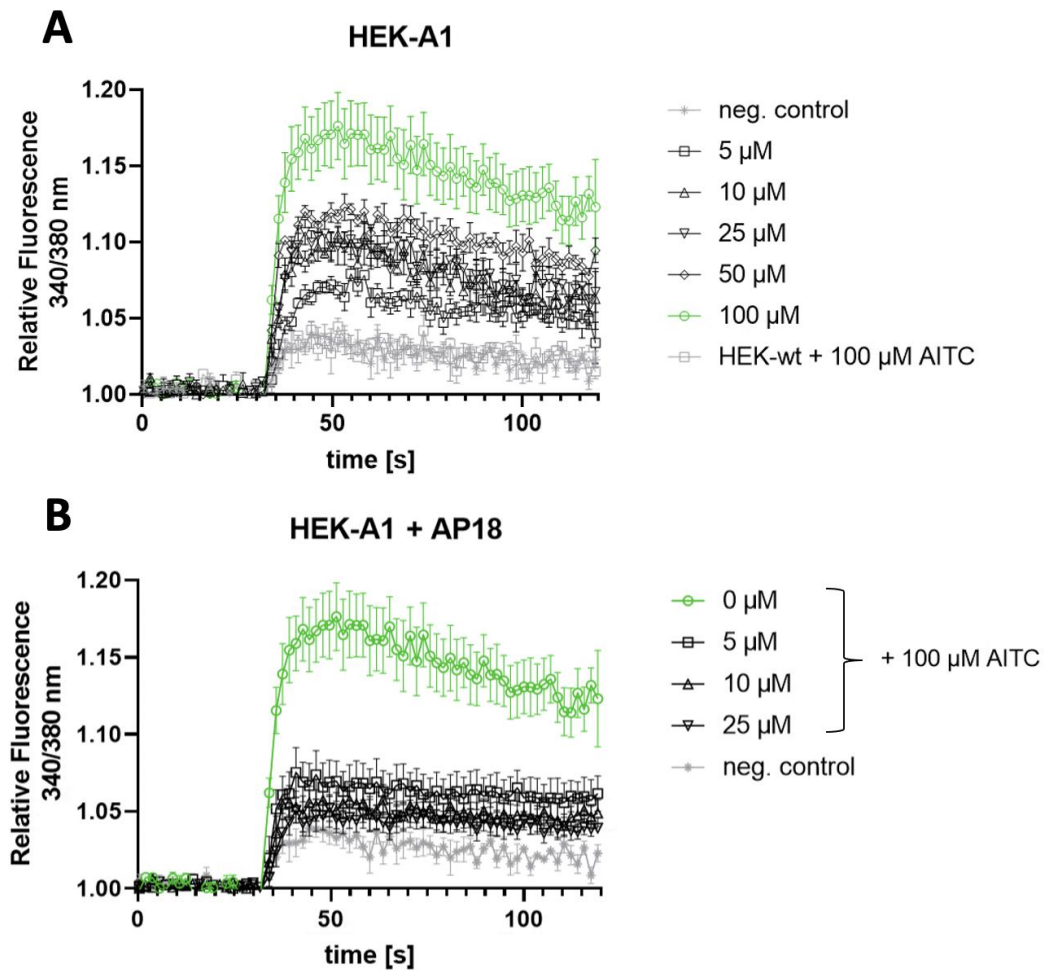


Figure SI 1: Changes in intracellular calcium concentration after stimulation with AITC detected by Fura-2 AM

HEK-A1 and HEK-wt cells were loaded with Fura-2 AM (c_{final} 2 μ M) and stimulated with different concentrations of AITC (5 μ M, 10 μ M, 25 μ M, 50 μ M and 100 μ M). DMEM was used as a negative control. The relative fluorescence signal increased with increasing AITC concentrations, suggesting hTRPA1 activation. HEK-wt cells were not affected by AITC (A). The antagonist AP18 (5 μ M, 10 μ M, and 25 μ M) was used to confirm that these signals were hTRPA1 specific. Calcium influx was decreased and almost abolished as AP18 concentrations rose, confirming hTRPA1 correct protein folding and, as a result, functioning (B).

Figure SI 2

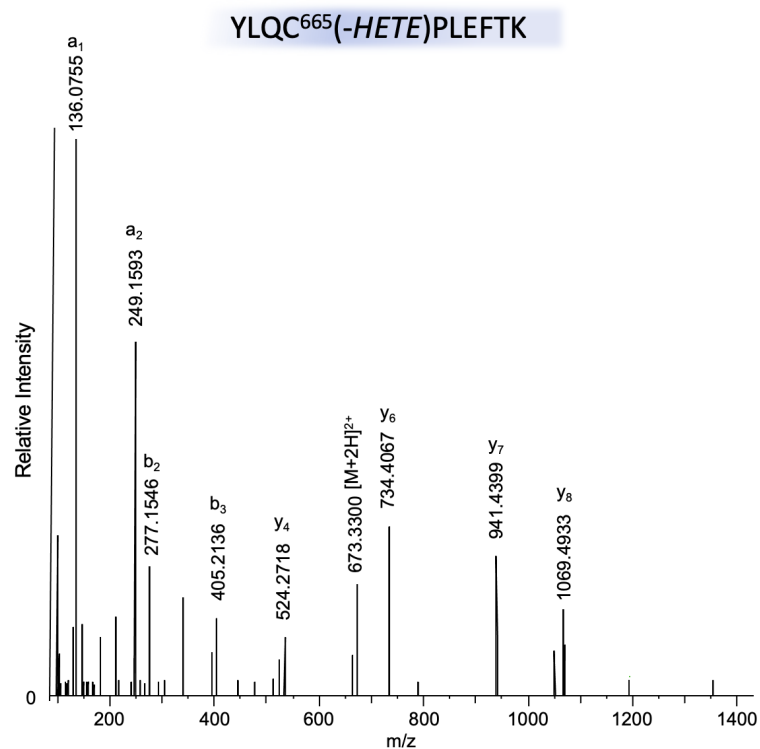


Figure SI 2: MS/HR MS spectrum of YLQC⁶⁶⁵(-HETE)PLEFTK containing the alkylated Cys⁶⁶⁵ residue

The spectrum was extracted from a μ LC-ESI MS/HR MS run showing the alkylated peptide eluting at t_R 11.46 min (Fig. 3 B). The sample was obtained from HEK-A1 cells exposed to SM for 1 h followed by IMS and trypsin-cleavage. Labelled signals were assigned to product ions as indicated and are listed in detail in Table SI 1. Due to minor intensities, signals at m/z 105.0369 and m/z 137.0089 are not labelled. When compared to their theoretical mass, all ions had a mass difference typically below 5.5 ppm.

Figure SI 3

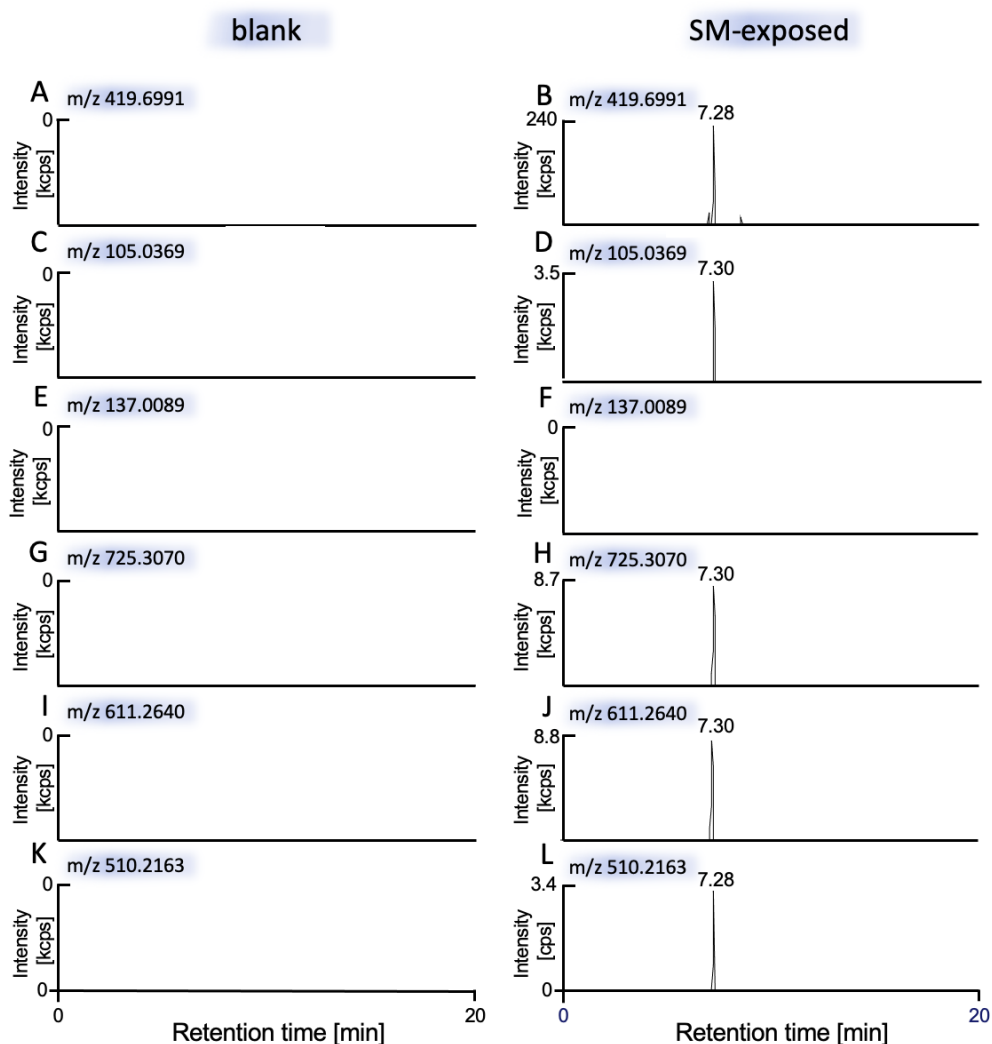


Figure SI 3: Detection of hexapeptide INTC⁴⁶²(-HETE)QR [M+2H]²⁺ using targeted μ LC-ESI MS/HR MS (PRM)

Results from a blank (negative control) not exposed to SM are shown in left column (A, C, E, G, I, K) and results of HEK-A1 cells exposed to SM are shown in right column (B, D, F, H, J, L). Human TRPA1 was extracted from HEK-A1 cells by IMS and subjected to trypsin-mediated proteolysis. The XIC of the alkylated peptide ([M+2H]²⁺ m/z 419.6991) is shown in part B (± 3 ppm) and the XIC of diverse product ions, assigned in Table SI 2 and Figure SI 3, are shown in part D (m/z 105.0369), F (m/z 137.0089), H (m/z 725.3070), J (m/z 611.2640) and L (m/z 510.2163) (± 10 ppm). No interferences were observed in the blank (A, C, E, G, I, K).

Figure SI 4

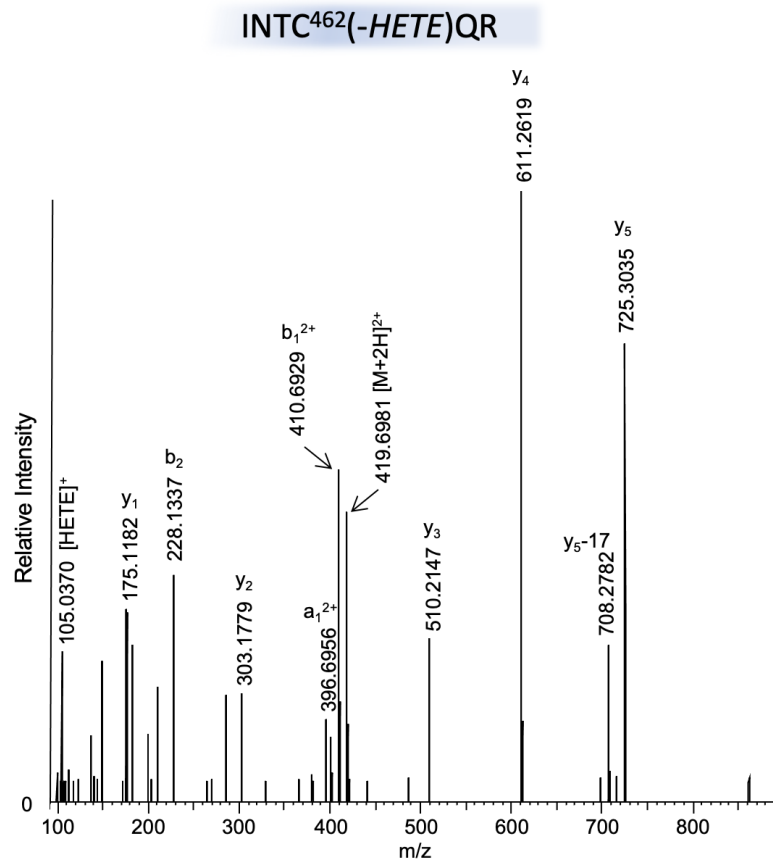


Figure SI 4: MS/HR MS spectrum of INTC⁴⁶²(-HETE)QR containing the alkylated Cys⁴⁶²

The spectrum was extracted from a μ LC-ESI MS/HR MS run showing the alkylated peptide eluting at t_R 7.28 min (Fig. SI 3). The sample was obtained from HEK-A1 cells exposed to SM for 1 h followed by IMS and trypsin-cleavage. Labelled signals were assigned to product ions as indicated and listed in detail in Table SI 2. Due to minor intensity, the signal at m/z 137.0089 is not labelled. When compared to their theoretical mass, all ions had a mass difference typically below 5.3 ppm.

Figure SI 5

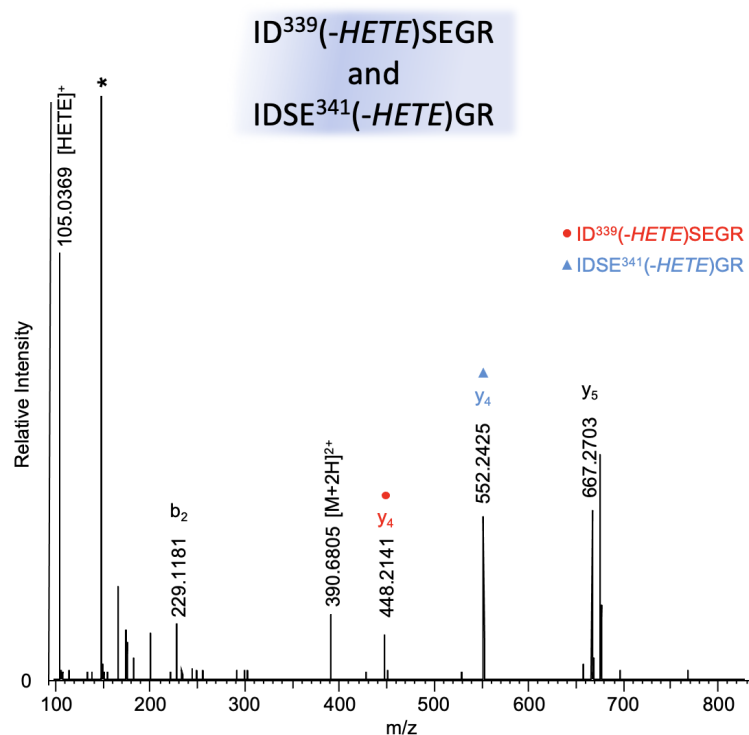


Figure SI 5: Mixed MS/HR MS spectrum of ID³³⁹(-HETE)SEGR containing the alkylated Asp³³⁹ and of IDSE³⁴¹(-HETE)GR containing the alkylated Glu³⁴¹

Due to coelution of the adducted peptides, the mixed spectrum was extracted from a μ LC-ESI MS/HR MS run showing two alkylated peptides eluting at t_R 7.49 min (Fig. 4). The sample was obtained from HEK-A1 cells exposed to SM for 1 h followed by IMS and trypsin-cleavage. Labelled signals were assigned to product ions as indicated (red circle only belonging to ID³³⁹(-HETE)SEGR and blue triangle only to IDSE³⁴¹(-HETE)GR). When compared to their theoretical mass, all ions had a mass difference typically below 5 ppm as listed in Table SI 3 and SI 4.

4 Paper II

Toxicology Letters 376 (2023) 51–59



Contents lists available at ScienceDirect

Toxicology Letters

journal homepage: www.journals.elsevier.com/toxicology-letters

Activation of the human TRPA1 channel by different alkylating sulfur and nitrogen mustards and structurally related chemotherapeutic drugs

Katharina Müller-Dott^{a,b}, Sarah Christine Raßmuß^a, Marc-Michael Blum^a, Horst Thiermann^a, Harald John^a, Dirk Steinritz^{a,b,*}

^a Bundeswehr Institute of Pharmacology and Toxicology, 80937 Munich, Germany

^b Walther-Straub-Institute of Pharmacology and Toxicology, Ludwig-Maximilians-University, 80336 Munich, Germany

ARTICLE INFO

Editor: Dr. Angela Mally

Keywords:

AP18
Bendamustine
Calcium
Chemical warfare agents
O-mustard
Sesquimustard

ABSTRACT

An important target in toxicology is the ion channel known as human transient receptor potential ankyrin 1 (hTRPA1). It is triggered by a variety of chemicals, including the alkylating chemical warfare agent sulfur mustard (SM). The activation potentials of structural analogs including O- and sesquimustard, nitrogen mustards (HN1, HN2, and HN3), and related chemotherapeutic drugs (bendamustine, cyclophosphamide, and ifosfamide) were examined in the current study. The aequorin assay was used to measure changes in intracellular calcium levels in human hTRPA1 overexpressing HEK293 cells. The XTT assay was used to determine cytotoxicity. The data presented here highlight that all investigated alkylating substances, with the exception of cyclophosphamide and ifosfamide, cause the activation of hTRPA1. Cytotoxicity and activation of hTRPA1 were found to be related. Compounds with high reactivity had higher cytotoxicity and vice versa. However, inhibiting hTRPA1 with the specific inhibitor AP18 could not reduce the cytotoxicity induced by alkylating agents. As a result, hTRPA1 does not play a significant role in the cytotoxicity of alkylating agents.

1. Introduction

Sulfur mustard (SM) is a chemical warfare agent that was deployed for the first time in World War I (Balali-Mood and Hefazi, 2005; Kehe and Szincz, 2005; Paromov et al. 2007). Although the use of chemical warfare agents is prohibited by Chemical Weapons Convention (CWC) that is controlled by the Organisation for the Prohibition of Chemical Weapons (OPCW), SM was deployed in various conflicts such as in the Syrian Arab Republic deployed by the terroristic group so called "Islamic state" (John et al. 2019; Sezigen et al. 2019). Various organs including skin, eyes and lungs are affected by SM (Kehe and Szincz, 2005;

Wattana and Bey, 2009; Ghabili et al. 2011; Rose et al. 2018; Müller-Dott et al. 2020). Toxicity is attributed to covalent modifications of various biomolecules, including proteins, lipids, and DNA, resulting in intra- and interstrand crosslinks (Ludlum et al. 1994; Kehe and Szincz, 2005). Among the targets are human transient receptor potential ankyrin 1 (hTRPA1) channels that were shown to be activated by SM and its monofunctional analogue 2-chloroethyl ethyl sulfide (CEES) (Stenger et al. 2015; Müller-Dott et al. 2022).

TRPA1 is a member of the family of chemosensory transient receptor potential (TRP) ion channels. It features a characteristic ankyrin repeat sequence at the N-terminus and is activated by different stimuli

Abbreviations: AITC, allyl isothiocyanate; AP18, 4-(4-chlorophenyl)-3-methyl-3-buten-2-one oxime; AU, absorbance units; $[Ca^{2+}]_i$, intracellular calcium concentration; CaM, Calmodulin; CEES, 2-chloroethyl ethyl sulfide; CWC, Chemical Weapons Convention; DCM, dichloromethane; DMEM, Dulbecco's modified eagle medium; DMSO, dimethyl sulfoxide; DTT, 1,4-dithiothreitol; FBS, fetal bovine serum; HEK-A1, HEK293 cells stably expressing hTRPA1; HEK-wt, HEK293 wildtype; HN1, bis(2-chloroethyl)ethylamine; HN2, bis(2-chloroethyl)methylamine; HN3, tris(2-chloroethyl)amine; hTRPA1, human transient receptor potential ankyrin 1; LC₅₀, lethal concentration resulting in 50% cell viability; NM, nitrogen mustards; NMR, nuclear magnetic resonance; OPCW, Organisation for the Prohibition of Chemical Weapons; PBS, phosphate buffered saline; PBS/Tween, 1x PBS containing 0.1% (v/v) Tween-20; PCR, polymerase chain reaction; P/S, penicillin/streptomycin solution; PVDF, polyvinylidene difluoride; Q, sesquimustard, 1,2-bis(2-chloroethylsulfanyl) ethane; RT, room temperature; SDS-PAGE, sodium dodecyl sulfate-polyacrylamide gel electrophoresis; SM, sulfur mustard, bis(2-chloroethyl) sulfide; T, O-mustard, bis(2-(2-chloroethylsulfanyl)ethyl)ether; TCEP-HCl, tris(2-carboxyethyl)phosphine-hydrochloride; TRP, transient receptor potential; XTT, 2,3-bis-(2-methoxy-4-nitro-5-sulphophenyl)-2 H-tetrazolium-5-carboxanilide.

* Correspondence to: Neuherbergstr. 11, 80937 Munich, Germany.

E-mail addresses: k.muellerdott@campus.lmu.de (K. Müller-Dott), s.rassmuss@labor-becker.de (S.C. Raßmuß), mblum@blum-scientific.de (M.-M. Blum), horstthiermann@bundeswehr.org (H. Thiermann), haraldjohn@bundeswehr.org (H. John), dirksteinritz@bundeswehr.org (D. Steinritz).

<https://doi.org/10.1016/j.toxlet.2023.01.007>

Received 4 November 2022; Received in revised form 11 January 2023; Accepted 20 January 2023

Available online 21 January 2023

0378-4274/© 2023 The Authors. Published by Elsevier B.V. This is an open access article under the CC BY-NC-ND license (<http://creativecommons.org/licenses/by-nc-nd/4.0/>).

including heat, mechanical stress and a variety of chemicals (Bandell et al. 2004; Wang and Woolf, 2005; Andersson et al. 2008). Therefore, hTRPA1 channels attracted notice as chemo- and nociceptor (Bandell et al. 2004; Bautista et al. 2005; Macpherson et al. 2006, 2007) and are associated with pain sensations or cough reflexes (Story et al. 2003; Bandell et al. 2004).

Although Stenger et al. (2015, 2017) have clearly proven SM-induced activation by SM, this finding has been under debate because SM is not known to cause immediate pain in vivo (Kehe and Szinicz, 2005). For this reason, this work aims to validate the hTRPA1 activation by SM-related alkylating compounds in vitro. The agents and compounds used included additional types of SM-related compounds such as sesquimustard (Q) and O-mustard (T) (Fig. 1A) (Gasson et al. 1948), nitrogen mustards (NM), namely bis(2-chloroethyl)ethylamine (HN1), bis(2-chloroethyl)methylamine (HN2) and tris(2-chloroethyl)amine (HN3) (Fig. 1B), as well as the NM-based chemotherapeutics bendamustine, cyclophosphamide and ifosfamide (Fig. 1C) (Singh et al. 2018; Dixit et al. 2023).

Both Q and T are SM-related compounds that were found to be much more toxic than SM: Q was first synthesized in 1921 (Bennett and Whincop, 1921) and revealed an increase in blister formation by a factor of five compared to SM (Gasson et al. 1948). T was first synthesized in the 1930 s and is 3.5 times more vesicant than SM (Watson and Griffin, 1992).

HN1, HN2 and HN3 were also synthesized in the 1920 s and 1930 s. Their alkylating and toxic properties were found to be comparable to those of SM (Kehe and Szinicz, 2005). Although intended as chemical warfare agents, NM have never been deployed in any conflict. Instead, HN1 was used to treat warts, while HN2 and HN3 were introduced as antineoplastic drugs in cancer treatment (Gilman, 1963; Mattes et al. 1986; DeVita and Chu, 2008; Mangerich and Esser, 2014; Singh et al. 2018). Severe side effects of the original NM resulted in the synthesis of better tolerated derivatives such as bendamustine, cyclophosphamide or ifosfamide that were used as chemotherapeutic drugs (Cheson and Rummel, 2009).

Bendamustine is a therapeutic drug for the treatment of chronic lymphocytic leukemia and multiple myeloma. Like SM, it is an alkylating compound resulting in DNA cross-links (Cheson and Rummel, 2009;

Chang and Kahl, 2012; Gentile et al. 2015; Lehmann and Wennerberg, 2021). Cyclophosphamide and ifosfamide, used for the treatment of various cancers, are prodrugs that require cytochrome P450-mediated activation, primarily in the liver (Zhang et al. 2008). All three chemotherapeutic drugs can cause exhaustion, nausea, vomiting, coughing, skin irritation, or hoarseness, symptoms that are very similar to those caused by SM. Burning, numbness and unpleasant feelings have also been reported (Zhang et al. 2008; Cheson and Rummel, 2009).

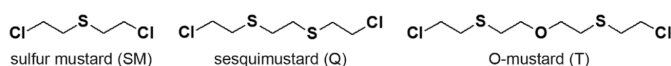
All agents and compounds described above have alkylating properties and thus, might also activate hTRPA1 and contribute to cytotoxicity as it has been reported and proposed for SM (Stenger et al. 2015). This aspect was assessed in the present study by addressing the following questions: i) is hTRPA1 also activated by other alkylating agents than SM? ii) does hTRPA1 activation correlate with cytotoxicity? and iii) does pre-treatment with a hTRPA1 specific antagonist attenuate cytotoxicity caused by the alkylating agents and compounds? To answer these questions, a hTRPA1-overexpressing HEK293 (HEK-A1) cell line was used. The calcium-sensitive photoprotein aequorin was used to study changes in intracellular calcium concentration ($[Ca^{2+}]_i$) as an effect of hTRPA1 activation. Cytotoxicity was evaluated using a cell viability assay (XTT, 2, 3-bis-(2-methoxy-4-nitro-5-sulphophenyl)-2 H-tetraazolium-5-carboxanilide).

2. Material and methods

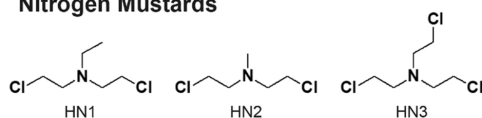
2.1. Material

Dulbecco's Modified Eagle Medium (DMEM) containing 4.5 g/L D-glucose, L-glutamine and pyruvate, fetal bovine serum (FBS), phosphate buffered saline (PBS) pH 7.4, penicillin/streptomycin solution (P/S) and 0.05% trypsin EDTA were all from Gibco by Life Technologies (Darmstadt, Germany). E-gel EX 1%, E-gel 1 kb plus express DNA ladder, NuPAGE MES SDS running buffer (20x), NuPAGE transfer buffer (20x), 4–12% Bis-Tris gels, as well as polyvinylidene difluoride (PVDF) membrane 0.2 μ m pore size were purchased from Invitrogen by Life Technologies (Karlsruhe, Germany). Casy ton was obtained from OMNI Life Sciences (Bremen, Germany). Digitonin, tris(2-carboxyethyl)phosphine-hydrochloride (TCEP-HCl), Tween-20, NaCl, allyl isothiocyanate

A Sulfur Mustards



B Nitrogen Mustards



C NM-based Chemotherapeutics

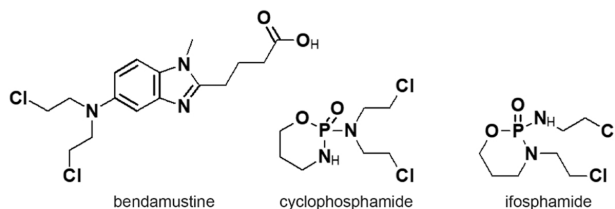


Fig. 1. Overview of the chemical structure of the different alkylating agents used in the present study. (A) Sulfur mustard (bis(2-chloroethyl) sulfide, SM), sesquimustard (1,2-bis(2-chloroethylsulfanyl) ethane, Q) and O-mustard (bis(2-(2-chloroethylsulfanyl)ethyl)ether, T) are characterized by two reactive side chains with chlorine atoms at both ends. (B) Nitrogen mustards such as HN1 (bis(2-chloroethyl)ethylamine), HN2 (bis(2-chloroethyl)methylamine) and HN3 (tris(2-chloroethyl)amine) are tertiary amines with vesicant activity (National Defense Research Committee, 1946). (C) The nitrogen mustard-based chemotherapeutics bendamustine, cyclophosphamide and ifosfamide have structural similarities to alkylating agents and purine analogs (Cheson and Rummel, 2009). Cyclophosphamide and ifosfamide belong to the group of phosphoramidate mustards (Lehmann and Wennerberg, 2021).

(AITC), dimethyl sulfoxide (DMSO), 1,4-dithiothreitol (DTT), NH_4HCO_3 , bendamustine, cyclophosphamide, ifosfamide, isopropanol and ethanol were purchased from Sigma-Aldrich (Steinheim, Germany). Dichloromethane (DCM, $\geq 99.8\%$ SupraSolv®) was from Merck (Darmstadt, Germany). Tris, HCl and sodium hypochlorite (NaOCl) solution for decontamination (12% Cl_2) were obtained from Carl Roth (Karlsruhe, Germany). Chameleon Duo marker, 4x protein loading dye, intercept blocking buffer PBS and IR Dye 800CW goat anti-rabbit antibody were obtained from LI-COR Biosciences (Bad Homburg, Germany). The primary antibody against hTRPA1 (DyLight 549) was from Abnova (Taipei, Taiwan). Cell proliferation kit II (XTT) was obtained from Roche Diagnostics GmbH (Mannheim, Germany). The RNeasy mini kit, the RT² first-strand kit, and the HotStar Taq plus master mix were both from Qiagen (Hilden, Germany). The forward (5'-TGTTTCTCAGTGACCA-CAAT-3') and reverse (5'-CTGTGAAGCATGGTCTCATGA-3') primer sequences utilized for hTRPA1 mRNA detection were delivered from Eurofins Genomics GmbH (Ebersberg, Germany). PromoFectin was purchased from PromoCell (Heidelberg, Germany). The coelenterazine was from p.j.k. (Kleinbittersdorf, Germany) and 4-(4-chlorophenyl)-3-methyl-3-buten-2-one oxime (AP18) was from Tocris Bioscience (Bristol, UK). The German Ministry of Defense made available HN1, HN2, HN3 and SM (purity of SM > 99%, assessed in-house by nuclear magnetic resonance (NMR) spectroscopy). T and Q were synthesized by chlorination of respective diol-compounds (Kaushik and Rana, 2005). Molecular structure and purity (> 95%) were confirmed by ¹H- and ¹³C NMR spectroscopy. Stock solutions of T and Q (150 mM) were prepared in DCM.

2.2. Cell culture

HEK293 wild-type cells (HEK-wt) and HEK-A1 cells, stably expressing the hTRPA1 channel, were kindly donated by the Walther-Straub-Institute (Ludwig-Maximilians-University, Munich, Germany). All cells were cultured in DMEM containing 1% (v/v) P/S and 10% (v/v) FBS in a humidified atmosphere at 37 °C and 5% (v/v) CO_2 (standard conditions). Splitting was performed every two to three days when cells attained 70–80% confluency. For detachment, cells were rinsed with 10 mL of PBS before 2 mL of trypsin was added for 2 min at 37 °C and 5% (v/v) CO_2 . Afterwards, 18 mL DMEM was added to inactivate trypsin. The cell number was determined using a Casy cell counter and analyzer TT (Innovatis GmbH, Bremen, Germany). The cells were then used for subsequent experiments or cultured at 37 °C and 5% (v/v) CO_2 in Cell Star® T175 flask (Greiner Bio-One GmbH, Frickenhausen, Germany).

2.3. Polymerase chain reaction

For RNA isolation, 5×10^6 HEK-wt or HEK-A1 cells were used. The RNeasy mini kit was utilized according to the manufacturer's instructions. RNA concentration was measured spectrophotometrically with an Infinite M200 PRO photometer using a NanoQuant plate and the i-control software 1.8.50.0 (Tecan, Switzerland). To synthesize cDNA from RNA, the RT² first strand kit was utilized. In summary, a total of 500 ng RNA was mixed with 2 μL GE buffer and filled up with RNase-free water to a total volume of 10 μL . The genomic DNA elimination mix was incubated for 5 min at 42 °C followed by a cooling period at 5 °C for 1 min using a Mastercycler nexus GX2 (Eppendorf, Hamburg, Germany). In a next step, the reverse-transcription mix was prepared using 4 μL 5x BC3 buffer, 1 μL P2 control, 2 μL RE3 reverse transcriptase and 3 μL RNase free water. This was mixed with 10 μL of the before incubated genomic DNA elimination mix and incubated at 42 °C for 15 min, followed by 5 min at 95 °C to stop the reaction. The mixture was cooled to 4 °C and filled up with 91 μL RNase free water.

hTRPA1 cDNA was amplified with a HotStar Taq plus master mix according to the manufacturer's protocol. Specific hTRPA1 primers (forward: 5'-TGTTTCTCAGTGACCA-3'; reverse: 5'-

CTGTGAAGCATGGTCTCATGA-3') were used and diluted in RNase-free water to a final concentration of 0.5 μM . The polymerase chain reaction (PCR) started with an initial heat activation step at 95 °C for 5 min, followed by denaturation at 94 °C for 30 s, annealing at 55 °C for 30 s and extension at 72 °C for 1 min. After 30 cycles, the final extension was run at 72 °C for 10 min to fill incomplete ends. Finally, the PCR product was cooled to 4 °C and was separated using 1% agarose electrophoresis for 10 min. Gel images were recorded using an E-gel power snap and camera (Invitrogen by Life Technologies, Karlsruhe, Germany).

2.4. Lysis of cells

For cell lysis, a digitonin lysis buffer containing 20 mM Tris, adjusted to pH 8.0, 150 mM NaCl, 5 mM TCEP-HCl and 1% (w/v) digitonin was freshly prepared. The medium was removed from T175 cell culture flask before 2 mL of lysis buffer was added. After 1 h of incubation at 4 °C, cells were scraped off and transferred to a clean tube. The lysate was then vortexed several times and incubated on ice for 1 h. Cell lysates were centrifuged for 15 min at 14,000 RCF and supernatants were transferred to clean tubes and kept at – 80 °C.

2.5. Western blot

For Western blot experiments, 15 μL of either HEK-A1 or HEK-wt whole cell lysate was combined with 8 μL loading buffer (60 μL 4x loading dye and 40 μL of 500 mM DTT in water) and placed on 4–12% Bis-Tris gels. As a marker, 3 μL Chameleon Duo was utilized. Sodium dodecyl sulfate-polyacrylamide gel electrophoresis (SDS-PAGE) was performed in ice-cold 1x NuPAGE MES SDS running buffer at constant voltage (200 V) for 40 min. After SDS-PAGE, proteins were transferred to a 0.2 μm PVDF membrane using the wet blotting technique. The membrane was activated for 30 s in methanol and a 1x NuPAGE transfer buffer containing 20% methanol was used for blotting. Blotting was carried out for 1 h at 25 V. The membrane was then blocked for 1 h on an orbital shaker in 1x PBS blocking buffer. The anti-hTRPA1 DyLight 549 antibody (C_{final} 1 $\mu\text{g}/\text{mL}$) was utilized as a primary antibody and was diluted in 4 mL 0.2% (v/v) Tween-20 in 1x PBS blocking buffer. The membrane was incubated with the primary antibody overnight and was then washed twice for 10 min with 1x PBS containing 0.1% (v/v) Tween-20 (PBS/Tween). Incubation with the secondary goat anti-rabbit antibody, which was diluted 1:7500 in 11 mL of 0.2% (v/v) Tween-20 in 1x PBS blocking buffer, was performed for 1 h. Afterwards, the membrane was washed twice with PBS/Tween. Images were recorded on an Odyssey® DLx imaging system (LI-COR Biosciences) using the integrated Image studio 5.2 software.

2.6. Measurement of intracellular Ca^{2+} -levels using the aequorin assay

Changes in $[\text{Ca}^{2+}]_i$, as an indicator of hTRPA1 activation, were investigated using the aequorin assay. For transfection, 12 μg of the aequorin plasmid (1000 ng/ μL) and 12 μL PromoFectin were diluted each in 500 μL DMEM. The two solutions were thoroughly mixed. The DNA-PromoFectin mixture was allowed to incubate for 30 min at room temperature (RT). Meanwhile, cells were detached as described before (see section: 2.2 Cell culture). Afterwards, 1 mL of the DNA-PromoFectin solution was added to $3\text{--}4 \times 10^6$ HEK-A1 cells in suspension and transferred to a T25 flask. Cells were then incubated for 72 h at standard conditions. Cells were washed with 2 mL of PBS, detached with 0.5 mL of trypsin and resuspended in 4.5 mL of medium. The cell suspension was incubated with 5 μL coelenterazine (in DMSO, C_{final} 5 μM) in the dark for 15 min at RT. Cells were then centrifuged at 525 RCF for 5 min. The supernatant was removed and the cell pellet was resuspended in 5 mL of DMEM without additives. Subsequently, 190 μL of the cell suspension, containing 2.5×10^5 cells, was transferred into each well of a white 96-well plate (Greiner Bio-One GmbH). The plate was placed in the pre-heated Infinity M200 PRO photometer (37 °C,

integration time 1000 ms). After recording the baseline for 10 s, 10 μL of the putative agonist was injected into a single well and luminescence was recorded for at least 75 s

AITC (freshly prepared to a final concentration of 25 μM) served as a positive control. All alkylating agents were dissolved in DCM (150 mM stock solution) and the dilutions were freshly prepared in DMEM immediately before injection. Final concentrations were 75 μM , 112.5 μM , 150 μM and 187.5 μM for SM, T and Q, each. Since the equimolar concentrations of NM and chemotherapeutic compounds did not show significant changes in $[\text{Ca}^{2+}]_i$, the final concentrations of all NM and chemotherapeutics were 666.7 μM , prepared from a 400 mM stock solution. For experiments using the hTRPA1 specific antagonist AP18, preincubation of the cell suspension was performed with AP18 to a final concentration of 40 μM . The preincubated suspension was then transferred to a white 96-well plate and after 10 s, 10 μL of the agonist solution was injected into each well. Changes in $[\text{Ca}^{2+}]_i$ were measured as previously described.

2.7. Cell viability assay

Cell viability was determined using the XTT assay. In summary, 50,000 HEK-A1 or HEK-wt cells were seeded into each well of a 96-well plate. After 24 h, cell culture medium was removed and 80 μL of fresh medium was added to each well. Mustard agents were diluted in DCM, while NM were diluted in 100% isopropanol containing 4 mg/mL of NH_4HCO_3 , and chemotherapeutics were directly dissolved in DMEM. A second dilution (1:2) was prepared in preheated medium. To minimize hydrolysis, 80 μL of the final stock solutions were immediately transferred to the respective wells. Final concentrations of SM, HN1, HN2 and HN3 ranged from 0.05 μM to 3000 μM . For T and Q final concentrations were between 3.13 μM and 2400 μM , and for all chemotherapeutics from 0.029 mM to 30 mM. A permeable seal was applied to the 96-well plate which was then incubated for 24 h under standard conditions. In the case of pre-treatment with AP18, the hTRPA1 inhibitor was added prior to the medium with a final concentration of 40 μM AP18.

After 24 h, the medium was removed and the XTT assay was performed according to the manufacturer's protocol. In brief, 150 μL of an XTT-master mix (10.2 mL medium, 5 mL XTT-solution and 100 μL XTT-coupling reagent) was added to each well. The plate was incubated under standard conditions until the measured absorbance at 450 nm (Infinite M200 PRO photometer, 9 nm bandwidth, 15 flashes per well) reached values between 1.3 absorbance units (AU) and 1.7 AU for the negative control. Absorbance at the reference wavelength 630 nm was subtracted.

2.8. Correlation between human TRPA1 activation and cytotoxicity

To facilitate a comparison of the maximum activation of hTRPA1 caused by the different agonists, a normalization was calculated as follows: the maximum amplitude of the respective group was identified and divided by the concentration of the agonist. Results for SM were set to 1 and all other values were normalized accordingly. The concentration decreasing cell viability to 50% (lethal concentration 50, LC_{50}) of each compound was calculated. The calculated value was subtracted from 1, followed by a normalization to the LC_{50} of SM, which was thereby set to 1. The activation-cytotoxicity ratio was calculated by dividing the values of normalized activation by normalized cytotoxicity. The mean value was calculated by dividing the mean activation of hTRPA1 by the mean cytotoxicity value. Lower limits were determined by dividing the lowest activation value by the lowest cytotoxicity value and vice versa.

2.9. Statistics

GraphPad Prism v9.3.1 (San Diego, USA) was used to calculate non-linear curve fitting (log(inhibitor) vs. response-variable slope, top

constraint = 100, bottom constraint = 0) for XTT data. The LC_{50} and the corresponding 95% confidence interval were calculated from the fitted curve. R statistical software (R Core Team, 2022) with RStudio (R Studio Team, 2022) was used for all other statistical calculations. Graphical output was done using ggplot from the tidyverse package (Wickham et al. 2019).

3. Results and discussion

In the present study, we evaluated hTRPA1 activation by SM and SM-related alkylating agents, different NM as well as NM-derived chemotherapeutics. Furthermore, an activation-cytotoxicity index was calculated to correlate hTRPA1 activation and cytotoxicity. Finally, the effect of the hTRPA1 specific antagonist AP18 on agent-induced cytotoxicity was assessed.

3.1. Human TRPA1 expression in overexpressing HEK-A1 cells

hTRPA1 expression in HEK-A1 cells was investigated by PCR and Western blot technique. HEK-wt cells, that do not express hTRPA1, were used as negative control. A specific hTRPA1 mRNA band at approx. 600 bp was found in HEK-A1 cells while no signal was detected in HEK-wt cells (Fig. 2A). At the protein level, a characteristic double band for hTRPA1 was detected in HEK-A1 cells at approximately 125 kDa corresponding to the molecular weight of the channel (Virk et al. 2019). The double band was most likely generated by posttranslational modifications not further specified in the literature (UniProt No. O75762). As expected, no bands were observed in HEK-wt cells, indicating that hTRPA1 was not expressed in these cells (Fig. 2B).

3.2. Human TRPA1 activation by different alkylating agents

hTRPA1 activation was determined using an aequorin luminescence-based functional calcium assay to measure changes in $[\text{Ca}^{2+}]_i$. Aequorin, a calcium sensitive photoprotein derived from the jellyfish *Aequorea victoria*, has been intensively studied as a calcium indicator in cells (Shimomura et al. 1974; Kendall and Badminton, 1998). Although the aequorin assay is more technical than the fluorescence-based Fura-2 AM assay, it was chosen since Fura-2 is directly impacted by SM (Stenger et al. 2015). The aequorin test, on the other hand, might be difficult to interpret and compare between studies: Strong and rapid rises in $[\text{Ca}^{2+}]_i$ can result in steep response curves, whereas delayed responses to applied stimuli result in sigmoidal-shaped curves. Furthermore, a drop in luminescence signal might be produced by a decrease in $[\text{Ca}^{2+}]_i$ or low coelenterazine levels. A lack of coelenterazine can be ruled out in our experiments because the hTRPA1-specific agonist AITC (Bandell et al. 2004; Hinman et al. 2006), which was used as positive control, caused luminescence signals greater than in all other alkylating agents tested (Suppl. Fig. S1). Ethanol tested as solvent control had no effect on $[\text{Ca}^{2+}]_i$, demonstrating that the detected signal for AITC was caused by

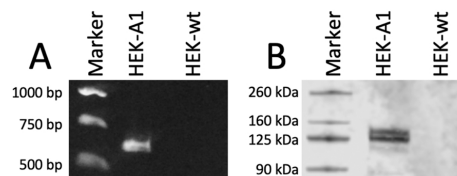


Fig. 2. : hTRPA1 mRNA and protein in HEK-A1 and HEK-wt cells. (A) Detection of hTRPA1 mRNA expression by PCR in HEK-A1 and HEK-wt cells revealed specific mRNA expression in HEK-A1, but not in HEK-wt cells. (B) Western blot of HEK-A1 and HEK-wt protein lysates using an anti-hTRPA1 antibody revealed a characteristic double band for hTRPA1 at 125 kDa in HEK-A1, but not in HEK-wt cells.

changes in $[Ca^{2+}]_i$, confirming hTRPA1 activation. Further solvent controls such as DCM, DMEM and HCl did also not effect $[Ca^{2+}]_i$ (Suppl. Fig. S1).

Since CEES and SM have already been shown to activate the hTRPA1 channel (Stenger et al. 2015), it was assumed that SM-related alkylating agents such as T and Q, as well as NM and chemotherapeutic agents would likewise activate the hTRPA1. Due to the high lipophilicity of the solvent DCM and to reduce the final solvent concentration during the measurement, the highest possible concentration of the agent was 187.5 μ M. Thus, final concentrations of the mustard agents were 75 μ M,

112.5 μ M, 150 μ M and 187.5 μ M. To validate that the changes in $[Ca^{2+}]_i$ were specifically mediated by hTRPA1, the hTRPA1-specific antagonist AP18 was used.

After injection, each SM concentration showed an increase in the luminescence signal indicating an increase in $[Ca^{2+}]_i$ as already documented by Stenger et al. (2015) (Fig. 3A). After exposure to either 187.5 μ M T or Q, maximum levels were induced 5–10 s after injection and furthermore resulted in a long-lasting signal with comparable levels of luminescence. Even after about 80 s, the baseline was not reached. Similar peak intensities were recorded, showing that T and Q have

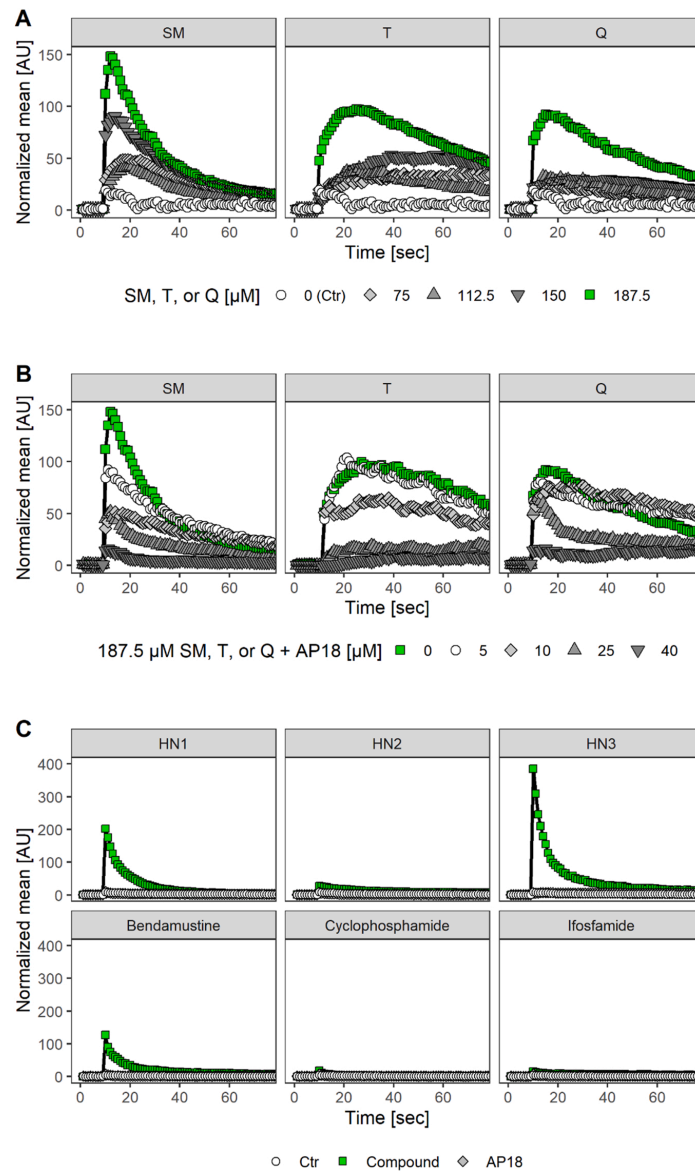


Fig. 3. : Changes in $[Ca^{2+}]_i$ after exposure to different alkylating agents.

comparable potencies, while the maximum signal was lower when compared to SM. In general, SM and T concentrations ranging from 75 μM to 150 μM resulted in a dose-dependent decrease of $[\text{Ca}^{2+}]_i$. In the case of Q, similar peak intensities were measured for 75 μM , 112.5 μM and 150 μM Q. The amplitude at 187.5 μM Q was twice as large as at concentrations between 75 M and 150 M Q, as shown in Fig. 3A. Furthermore, the solvent control DCM revealed minimal changes in $[\text{Ca}^{2+}]_i$ for around 10 s after injection, suggesting that hTRPA1 was mechanically activated (Story and Gereau, 2006; Petrus et al. 2007) (Suppl. Fig. S1). Taken together, the effects of SM, Q, and T on hTRPA1 activation were convincingly demonstrated (Fig. 3A). Long-lasting signals for T and Q may imply an irreversible alteration at the hTRPA1 channel, as demonstrated by Hinman et al. (2006) who observed that currents induced by N-methyl maleimide persisted. SM-induced protein modifications are thought to be fairly persistent (John et al. 2019) and Blum et al. (2020) showed enhanced reactivity of Q with cysteine residues in human serum albumin. This could explain the long-lasting hTRPA1 activation observed as a result of persistent protein modifications generated by Q within the hTRPA1 channel. The mustard agents did not reach the peak intensity of AITC (25 μM , maximum peak intensity 1500 AU, Suppl. Fig. S1), indicating a lower potency of the tested compounds, as previously reported by Stenger et al. for SM (2015).

Experiments were repeated using the highest concentration of 187.5 μM SM, T and Q in the presence of the specific hTRPA1 antagonist AP18 to validate that the recorded signals were related to hTRPA1 activation (Fig. 3B). AP18 concentrations were chosen between 5 μM and 40 μM because 5 μM had only minimal effect on agonist-induced activation while 40 μM resulted in full blocking. The use of 10 μM and 25 μM AP18 reduced the elevation of $[\text{Ca}^{2+}]_i$ caused by SM, Q and T. With 25 μM AP18 pre-treatment before T exposure or 40 μM AP18 for SM and Q, full hTRPA1 inhibition was observed. In general, when AP18 concentrations increased, the luminescence signal diminished in a dose-dependent manner.

Following that, the activation of hTRPA1 by the structurally related NM alkylating agents HN1, HN2, and HN3, as well as the NM-related chemotherapeutics bendamustine, cyclophosphamide, and ifosfamide, was investigated (Fig. 3C). We concentrated on SM-related mustard agents in this investigation. Experiments with NM and NM-based chemotherapeutics were conducted as proof of concept, and hence just a single concentration was employed to demonstrate hTRPA1 activation. Concentrations comparable to those used in mustard agent experiments had no effect on $[\text{Ca}^{2+}]_i$. However, at 666.7 μM , a distinct response was seen. The NM-induced activation was assessed once more following pre-treatment with 40 μM AP18. The absence of the previously detected signals proved that NM-induced hTRPA1 activation was the cause of them. Since all of the NM and bendamustine were obtained in their hydrochloride form, equimolar amounts of HCl were also used to exclude an activation effect of HCl. Since the HCl signals resembled those of the negative control, they could be neglected. (Suppl. Fig. S1).

HN1 and HN3 demonstrated a significant increase in relative luminescence that was absent in the presence of AP18. HN3 had a higher activation potential than HN1. For HN2, only slight but still noticeable increases in $[\text{Ca}^{2+}]_i$ were detected. HN3s chemical structure may increase its reactivity with the hTRPA1 channel. HN3 has an additional chloroethyl group as a side chain, giving it three reactive side chains, whereas HN1 only has an ethyl group and HN2 only has a methyl group. As a result, HN1 and HN2 only contain two reactive side chains (DeVita and Chu, 2008; Lehmann and Wennerberg, 2021). As a result, the additional reactive side chain in HN3 may increase the activation potential of hTRPA1 when compared to HN1 and H2. Furthermore, hydrolysis of HN3 is thought to be lower than that of HN1 and HN2 (Munro et al. 1999). This could result in longer-lasting HN3 concentrations at hTRPA1 locations, resulting in the rise in $[\text{Ca}^{2+}]_i$ seen in our study. However, NM did not provide a long-lasting signal as compared to mustard agents. The low activation potential of HN2 was unexpected,

but it was found repeatedly without a clear explanation.

Furthermore, the activation of hTRPA1 by three alkylating chemotherapeutics was investigated. Bendamustine increased relative luminescence to a level moderately lower than the maximal level of HN1. There were no changes in $[\text{Ca}^{2+}]_i$ with ifosfamide or cyclophosphamide. Because the two prodrugs require metabolic activation by cytochrome P450 enzymes (Zhang et al. 2008), neither cyclophosphamide nor ifosfamide were expected to directly activate hTRPA1. No changes in $[\text{Ca}^{2+}]_i$ were observed after AP18 pre-treatment, indicating that the observed activation mediated by bendamustine exposure was hTRPA1 specific.

The lower efficacy of SM, T, and Q might indicate that AITC and the alkylating compounds target alternative amino acid residues in hTRPA1. AITC, according to Hinman et al. (2006), primarily targets the three cysteines Cys⁶²¹, Cys⁶⁴¹, and Cys⁶⁶⁵ that are essential for activation by sulphydryl-selective electrophiles. Müller-Dott et al. (2022) demonstrated that SM also targets Cys⁶⁶⁵ and additionally Cys⁶⁶², but not Cys⁶⁴¹. Since Cys⁶²¹ was not detected in that study, it is unknown whether SM alkylates this residue. However, additional modifications of aspartic acid and glutamic acid residues of hTRPA1 were observed following SM exposure (Müller-Dott et al. 2022). Q and T are also expected to alkylate the SM-targeted amino acid residues, but this has yet to be studied. Future research should also identify the amino acid residues that are targeted by the N-alkylating compounds.

The intracellular downstream effect of hTRPA1 activation may be related to the Ca^{2+} -levels attained and hence differs between AITC and alkylating agents. Calmodulin (CaM), for example, has been shown to bind to TRPA1 channels (Hasan et al. 2017), and the lobes of CaM can selectively decode Ca^{2+} in different ways due to their varying spatial affinities to Ca^{2+} (Ben-Johny and Yue, 2014). Furthermore, Ca^{2+} -ions are the most significant endogenous regulators of hTRPA1, enhancing and inhibiting its activity in response to chemical stimulus (Hu et al. 2021). Thus, future research should investigate the signaling that arises when hTRPA1 is stimulated by diverse stimuli with varying calcium levels.

Changes in $[\text{Ca}^{2+}]_i$ were measured in HEK-A1 cells using aequorin assay. Injection of the freshly prepared agents/compounds was performed after 10 s. The graphs show the mean values of the baseline corrected data. All experiments were conducted with $n = 3$. (A) Luminescence measurement after injection of SM, T or Q in concentrations of 75 μM (rhombus), 112.5 μM (triangle), 150 μM (upside down triangle) and 187.5 μM (green square) SM. All concentrations used showed an increase in $[\text{Ca}^{2+}]_i$, clearly demonstrating activation of hTRPA1. The solvent control (DCM, circle) was measured in the absence of an alkylating agent and was labeled "ctr". (B) Measurement of luminescence after injection of 187.5 μM SM, T, or Q (named AP18 Q, green squares) after pre-treatment with AP18 in the concentrations of 5 μM (circle), 10 μM (rhombus), 25 μM (triangle) and 40 μM (upside down triangle) AP18. Increasing AP18 concentrations resulted in a decrease in luminescence. The highest AP18 concentration prevented $[\text{Ca}^{2+}]_i$ and indicating that hTRPA1 was completely blocked. (C) Luminescence measurement after injection of HN1, HN2, HN3, bendamustine, cyclophosphamide and ifosfamide in the concentrations of 666.7 μM (green squares) and pre-treatment with 40 μM AP18 (rhombus). An increase in the luminescence signal was observed for all three nitrogen mustards and bendamustine, indicating hTRPA1 activation. Incubation with AP18 prevented changes of $[\text{Ca}^{2+}]_i$ (circle).

3.3. Cytotoxicity of alkylating agents

To examine the cytotoxicity of the various alkylating agents, cell viability was assessed using the XTT assay. Table 1 summarizes the calculated LC_{50} values, indicating a 50% reduction of in vitro cell viability, and the related 95% confidence intervals of the non-linear curve fit at the LC_{50} . When compared to HEK-wt cells, HEK-A1 cells were significantly more susceptible to SM, Q, and all NM. LC_{50} of T

Table 1

Cytotoxicity of different alkylating substances in HEK-A1 and HEK-wt cells and protective effect of AP18 in HEK-A1 cells using the XTT assay. LC₅₀ values and the corresponding 95% confidence interval are shown, values marked with * show significant difference compared to HEK-A1 cells. All experiments were conducted with n = 3.

	HEK-A1		HEK-A1 40 μM AP18		HEK-wt	
SM	66.8	(50.4–87.4)	101.5	(66.9–157.1)	247.6	(155.2–412.0)*
T	131.5	(86.5–200.7)	38.4	(27.1–54.1)*	241.5	(169.0–347.8)
Q	42.2	(30.9–57.6)	24.8	(16.8–36.1)	170.3	(123.6–237.6)*
HN1	215.1	(170.5–273.1)	154.1	(119.5–199.6)	624.1	(445.4–905.2)*
HN2	91.2	(75.0–111.3)	124.8	(94.5–166.4)	380.2	(258.7–577.3)*
HN3	232.9	(205.0–264.8)	440.6	(299.7–663.0)*	661.6	(529.5–837.3)*
Bendamustine	687.4	(506.8–971.6)	1784	(1069–3287)*	1160	(853.0–1743)
Cyclophosphamide	19,793	(17,430–22,559)	21,169	(15,583–19,496)	14,440	(17,902–25,204)
Ifosfamide	13,926	(12,693–15,286)	13,245	(11,646–15,124)	17,283	(15,033–19,946)

varied by nearly a factor two from SM, but failed to reach significance due to variance in both groups. In the Supplementary, Figs. S2 provide dose-response curves as well as a graphical representation of the calculated LC₅₀ values in HEK-A1 cells. The greater toxicity of Q in contrast to SM might be attributed to its enhanced reactivity, as demonstrated by Blum et al. (2020) for cysteine residues in human serum albumin. In our investigation, the cytotoxicity of HN2 was shown to be equivalent to that of SM. This finding is consistent with the findings of Mangerich et al. (2016). Our in vitro findings are consistent with the toxicity observed in mice after percutaneous exposure to HN1, HN2, and HN3: HN2 was found to be more harmful than HN1 and HN3 (Emadi et al. 2012). When compared to other alkylating compounds, the cytotoxicity of the examined chemotherapeutics was reduced. The cytotoxicity of the pro-drugs ifosfamide and cyclophosphamide was essentially non-existent, as predicted, but bendamustine as an active agent was obviously cytotoxic.

3.4. Correlation between human TRPA1 activation and cytotoxicity

Because the concentrations of the various agonists differed, the aquorin assay results had to be normalized to the concentrations of the agonist. A correlation between hTRPA1 activation (relative potencies)

and cytotoxicity was feasible using this approach (Fig. 4). Almost all alkylating agents exhibited a relationship between hTRPA1 activation and cell viability: cytotoxicity increased synchronously with hTRPA1 activation. Only Q and HN2, and to a lesser extent HN3, did not precisely adhere to that correlation. Q was more cytotoxic than SM but had almost the same activation potential. HN2, on the other hand, demonstrated comparable cytotoxicity to SM but no comparable activation potential of hTRPA1 (Fig. 4A). An activation-cytotoxicity ratio was calculated to illustrate the relationship between hTRPA1 activation and cytotoxicity. The results for SM, which was used as the reference compound, were calculated with a lower threshold of 0.4 and a 2.2-fold higher threshold (shown in gray in Fig. 4B). If the estimated mean value of the various substances was between the lower and upper thresholds, a comparable ratio was assumed, demonstrating a link between activation potential and cytotoxicity. Except for HN2, all of the alkylating agents investigated had ratios that were equivalent to SM. Bendamustine's cytotoxicity was rather modest, which explains the variation in the calculated ratio. The lower HN3 threshold was within the range of the computed SM threshold limits and hence was not regarded substantially different. Only HN2 differed significantly, which can be explained to the lack of hTRPA1 activation.

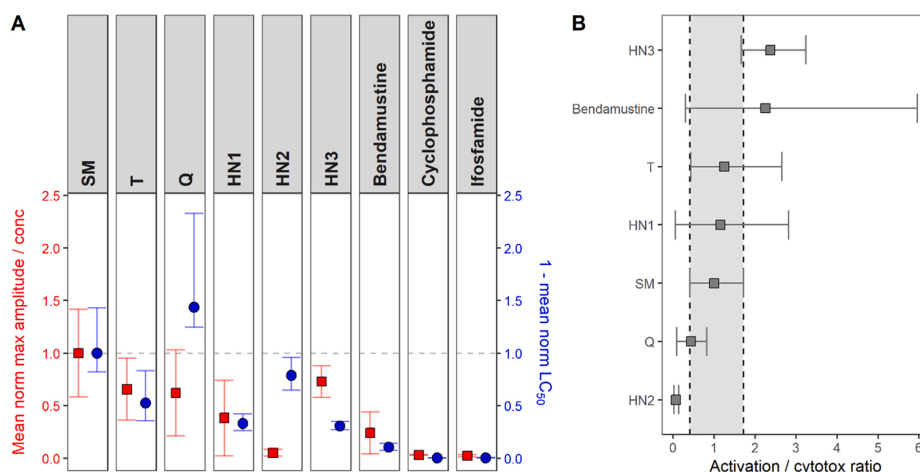


Fig. 4. Correlation of normalized activation potential and normalized LC₅₀ values. (A) The mean normalized maximal amplitude divided by the concentration used (red square, left y-axis) is presented together with 1 minus the mean normalized LC₅₀ (blue circle, right y-axis). The activation of hTRPA1 increased with increasing cytotoxicity, with some variances for Q, HN2, and HN3. Red squares also indicate the corresponding potencies in relation to SM (potency = 1). (B) A relationship between hTRPA1 activation and cytotoxicity was visualized by calculating the activation-cytotoxicity ratio which was between 0.4 and 2.2 for SM (indicated by dashed lines and gray area). A relationship was found for almost all the alkylating compounds with an exception for HN2. The determined threshold values in this case were outside of SM's threshold limits.

3.5. Effect of AP18 on cytotoxicity

Elevated $[Ca^{2+}]_i$ has been reported as mediator of apoptosis (Wang and Youle, 2009; Marchi et al. 2018), hence reducing it might prevent cell death. Table 1 shows that pre-treatment of HEK-A1 cells with the hTRPA1 specific antagonist AP18 prior to exposure to the various alkylating chemicals did not provide consistent results. Cytotoxicity was partially decreased for SM and HN2, and more distinct for HN3, but elevated in the presence of AP18 for T, Q, and HN1. However, we could not find a consistent trend, and the benefits of AP18 were quite minor in our experiments. Our findings are consistent with those of Stenger et al. (2015), who found that AP18 had no major influence on in vitro cytotoxicity when the LC₅₀ value was considered. Sawyer and Hamilton (2000) similarly revealed that SM cytotoxicity in keratinocytes was not reliant on $[Ca^{2+}]_i$, as our data suggested. This suggests that alternative mechanisms are involved in the cytotoxicity of alkylating agents.

4. Conclusion

Despite the fact that SM does not cause acute pain, we demonstrated that SM, the SM-related drugs Q and T, the NM HN1, HN2, and HN3, and the NM-derived chemotherapeutic drug bendamustine consistently activated hTRPA1. A link was found between hTRPA1 activation and cytotoxicity: alkylating compounds with lower activation potential were found to be less toxic than SM, and vice versa. However, inhibition of hTRPA1 had little influence on the LC₅₀, showing that hTRPA1 is not the main factor in alkylating agent-induced cytotoxicity. As a result, we conclude that hTRPA1 activation by diverse alkylating agents merely reflects the overall chemical reactivity. Future research should concentrate on investigating cellular consequences following hTRPA1 activation by alkylating chemicals that go beyond cytotoxicity.

Funding

The research was supported by the Deutsche Forschungsgemeinschaft (DFG) Research Training Group (RTG) 2338 P03, which was awarded to Horst Thiermann and Dirk Steinritz.

Declaration of Competing Interest

The authors state that they have no financial or personal relationships that may be considered as competing interests.

Data Availability

Data will be made available on request.

Acknowledgements

The authors thank Tilo Kliemt (Ludwig-Maximilians-University, Munich, Germany) for his excellent work and for performing preliminary experiments.

Appendix A. Supporting information

Supplementary data associated with this article can be found in the online version at [doi:10.1016/j.toxlet.2023.01.007](https://doi.org/10.1016/j.toxlet.2023.01.007).

References

- Andersson, D.A., Gentry, C., Moss, S., Bevan, S., 2008. Transient receptor potential A1 is a sensory receptor for multiple products of oxidative stress. *J. Neurosci.* 28, 2485–2494. <https://doi.org/10.1523/JNEUROSCI.5369-07.2008>.
- Balali-Mood, M., Hefazi, M., 2005. Clinical toxicology of sulfur mustard. *Arch. Iran. Med.* 8, 162–179.
- Bandell, M., Story, G.M., Hwang, S.W., et al., 2004. Noxious cold ion channel TRPA1 is activated by pungent compounds and bradykinin. *Neuron* 41, 849–857. [https://doi.org/10.1016/s0896-6273\(04\)00150-3](https://doi.org/10.1016/s0896-6273(04)00150-3).
- Bautista, D.M., Movahed, P., Hinman, A., et al., 2005. Pungent products from garlic activate the sensory ion channel TRPA1. *Proc. Natl. Acad. Sci. USA* 102, 12248–12252. <https://doi.org/10.1073/pnas.0505356102>.
- Ben-Johny, M., Yue, D.T., 2014. Calmodulin regulation (calmodulation) of voltage-gated calcium channels. *J. Gen. Physiol.* 143, 679–692. <https://doi.org/10.1085/jgp.201311153>.
- Bennett, G.M., Whincop, E.M., 1921. Some derivatives of monothioethylene glycol. *J. Chem. Soc.* 119, 1860–1864.
- Blum, M.M., Richter, A., Siegert, M., et al., 2020. Adduct of the blistering warfare agent sesquimustard with human serum albumin and its mass spectrometric identification for biomedical verification of exposure. *Anal. Bioanal. Chem.* 412, 7723–7737. <https://doi.org/10.1007/s00216-020-02917-w>.
- Chang, J.E., Kahl, B.S., 2012. Bendamustine for treatment of chronic lymphocytic leukemia. *Expert Opin. Pharm.* 13, 1495–1505. <https://doi.org/10.1517/14656566.2012.693163>.
- Cheson, B.D., Rummel, M.J., 2009. Bendamustine: Rebirth of an old drug. *J. Clin. Oncol.* 27, 1492–1501. <https://doi.org/10.1200/JCO.2008.18.7252>.
- DeVita, V.T., Chu, E., 2008. A history of cancer chemotherapy. *Cancer Res* 68, 8643–8653. <https://doi.org/10.1158/0008-5472.CAN-07-6611>.
- Dixit, P., Jeyaseelan, C., Gupta, D., 2023. Nitrogen mustard: a promising class of anti-cancer chemotherapeutics – a review. *Biointerface Res Appl. Chem.* 161, 1–27. <https://doi.org/10.33263/BRIACI32.161>.
- Emadi, S.N., Soroush, M., Kafashi, M., et al., 2012. Comparison late cutaneous complications between exposure to sulfur mustard and nerve agents. *Cutan. Ocul. Toxicol.* 31, 214–219. <https://doi.org/10.3109/15569527.2011.641196>.
- Gasson, E.J., McCombie, H., Williams, A.H., Woodward, F.N., 1948. New organic sulphur vesicants: 1: 2-di-(2-chloroethylthio)ethane and its analogues. *J. Chem. Soc.* 16, 44–46. <https://doi.org/10.1039/jr9480000044>.
- Gentile, M., Vigna, E., Recchia, A.G., et al., 2015. Bendamustine in multiple myeloma. *Eur. J. Haematol.* 95, 377–388. <https://doi.org/10.1111/ejh.12609>.
- Ghabili, K., Agutter, P., Ghanei, M., et al., 2011. Sulfur mustard toxicity: history, chemistry, pharmacokinetics, and pharmacodynamics. *Crit. Rev. Toxicol.* 41, 384–403. <https://doi.org/10.3109/10408444.2010.541224>.
- Gilman, A., 1963. The initial clinical trial of nitrogen mustard. *Am. J. Surg.* 105, 574–578. [https://doi.org/10.1016/0002-9610\(63\)90232-0](https://doi.org/10.1016/0002-9610(63)90232-0).
- Hasan, R., Leeson-Payne, A.T.S., Jaggar, J.H., Zhang, X., 2017. Calmodulin is responsible for Ca²⁺-dependent regulation of TRPA1 Channels. *Sci. Rep.* 7, 1–13. <https://doi.org/10.1038/srep45098>.
- Hinman, A., Chuang, H.-h., Bautista, D.M., Julius, D., 2006. TRP channel activation by reversible covalent modification. *Proc. Natl. Acad. Sci.* 103, 19564–19568. <https://doi.org/10.1073/pnas.0609598103>.
- Hu, F., Song, X., Long, D., 2021. Transient receptor potential ankyrin 1 and calcium: Interactions and association with disease (Review). *Exp. Ther. Med* 22, 1–7. <https://doi.org/10.3892/etm.2021.10897>.
- John, H., Koller, M., Worek, F., et al., 2019. Forensic evidence of sulfur mustard exposure in real cases of human poisoning by detection of diverse albumin-derived protein adducts. *Arch. Toxicol.* 93, 1881–1891. <https://doi.org/10.1007/s00204-019-02461-2>.
- Kaushik, M.P., Rana, H., 2005. Facile one-step synthesis of dithiaalkanedioles. *Org. Prep. Proced. Int* 37, 268–272. <https://doi.org/10.1080/00304940509354957>.
- Kehe, K., Szincz, L., 2005. Medical aspects of sulphur mustard poisoning. *Toxicology* 214, 198–209. <https://doi.org/10.1016/j.tox.2005.06.014>.
- Kendall, J.M., Badminton, M.N., 1998. Aequorea victoria bioluminescence moves into an exciting new era. *Trends Biotechnol.* 16, 216–224. [https://doi.org/10.1016/s0167-7799\(98\)01184-6](https://doi.org/10.1016/s0167-7799(98)01184-6).
- Lehmann, F., Wennerberg, J., 2021. Evolution of nitrogen-based alkylating anticancer agents. *Processes* 9, 1–10. <https://doi.org/10.3390/pr9020377>.
- Ludlum, D., Austin-Ritchie, P., Hagopian, M., et al., 1994. Detection of sulfur mustard-induced DNA modifications. *Chem. Biol. Inter.* 91, 39–49. [https://doi.org/10.1016/0009-2797\(94\)90005-1](https://doi.org/10.1016/0009-2797(94)90005-1).
- Macpherson, L.J., Dubin, A.E., Evans, M.J., et al., 2007. Noxious compounds activate TRPA1 ion channels through covalent modification of cysteines. *Nature* 445, 541–545. <https://doi.org/10.1038/nature05544>.
- Macpherson, L.J., Hwang, S.W., Miyamoto, T., et al., 2006. More than cool: Promiscuous relationships of menthol and other sensory compounds. *Mol. Cell Neurosci.* 32, 335–343. <https://doi.org/10.1016/j.mcn.2006.05.005>.
- Mangerich, A., Debiak, M., Birtel, M., et al., 2016. Sulfur and nitrogen mustards induce characteristic poly(ADP-ribosyl)ation responses in HaCaT keratinocytes with distinctive cellular consequences. *Toxicol. Lett.* 244, 56–71. <https://doi.org/10.1016/j.toxlet.2015.09.010>.
- Mangerich, A., Esser, C., 2014. Chemical warfare in the First World War: reflections 100 years later. *Arch. Toxicol.* 88, 1909–1911. <https://doi.org/10.1007/s00204-014-1370-z>.
- Marchi, S., Patergnani, S., Missiroli, S., et al., 2018. Mitochondrial and endoplasmic reticulum calcium homeostasis and cell death. *Cell Calcium* 69, 62–72. <https://doi.org/10.1016/j.ceca.2017.05.003>.
- Mattes, W.B., Hartley, J.A., Kohn, K.W., 1986. DNA sequence selectivity of guanine-N7 alkylation by nitrogen mustards. *Nucleic Acids Res* 14, 2971–2987. <https://doi.org/10.1093/nar/14.7.2971>.
- Müller-Dott, K., Thiermann, H., John, H., Steinritz, D., 2022. Isolation of human TRPA1 channel from transfected HEK293 cells and identification of alkylation sites after sulfur mustard exposure. *Arch. Toxicol.* <https://doi.org/10.1007/s00204-022-03411-1>.

K. Müller-Dott et al.

Toxicology Letters 376 (2023) 51–59

- Müller-Dott, K., Thiermann, H., Steinritz, D., Popp, T., 2020. Effect of sulfur mustard on melanogenesis in vitro. *Toxicol. Lett.* 319, 197–203. <https://doi.org/10.1016/j.toxlet.2019.11.014>.
- Munro, N.B., Talmage, S.S., Griffin, G.D., et al., 1999. The sources, fate, and toxicity of chemical warfare agent degradation products. *Environ. Health Perspect.* 107, 933–974. <https://doi.org/10.1289/ehp.99107933>.
- National Defense Research Committee (1946) Chemical warfare agents and related chemical problems, Parts III-VI.
- Paromov, V., Suntres, Z., Smith, M., Stone, W.L., 2007. Sulfur mustard toxicity following dermal exposure: role of oxidative stress, and antioxidant therapy. *J. Burns Wounds* 7, 60–85.
- Petrus, M., Peier, A.M., Bandell, M., et al., 2007. A role of TRPA1 in mechanical hyperalgesia is revealed by pharmacological inhibition. *Mol. Pain.* 3, 1–8. <https://doi.org/10.1186/1744-8069-3-40>.
- R Core Team, 2022. R: A Language and Environment for Statistical Computing. R Found. Stat. Comput.
- R Studio Team, 2022. RStudio: Integrated Development Environment for R. RStudio, PBC. (<http://www.rstudio.com/>)
- Rose, D., Schmidt, A., Brandenburger, M., et al., 2018. Sulfur mustard skin lesions: a systematic review on pathomechanisms, treatment options and future research directions. *Toxicol. Lett.* 293, 82–90. <https://doi.org/10.1016/j.toxlet.2017.11.039>.
- Sawyer, T.W., Hamilton, M.G., 2000. Effect of intracellular calcium modulation on sulfur mustard cytotoxicity in cultured human neonatal keratinocytes. *Toxicol. Vitr* 14, 149–157. [https://doi.org/10.1016/S0887-2333\(00\)00005-9](https://doi.org/10.1016/S0887-2333(00)00005-9).
- Sezigen, S., Ivelik, K., Ortatati, M., et al., 2019. Victims of chemical terrorism, a family of four who were exposed to sulfur mustard. *Toxicol. Lett.* 303, 9–15. <https://doi.org/10.1016/j.toxlet.2018.12.006>.
- Shimomura, O., Johnson, F.H., Morise, H., 1974. Mechanism of the luminescent intramolecular reaction of aequorin. *Biochemistry* 13, 3278–3286. <https://doi.org/10.1021/bi00713a016>.
- Singh, R.K., Kumar, S., Prasad, D.N., Bhardwaj, T.R., 2018. Therapeutic journey of nitrogen mustard as alkylating anticancer agents: Historic to future perspectives. *Eur. J. Med Chem.* 151, 401–433. <https://doi.org/10.1016/j.ejmech.2018.04.001>.
- Stenger, B., Popp, T., John, H., et al., 2017. N-Acetyl-L-cysteine inhibits sulfur mustard-induced and TRPA1-dependent calcium influx. *Mol. Toxicol.* 91, 2179–2189. <https://doi.org/10.1007/s00204-016-1873-x>.
- Stenger, B., Zehfuß, F., Mückter, H., et al., 2015. Activation of the chemosensing transient receptor potential channel A1 (TRPA1) by alkylating agents. *Arch. Toxicol.* 89, 1631–1643. <https://doi.org/10.1007/s00204-014-1414-4>.
- Story, G.M., Gereau, R.W., 2006. Numbing the senses: role of TRPA1 in mechanical and cold sensation. *Neuron* 50, 177–190. <https://doi.org/10.1016/j.neuron.2006.04.006>.
- Story, G.M., Peier, A.M., Reeve, A.J., et al., 2003. ANKTM1, a TRP-like channel expressed in nociceptive neurons, is activated by cold temperatures. *Cell* 112, 819–829. [https://doi.org/10.1016/S0092-8674\(03\)00158-2](https://doi.org/10.1016/S0092-8674(03)00158-2).
- Virk, H.S., Rekas, M.Z., Biddle, M.S., et al., 2019. Validation of antibodies for the specific detection of human TRPA1. *Sci. Rep.* 9, 1–9. <https://doi.org/10.1038/s41598-019-55133-7>.
- Wang, C., Youle, R.J., 2009. The role of mitochondria in apoptosis. *Annu Rev. Genet* 43, 95–118. <https://doi.org/10.1146/annurev-genet-102108-134850>.
- Wang, H., Woolf, C.J., 2005. Pain TRPs. *Neuron* 46, 9–12. <https://doi.org/10.1016/j.neuron.2005.03.011>.
- Watson, A.P., Griffin, G.D., 1992. Toxicity of vesicant agents scheduled for destruction by the chemical stockpile disposal program. *Environ. Health Perspect.* 98, 259–280. <https://doi.org/10.1289/ehp.9298259>.
- Wattana, M., Bey, T., 2009. Mustard gas or sulfur mustard: an old chemical agent as a new terrorist threat. *Prehosp. Disaster Med* 24, 19–29. <https://doi.org/10.1017/S1049023x0000649X>.
- Wickham, H., Averick, M., Bryan, J., et al., 2019. Welcome to the Tidyverse. *J. Open Source Softw.* 4, 1686. <https://doi.org/10.21105/joss.01686>.
- Zhang, J., Tian, Q., Zhou, S.-F., 2008. Clinical pharmacology of cyclophosphamide and ifosfamide. *Curr. Drug Ther.* 1, 55–84. <https://doi.org/10.2174/157488506775268515>.

4.1 Supplementary material Paper I

Supplementary Material

Activation of the human TRPA1 channel by different alkylating sulfur and nitrogen mustards and structurally related chemotherapeutic drugs

Katharina Müller-Dott^{1,2}, Sarah Christine Raßmuß¹, Marc-Michael Blum¹, Horst Thiermann¹, Harald John¹, Dirk Steinritz^{*1,2}

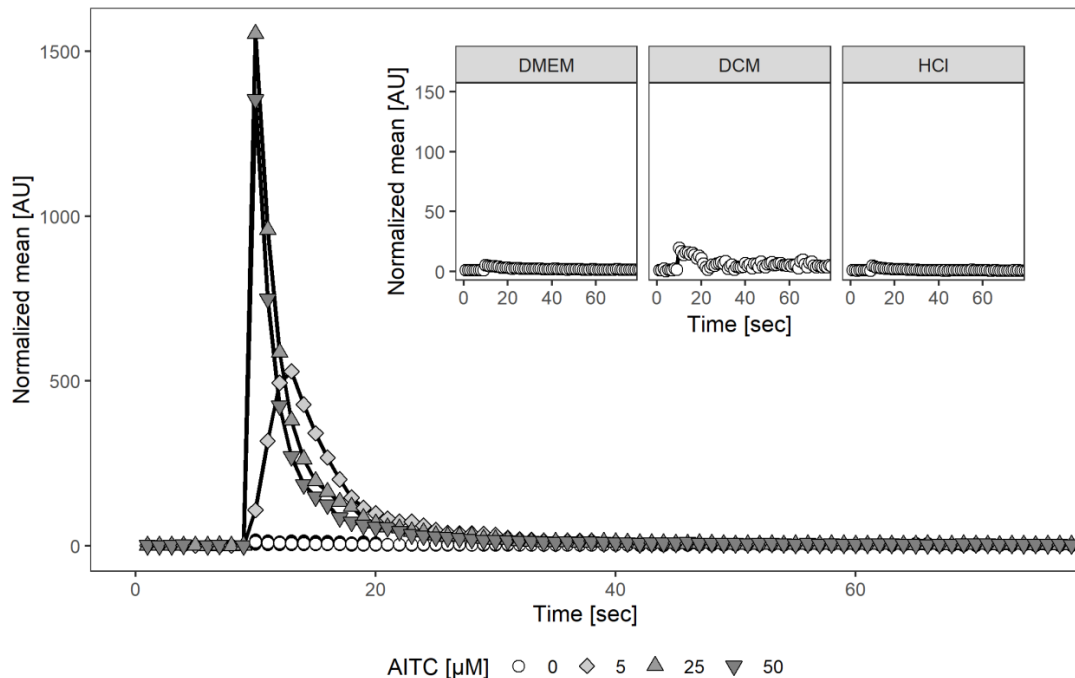


Figure S1: Changes in $[Ca^{2+}]_i$ after exposure to AITC, DMEM, DCM and HCl

Luminescence measurement of HEK-A1 cells after injection of allyl isothiocyanate (AITC) in the concentrations of 5 μM (rhombus), 25 μM (triangle) and 50 μM (upside down triangle) and after injection of DMEM and dichloromethane (DCM) as well as HCl (675 μM). $[Ca^{2+}]_i$ was assessed using the aequorin assay. Injection of the freshly prepared AITC as well as the solvents was performed after recording the baseline for 10 s. An increase in luminescence indicating a rise of $[Ca^{2+}]_i$ was observed for all applied AITC concentrations. The highest concentrations (25 μM and 50 μM) resulted in similar peak intensity indicating maximum hTRPA1 activation. Injection of DMEM and HCl resulted in only small and negligible increases in $[Ca^{2+}]_i$, which might be attributed to mechanical activation of hTRPA1. DCM caused a little rise in luminescence, which recovered to baseline 10 s after injection. The graph depicts baseline adjusted data. All investigations were carried out using a sample size of three.

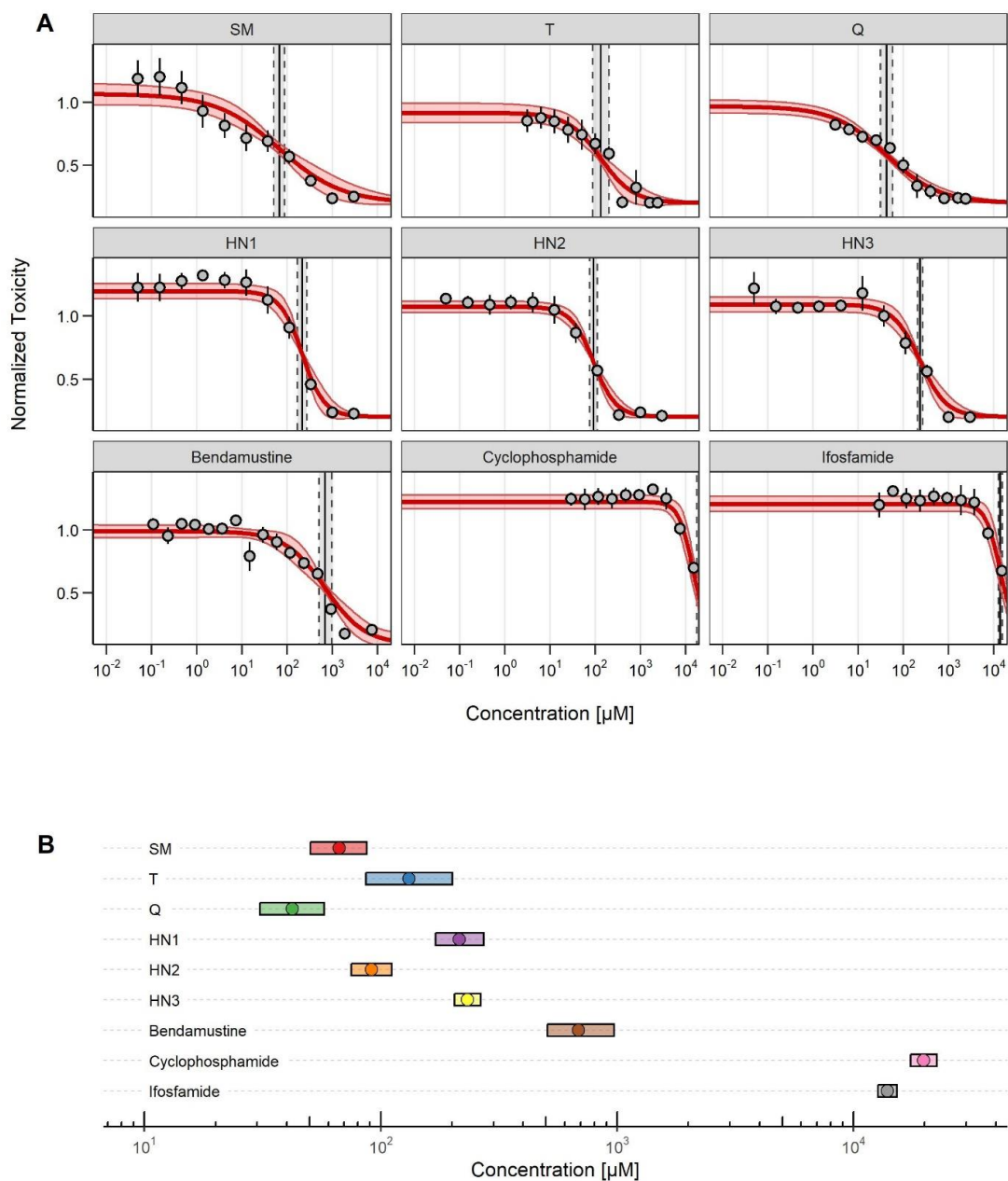


Figure S2: Analysis of dose-response data from HEK-A1 cells following exposure to alkylating chemicals

(A) Dose-response curves demonstrating cell viability of HEK-A1 cells 24 hours following exposure to SM, NM, or chemotherapeutic drugs as determined by the XTT assay. The red lines show the dose-response modeling findings using the LL.4 function with no upper or lower bounds. The 95%-CI of the curve fit is shown in light red. Dots represent means \pm SEM. Every experiment had three biological replicates ($n=3$), each with up to four technical replicates. The predicted LC_{50} concentration is indicated by gray vertical solid lines, with lower and upper limits indicated by dashed lines. (B) Synopsis of the computed LC_{50} values with lower and upper limits.

5 Summary

The chemical warfare agent sulfur mustard (SM) has been used in various conflicts through-out history even though it has been banned by international conventions. DNA alkylation has been reported as the primary molecular mechanism, however, alkylation of other proteins has also been described. It was shown that SM can directly activate human TRPA1 (hTRPA1) channels which are primarily found in sensory neurons. These channels play a crucial role in detecting and responding to various chemicals, environmental stimuli and in the perception of pain. They can be activated by a wide range of chemical irritants, such as mustard oil, cinnamaldehyde and AITC. The activation mechanism of the hTRPA1 channel by SM has not been researched so far.

As a result, Paper I focused on the interaction of SM with the hTRPA1 channel utilizing hTRPA1 overexpressing HEK293 cells. IMS was used to isolate hTRPA1 from transfected HEK293 cells. For the sensitive and selective detection of alkylation sites, a μ LC-ESI MS/HR MS approach was developed. After SM exposure, hTRPA1 channel modifications at Cys⁴⁶² and Cys⁶⁶⁵, as well as Asp³³⁹ and Glu³⁴¹, were detected for the first time. These may also play a role in hTRPA1 activation. hTRPA1 is thought to be a target for other SM-related chemical warfare agents, thus, analogous adducts could be analyzed utilizing the described analytical method.

Paper II investigated the activation potential of SM and SM-related alkylating agents such as Q, T, nitrogen mustards and chemotherapeutic compounds. In hTRPA1 overexpressing HEK293 cells, the aequorin assay was utilized to assess changes in $[Ca^{2+}]_i$. The findings reported in Paper II show that almost all studied alkylating compounds activated hTRPA1. Additionally, a relation between cytotoxicity and hTRPA1 activation was discovered. However, inhibition of the hTRPA1 using AP18 could not reduce the cytotoxicity induced by alkylating agents. As a consequence, hTRPA1 does not play a substantial role in cytotoxicity of the alkylating agents.

In conclusion, SM and SM-related alkylating agents activated the hTRPA1 channel. It was concluded that hTRPA1 activation by different alkylating agents merely reflects the overall chemical reactivity. Future research should concentrate on investigating cellular consequences following hTRPA1 activation by alkylating agents. Additionally, specific amino acid modifications were observed using μ LC-ESI MS/HR MS analysis. These SM-induced modifications were observed at cysteines as well as aspartic and glutamic acid residues. To determine the role of the altered amino acids, the modified residues will be altered and calcium measurements will be performed in future studies. This will provide further information on hTRPA1 activation.

6 Bibliography

- Anderson, D. R., Yourick, J. J., Moeller, R. B., Petrali, J. P., Young, G. D., & Byers, S. L. (1996). Pathologic changes in rat lungs following acute sulfur mustard inhalation. *Inhalation Toxicology*, *8*(3), 285–297. <https://doi.org/10.3109/08958379609005436>
- Andersson, D. A., Gentry, C., Moss, S., & Bevan, S. (2008). Transient receptor potential A1 is a sensory receptor for multiple products of oxidative stress. *Journal of Neuroscience*, *28*(10), 2485–2494. <https://doi.org/10.1523/JNEUROSCI.5369-07.2008>
- Bahia, P. K., Parks, T. A., Stanford, K. R., Mitchell, D. A., Varma, S., Stevens, S. M., & Taylor-Clark, T. E. (2016). The exceptionally high reactivity of Cys 621 is critical for electrophilic activation of the sensory nerve ion channel TRPA1. *Journal of General Physiology*, *147*(6), 451–465. <https://doi.org/10.1085/jgp.201611581>
- Balali-Mood, M., & Hefazi, M. (2005). Clinical toxicology of sulfur mustard. *Arch Iranian Med*, *8*(3), 162–179.
- Bandell, M., Story, G. M., Hwang, S. W., Viswanath, V., Eid, S. R., Petrus, M. J., Earley, T. J., & Patapoutian, A. (2004). Noxious cold ion channel TRPA1 is activated by pungent compounds and bradykinin. *Neuron*, *41*, 849–857. [https://doi.org/10.1016/s0896-6273\(04\)00150-3](https://doi.org/10.1016/s0896-6273(04)00150-3)
- Batal, M., Boudry, I., Mouret, S., Wartelle, J., Emorine, S., Bertoni, M., Bérard, I., Cléry-Barraud, C., & Douki, T. (2013). Temporal and spatial features of the formation of dna adducts in sulfur mustard-exposed skin. *Toxicology and Applied Pharmacology*. <https://doi.org/10.1016/j.taap.2013.10.010>
- Bautista, D. M., Jordt, S. E., Nikai, T., Tsuruda, P. R., Read, A. J., Poblete, J., Yamoah, E. N., Basbaum, A. I., & Julius, D. (2006). TRPA1 mediates the inflammatory actions of environmental irritants and proalgesic agents. *Cell*, *124*(6), 1269–1282. <https://doi.org/10.1016/j.cell.2006.02.023>
- Bautista, D. M., Movahed, P., Hinman, A., Axelsson, H. E., Sterner, O., Högestätt, E. D., Julius, D., Jordt, S. E., & Zygmunt, P. M. (2005). Pungent products from garlic activate the sensory ion channel TRPA1. *Proceedings of the National Academy of Sciences of the United States of America*, *102*(34), 12248–12252. <https://doi.org/10.1073/pnas.0505356102>
- Bautista, D. M., Pellegrino, M., & Tsunozaki, M. (2013). TRPA1: A gatekeeper for inflammation. *Annual Review of Physiology*, *75*(1), 181–200. <https://doi.org/10.1146/annurev-physiol-030212-183811>
- Bautista, D. M., Siemens, J., Glazer, J. M., Tsuruda, P. R., Basbaum, A. I., Stucky, C. L., Jordt, S. E., & Julius, D. (2007). The menthol receptor TRPM8 is the principal detector of environmental cold. *Nature*, *448*(7150), 204–208. <https://doi.org/10.1038/nature05910>

- Bennett, G. M., & Whincop, E. M. (1921). Some derivatives of monothioethylene glycol. *Journal of Chemical Society*, *119*, 1860–1864. <https://doi.org/10.1039/CT9211901860>
- Bessac, B. F., & Jordt, S. E. (2008). Breathtaking TRP channels: TRPA1 and TRPV1 in airway chemosensation and reflex control. *Physiology*, *23*(6), 360–370. <https://doi.org/10.1152/physiol.00026.2008>
- Bessac, B. F., & Jordt, S. E. (2010). Sensory detection and responses to toxic gases: Mechanisms, health effects, and countermeasures. *Proceedings of the American Thoracic Society*, *7*(4), 269–277. <https://doi.org/10.1513/pats.201001-004SM>
- Blum, M. M., Richter, A., Siegert, M., Thiermann, H., & John, H. (2020). Adduct of the blistering warfare agent sesquimustard with human serum albumin and its mass spectrometric identification for biomedical verification of exposure. *Analytical and Bioanalytical Chemistry*, *412*(28), 7723–7737. <https://doi.org/10.1007/s00216-020-02917-w>
- Bobb, A. J., Arfsten, D. P., & Jederberg, W. W. (2005). N-acetyl-L-cysteine as prophylaxis against sulfur mustard. *Military Medicine*, *170*(1), 52–56. <https://doi.org/10.7205/MILMED.170.1.52>
- Caterina, M. J., Schumacher, M. A., Tominaga, M., Rosen, T. A., Levine, J. D., & Julius, D. (1997). The capsaicin receptor: A heat-activated ion channel in the pain pathway. *Nature*, *389*(6653), 816–824. <https://doi.org/10.1038/39807>
- Chang, J. E., & Kahl, B. S. (2012). Bendamustine for treatment of chronic lymphocytic leukemia. *Expert Opinion on Pharmacotherapy*, *13*(10), 1495–1505. <https://doi.org/10.1517/14656566.2012.693163>
- Cheng, W., Sun, C., & Zheng, J. (2010). Heteromerization of TRP channel subunits: Extending functional diversity. *Protein and Cell*, *1*(9), 802–810. <https://doi.org/10.1007/s13238-010-0108-9>
- Cheson, B. D., & Rummel, M. J. (2009). Bendamustine: Rebirth of an old drug. *Journal of Clinical Oncology*, *27*(9), 1492–1501. <https://doi.org/10.1200/JCO.2008.18.7252>
- Clapham, D. E. (2003). TRP channels as cellular sensors. *Nature*, *426*(6966), 517–524. <https://doi.org/10.1038/nature02196>
- Cosens, D. J., & Manning, A. (1969). Abnormal electroretinogram from a drosophila mutant. *Nature*, *224*, 285–287. <https://doi.org/10.1038/224488a0>
- DeVita, V. T., & Chu, E. (2008). A history of cancer chemotherapy. *Cancer Research*, *68*(21), 8643–8653. <https://doi.org/10.1158/0008-5472.CAN-07-6611>
- Evison, D. (2002). Regular review: Chemical weapons. *BMJ*, *324*(7333), 332–335. <https://doi.org/10.1136/bmj.324.7333.332>
- Firooz, A., Sadr, B., Davoudi, S. M., Nassiri-Kashani, M., Panahi, Y., & Dowlati, Y. (2011). Long-term skin damage due to chemical weapon exposure. *Cutaneous and Ocular Toxicology*, *30*(1), 64–68. <https://doi.org/10.3109/15569527.2010.529547>
- Fischer, M. J., Leffler, A., Niedermirtl, F., Kistner, K., Eberhardt, M., Reeh, P. W., & Nau, C. (2010). The general anesthetic propofol excites nociceptors by activating TRPV1 and TRPA1 rather than GABAA receptors. *Journal of*

- Biological Chemistry*, 285(45), 34781–34792. <https://doi.org/10.1074/jbc.M110.143958>
- Gasson, E. J., McCombie, H., Williams, A. H., & Woodward, F. N. (1948). New organic sulphur vesicants; 1: 2-di-(2-chloroethylthio)ethane and its analogues. *Journal of the Chemical Society*, 16, 44–46. <https://doi.org/10.1039/jr9480000044>
- Gentile, M., Vigna, E., Recchia, A. G., Morabito, L., Mendicino, F., Giagnuolo, G., & Morabito, F. (2015). Bendamustine in multiple myeloma. *European Journal of Haematology*, 95(5), 377–388. <https://doi.org/10.1111/ejh.12609>
- Ghabili, K., Agutter, P., Ghanei, M., Ansarin, K., Panahi, Y., & Shoja, M. (2011). Sulfur mustard toxicity: History, chemistry, pharmacokinetics, and pharmacodynamics. *Critical Reviews in Toxicology*, 41(5), 384–403. <https://doi.org/10.3109/10408444.2010.541224>
- Gilman, A. (1963). The initial clinical trial of nitrogen mustard. *The American Journal of Surgery*, 105(5), 574–578. [https://doi.org/10.1016/0002-9610\(63\)90232-0](https://doi.org/10.1016/0002-9610(63)90232-0)
- Graham, J. S., & Schoneboom, B. A. (2013). Historical perspective on effects and treatment of sulfur mustard injuries. *Chemico-Biological Interactions*, 206(3), 512–522. <https://doi.org/10.1016/j.cbi.2013.06.013>.
- Hall, B. E., Prochazkova, M., Sapio, M. R., Minetos, P., Kurochkina, N., Binukumar, B. K., Amin, N. D., Terse, A., Joseph, J., Raithel, S. J., Mannes, A. J., Pant, H. C., Chung, M. K., Iadarola, M. J., & Kulkarni, A. B. (2018). Phosphorylation of the transient receptor potential ankyrin 1 by cyclin-dependent kinase 5 affects chemo-nociception. *Scientific Reports*, 8(1), 1–12. <https://doi.org/10.1038/s41598-018-19532-6>
- Hardie, R. C., & Minke, B. (1992). The TRP gene is essential for a light-activated Ca²⁺ channel in drosophila photoreceptors. *Neuron*, 8(4), 643–651. [https://doi.org/10.1016/0896-6273\(92\)90086-S](https://doi.org/10.1016/0896-6273(92)90086-S)
- Hemme, M., Fidder, A., Oeveren, D. v. d. R.-v., van der Schans, M. J., & Noort, D. (2021). Mass spectrometric analysis of adducts of sulfur mustard analogues to human plasma proteins: Approach towards chemical provenancing in biomedical samples. *Analytical and Bioanalytical Chemistry*, 413, 4023–4036. <https://doi.org/10.1007/s00216-021-03354-z>
- Hinman, A., Chuang, H.-h., Bautista, D. M., & Julius, D. (2006). TRP channel activation by reversible covalent modification. *Proceedings of the National Academy of Sciences*, 103(51), 19564–19568. <https://doi.org/10.1073/pnas.0609598103>
- Ishimaru, Y., & Matsunami, H. (2009). Transient receptor potential (TRP) channels and taste sensation. *Journal of Dental Research*, 88(3), 212–218. <https://doi.org/10.1177/0022034508330212>
- Jenner, J., & Graham, S. J. (2013). Treatment of sulphur mustard skin injury. *Chemico-Biological Interactions*, 206(3), 491–495. <https://doi.org/10.1016/j.cbi.2013.10.015>
- John, H., Koller, M., Worek, F., Thiermann, H., & Siegert, M. (2019). Forensic evidence of sulfur mustard exposure in real cases of human poisoning by

- detection of diverse albumin-derived protein adducts. *Archives of Toxicology*, *93*(7), 1881–1891. <https://doi.org/10.1007/s00204-019-02461-2>
- Jordt, S. E., Bautista, D. M., Chuang, H. H., McKemy, D. D., Zygmunt, P. M., Högestätt, E. D., Meng, I. D., & Julius, D. (2004). Mustard oils and cannabinoids excite sensory nerve fibres through the TRP channel ANKTM1. *Nature*, *427*(6971), 260–265. <https://doi.org/10.1038/nature02282>
- Kehe, K., Balszuweit, F., Emmeler, J., Kreppel, H., Jochum, M., & Thiermann, H. (2008). Sulfur mustard research—strategies for the development of improved medical therapy. *ePlasty*, *8*(32), 312–332.
- Kehe, K., Balszuweit, F., Steinritz, D., & Thiermann, H. (2009). Molecular toxicology of sulfur mustard-induced cutaneous inflammation and blistering. *Toxicology*, *263*(1), 12–19. <https://doi.org/10.1016/j.tox.2009.01.019>
- Kehe, K., & Szinicz, L. (2005). Medical aspects of sulphur mustard poisoning. *Toxicology*, *214*, 198–209. <https://doi.org/10.1016/j.tox.2005.06.014>
- Koivisto, A., & Pertovaara, A. (2015). Transient receptor potential ankyrin 1 channel antagonists for pain relief. In *TRP channels as therapeutic targets: From basic science to clinical use* (pp. 145–162). Elsevier Inc. <https://doi.org/10.1016/B978-0-12-420024-1.00009-6>
- Kwan, K. Y., Allchorne, A. J., Vollrath, M. A., Christensen, A. P., Zhang, D. S., Woolf, C. J., & Corey, D. P. (2006). TRPA1 contributes to cold, mechanical, and chemical nociception but is not essential for hair-cell transduction. *Neuron*, *50*(2), 277–289. <https://doi.org/10.1016/j.neuron.2006.03.042>
- Lehmann, F., & Wennerberg, J. (2021). Evolution of nitrogen-based alkylating anticancer agents. *Processes*, *9*(2), 1–10. <https://doi.org/10.3390/pr9020377>
- Ludlum, D., Austin-Ritchie, P., Hagopian, M., Niu, T.-Q., & Yu, D. (1994). Detection of sulfur mustard-induced DNA modifications. *Chemico-Biological Interactions*, *91*(1), 39–49. [https://doi.org/10.1016/0009-2797\(94\)90005-1](https://doi.org/10.1016/0009-2797(94)90005-1)
- Lüling, R., John, H., Gudermann, T., Thiermann, H., Mückter, H., Popp, T., & Steinritz, D. (2018). Transient receptor potential channel A1 (TRPA1) regulates sulfur mustard-induced expression of heat shock 70 kDa protein 6 (HSPA6) in vitro. *Cells*, *7*(9), 126. <https://doi.org/10.3390/cells7090126>
- Lüling, R., Schmeißer, W., Siegert, M., Mückter, H., Dietrich, A., Thiermann, H., Gudermann, T., John, H., & Steinritz, D. (2021). Identification of creatine kinase and alpha-1 antitrypsin as protein targets of alkylation by sulfur mustard. *Drug Testing and Analysis*, *13*(2), 268–282. <https://doi.org/10.1002/dta.2916>
- Macpherson, L. J., Dubin, A. E., Evans, M. J., Marr, F., Schultz, P. G., Cravatt, B. F., & Patapoutian, A. (2007). Noxious compounds activate TRPA1 ion channels through covalent modification of cysteines. *Nature*, *445*(7127), 541–545. <https://doi.org/10.1038/nature05544>
- Macpherson, L. J., Geierstanger, B. H., Viswanath, V., Bandell, M., Eid, S. R., Hwang, S., Patapoutian, A., & Diego, S. (2005). The pungency of garlic: Activation of TRPA1 and TRPV1 in response to allicin. *Current Biology*, *15*, 929–934. <https://doi.org/10.1016/j.cub.2005.04.018>

- Macpherson, L. J., Hwang, S. W., Miyamoto, T., Dubin, A. E., Patapoutian, A., & Story, G. M. (2006). More than cool: Promiscuous relationships of menthol and other sensory compounds. *Molecular and Cellular Neuroscience*, *32*(4), 335–343. <https://doi.org/10.1016/j.mcn.2006.05.005>
- Mangerich, A., Debiak, M., Birtel, M., Ponath, V., Balszuweit, F., Lex, K., Martello, R., Burckhardt-Boer, W., Strobelt, R., Siegert, M., Thiermann, H., Steinritz, D., Schmidt, A., & Bürkle, A. (2016). Sulfur and nitrogen mustards induce characteristic poly(adp-ribosyl)ation responses in hacat keratinocytes with distinctive cellular consequences. *Toxicology Letters*, *244*, 56–71. <https://doi.org/10.1016/j.toxlet.2015.09.010>
- Mangerich, A., & Esser, C. (2014). Chemical warfare in the first world war: Reflections 100 years later. *Archives of Toxicology*, *88*(11), 1909–1911. <https://doi.org/10.1007/s00204-014-1370-z>
- Masta, A., Gray, P. J., & Phillips, D. R. (1996). Effect of sulphur mustard on the initiation and elongation of transcription. *Carcinogenesis*, *17*(3), 525–532. <https://doi.org/10.1093/carcin/17.3.525>
- Mattes, W. B., Hartley, J. A., & Kohn, K. W. (1986). DNA sequence selectivity of guanine-N7 alkylation by nitrogen mustards. *Nucleic Acids Research*, *14*(7), 2971–2987. <https://doi.org/10.1093/nar/14.7.2971>
- Meents, J. E., Ciotu, C. I., & Fischer, M. J. (2019). TRPA1: A molecular view. *Journal of Neurophysiology*, *121*(2), 427–443. <https://doi.org/10.1152/jn.00524.2018>
- Montell, C., & Rubin, G. M. (1989). Molecular characterization of the drosophila TRP locus: A putative integral membrane protein required for phototransduction. *Neuron*, *2*(4), 1313–1323. [https://doi.org/10.1016/0896-6273\(89\)90069-X](https://doi.org/10.1016/0896-6273(89)90069-X)
- Mukhopadhyay, I., Gomes, P., Aranake, S., Shetty, M., Karnik, P., Damle, M., Kuruganti, S., Thorat, S., & Khairatkar-Joshi, N. (2011). Expression of functional TRPA1 receptor on human lung fibroblast and epithelial cells. *Journal of Receptors and Signal Transduction*, *31*(5), 350–358. <https://doi.org/10.3109/10799893.2011.602413>
- Müller-Dott, K., Thiermann, H., Steinritz, D., & Popp, T. (2020). Effect of sulfur mustard on melanogenesis in vitro. *Toxicology Letters*, *319*, 197–203. <https://doi.org/10.1016/j.toxlet.2019.11.014>
- National Defense Research Committee. (1946). *Chemical warfare agents and related chemical problems, parts iii-vi*.
- Nilius, B., Appendino, G., & Owsianik, G. (2012). The transient receptor potential channel TRPA1: from gene to pathophysiology. *Pflügers Archiv European Journal of Physiology*, *464*(5), 425–458. <https://doi.org/10.1007/s00424-012-1158-z>
- Nilius, B., & Flockerzi, V. (2014). Mammalian transient receptor potential (TRP) cation channels. In *Handbook of experimental pharmacology* (pp. 729–1290, Vol. 223).
- Nilius, B., & Owsianik, G. (2013). Transient receptor potential family of ion channels. *Encyclopedia of Pain*, 4037–4037. https://doi.org/10.1007/978-3-642-28753-4_202324

- Papirmeister, B., Feister, A., SI, S. R., & Ford, R. (1991). Medical defense against mustard gas: Toxic mechanisms and pharmacological implications. *CRC Press: Boca Raton, FL*, 91–122.
- Paromov, V., Suntres, Z., Smith, M., & Stone, W. L. (2007). Sulfur mustard toxicity following dermal exposure: Role of oxidative stress, and antioxidant therapy. *Journal of Burns and Wounds*, 7, 60–85.
- Paulsen, C. E., Armache, J. P., Gao, Y., Cheng, Y., & Julius, D. (2015). Structure of the TRPA1 ion channel suggests regulatory mechanisms. *Nature*, 344(6188), 1173–1178. <https://doi.org/10.1126/science.1249098>. Sleep
- Pedersen, S. F., Owsianik, G., & Nilius, B. (2005). TRP channels: An overview. *Cell Calcium*, 38(3-4), 233–252. <https://doi.org/10.1016/j.ceca.2005.06.028>
- Phillips, R. C. (2005). *The guide to US army museums*.
- Popp, T., Lüling, R., Boekhoff, I., Seeger, T., Branoner, F., & Gudermann, T. (2018). Immediate responses of the cockroach *blaptica dubia* after the exposure to sulfur mustard. *Archives of Toxicology*, 92(1), 337–346. <https://doi.org/10.1007/s00204-017-2064-0>
- Razavi, S. M., Saghafinia, M., Davoudi, S. M., & Salamati, P. (2013). The effects of sulfur mustard on the skin and their management: Reviewing the studies conducted on Iranian chemical victims. *Iranian Journal of Dermatology*, 16(63), 21–30.
- Razavi, S. M., Salamati, P., Saghafinia, M., & Abdollahi, M. (2012). A review on delayed toxic effects of sulfur mustard in Iranian veterans. *DARU, Journal of Pharmaceutical Sciences*, 20(1), 1–8. <https://doi.org/10.1186/2008-2231-20-51>
- Rice, P. (2003). Sulphur mustard injuries of the skin pathophysiology and management. *Toxicol Rev*, 22(2), 111–118. <https://doi.org/10.2165/00139709-200322020-00006>
- Rodgers, G. C., & Condurache, C. T. (2010). Antidotes and treatments for chemical warfare/terrorism agents: An evidence-based review. *Clinical Pharmacology and Therapeutics*, 88(3), 318–327. <https://doi.org/10.1038/clpt.2010.152>
- Rose, D., Schmidt, A., Brandenburger, M., Sturmheit, T., Zille, M., & Boltze, J. (2018). Sulfur mustard skin lesions: A systematic review on pathomechanisms, treatment options and future research directions. *Toxicology Letters*, 293, 82–90. <https://doi.org/10.1016/j.toxlet.2017.11.039>
- Sadofsky, L. R., Boa, A. N., Maher, S. A., Birrell, M. A., Belvisi, M. G., & Morice, A. H. (2011). TRPA1 is activated by direct addition of cysteine residues to the N-hydroxysuccinyl esters of acrylic and cinnamic acids. *Pharmacological Research*, 63(1), 30–36. <https://doi.org/10.1016/j.phrs.2010.11.004>
- Schmeißer, W., Lüling, R., Steinritz, D., Thiermann, H., Rein, T., & John, H. (2022). Transthyretin as a target of alkylation and a potential biomarker for sulfur mustard poisoning: Electrophoretic and mass spectrometric identification and characterization. *Drug Testing and Analysis*, 14(1), 80–91. <https://doi.org/10.1002/dta.3146>

- Schmidt, A., Steinritz, D., Rudolf, K. D., Thiermann, H., & Striepling, E. (2018). Accidental sulfur mustard exposure: A case report. *Toxicology Letters*, *293*, 62–66. <https://doi.org/10.1016/j.toxlet.2017.11.023>
- Sezigen, S., Ivelik, K., Ortatatli, M., Almacioglu, M., Demirkasimoglu, M., Eyison, R., Kunak, Z., & Kenar, L. (2019). Victims of chemical terrorism, a family of four who were exposed to sulfur mustard. *Toxicology Letters*, *303*, 9–15. <https://doi.org/10.1016/j.toxlet.2018.12.006>
- Shakarjian, M. P., Heck, D. E., Gray, J. P., Sinko, P. J., Gordon, M. K., Casillas, R. P., Heindel, N. D., Gerecke, D. R., Laskin, D. L., & Laskin, J. D. (2009). Mechanisms mediating the vesicant actions of sulfur mustard after cutaneous exposure. *Toxicological Sciences*, *114*(1), 5–19. <https://doi.org/10.1093/toxsci/kfp253>
- Singh, R. K., Kumar, S., Prasad, D. N., & Bhardwaj, T. R. (2018). Therapeutic journey of nitrogen mustard as alkylating anticancer agents: Historic to future perspectives. *European Journal of Medicinal Chemistry*, *151*, 401–433. <https://doi.org/10.1016/j.ejmech.2018.04.001>
- Smith, K. J., Hurst, C. G., Moeller, R. B., Skelton, H. G., & Sidell, F. R. (1995). Sulfur mustard: Its continuing threat as a chemical warfare agent, the cutaneous lesions induced, progress in understanding its mechanism of action, its long-term health effects, and new developments for protection and therapy. *Journal of the American Academy of Dermatology*, *32*(5 Part 1), 765–776. [https://doi.org/10.1016/0190-9622\(95\)91457-9](https://doi.org/10.1016/0190-9622(95)91457-9)
- Steinritz, D., Stenger, B., Dietrich, A., Gudermann, T., & Popp, T. (2018). TRPs in tox: Involvement of transient receptor potential-channels in chemical-induced organ toxicity-a structured review. *Cells*, *7*(8), 98. <https://doi.org/10.3390/cells7080098>
- Stenger, B., Zehfuß, F., Mückter, H., Schmidt, A., Balszuweit, F., Schäfer, E., Büch, T., Gudermann, T., Thiermann, H., & Steinritz, D. (2015). Activation of the chemosensing transient receptor potential channel A1 (TRPA1) by alkylating agents. *Archives of Toxicology*, *89*(9), 1631–1643. <https://doi.org/10.1007/s00204-014-1414-4>
- Story, G. M., Peier, A. M., Reeve, A. J., Eid, S. R., Mosbacher, J., Hricik, T. R., Earley, T. J., Hergarden, A. C., Andersson, D. A., Hwang, S. W., McIntyre, P., Jegla, T., Bevan, S., & Patapoutian, A. (2003). ANKTM1, a TRP-like channel expressed in nociceptive neurons, is activated by cold temperatures. *Cell*, *112*(6), 819–829. [https://doi.org/10.1016/S0092-8674\(03\)00158-2](https://doi.org/10.1016/S0092-8674(03)00158-2)
- Suo, Y., Wang, Z., Zubcevic, L., Hsu, A. L., He, Q., Borgnia, M. J., Ji, R.-R., & Lee, S.-Y. (2019). Structural insights into electrophile irritant sensing by the human TRPA1 channel. *Neuron*, *105*, 1–13. <https://doi.org/10.1016/j.neuron.2019.11.023>
- Takahashi, N., Mizuno, Y., Kozai, D., Yamamoto, S., Kiyonaka, S., Shibata, T., Uchida, K., & Mori, Y. (2008). Molecular characterization of TRPA1 channel activation by cysteine-reactive inflammatory mediators. *Channels*, *2*(4), 287–298. <https://doi.org/10.4161/chan.2.4.6745>

- Talavera, K., Startek, J. B., Alvarez-Collazo, J., Boonen, B., Alpizar, Y. A., Sanchez, A., Naert, R., & Nilius, B. (2020). Mammalian transient receptor potential TRPA1: from structure to disease. *Physiol Rev*, *100*(2), 725–803. <https://doi.org/10.1152/physrev.00005.2019>
- Veress, L. A., O'Neill, H. C., Hendry-Hofer, T. B., Loader, J. E., Rancourt, R. C., & White, C. W. (2010). Airway obstruction due to bronchial vascular injury after sulfur mustard analog inhalation. *American Journal of Respiratory and Critical Care Medicine*, *182*(11), 1352–1361. <https://doi.org/10.1164/rccm.200910-1618OC>
- Wang, H., & Woolf, C. J. (2005). Pain TRPs. *Neuron*, *46*(1), 9–12. <https://doi.org/10.1016/j.neuron.2005.03.011>
- Wang, L., Cvetkov, T. L., Chance, M. R., & Moiseenkova-Bell, V. Y. (2012). Identification of in vivo disulfide conformation of TRPA1 ion channel. *Journal of Biological Chemistry*, *287*(9), 6169–6176. <https://doi.org/10.1074/jbc.M111.329748>
- Watson, A. P., & Griffin, G. D. (1992). Toxicity of vesicant agents scheduled for destruction by the chemical stockpile disposal program. *Environmental Health Perspectives*, *98*(2), 259–280. <https://doi.org/10.1289/ehp.9298259>
- Wattana, M., & Bey, T. (2009). Mustard gas or sulfur mustard: An old chemical agent as a new terrorist threat. *Prehospital and Disaster Medicine*, *24*(1), 19–29. <https://doi.org/10.1017/S1049023X0000649X>
- Worek, F., Seeger, T., Neumaier, K., Wille, T., & Thiermann, H. (2016). Blaptica dubia as sentinels for exposure to chemical warfare agents – a pilot study. *Toxicology Letters*, *262*, 12–16. <https://doi.org/10.1016/j.toxlet.2016.09.006>
- Young, R. A., & Bast, C. (2009). Chapter 8 - Mustards and vesicants. In *Handbook of toxicology of chemical warfare agents* (pp. 93–108). <https://doi.org/10.1016/B978-0-12-800159-2.00008-7>
- Zhang, J., Tian, Q., & Zhou, S.-F. (2008). Clinical pharmacology of cyclophosphamide and ifosfamide. *Current Drug Therapy*, *1*(1), 55–84. <https://doi.org/10.2174/157488506775268515>

Acknowledgements

I would like to express my appreciation and gratitude to the individuals and organizations that helped me obtain my PhD in Medical Research. Their encouragement, knowledge, and support have been essential throughout this remarkable journey.

First and foremost, I would like to thank Prof. Dr. Gudermann, the GRK2338's speaker, for his dedication to academic excellence and the outstanding scientific program provided by the Research Training Group, as well as the opportunity to write my PhD thesis at Ludwig-Maximilians-Universität in Munich.

Prof. Dr. Dirk Steinritz and Prof. Dr. Harald John, my PhD supervisors, deserve special recognition. Their knowledge, strong support, and insightful advice have been invaluable in developing my research idea and guiding me through the complexity of my research project. I would also want to thank Prof. Dr. Horst Thiermann and the Bundeswehr Institute of Pharmacology and Toxicology in Munich for providing me with the opportunity to complete my dissertation under exceptional working conditions. This PhD dissertation would not have been completed without their support and dedicated engagement throughout the process. I would like to express my gratitude for your patience and understanding throughout the years.

I would also like to thank my Bachelor and Master students Sarah Raßmuß, Thilo Kliemt, Doreen Reuter and Anna Hellmann for their enthusiasm for cell culture, Western blot experiments, and research on the human TRPA1 channel.

Thank you to my colleagues and friends at the GRK2338 and the Bundeswehr Institute of Pharmacology and Toxicology, particularly Anja Köhler, Bernd Stenger, Jonas Tigges, Marina Dentzel, Markus Siegert, Sabrina Brockmüller, Simone Rothmiller, and Tamara Kranawetvogl, for engaging in intellectual discussion, encouraging advice and support, and the fantastic activities outside of the lab. I am thankful that colleagues have turned into friends who have made this experience unforgettable.

Most significantly, none of this would have been possible without the support of my family. I would like to acknowledge the immeasurable love, encouragement and understanding of my parents Carmen and Christoph Müller-Dott as well as my partner Nils Diehl. Their patience, understanding and belief in me have provided the strength and motivation to pursue my passion for research.

Just as importantly, I want to thank my daughter Lilly for her endless love.